WISSENSCHAFTSZENTRUM WEIHENSTEPHAN FÜR ERNÄHRUNG, LANDNUTZUNG UND UMWELT

LEHRSTUHL FÜR ENTWICKLUNGSGENETIK

Mechanisms regulating GABAergic neurogenesis in the developing mouse midbrain

Clara Elisabeth Teresa Agathe Tabea Zoe Wende

Vollständiger Abdruck der von der Fakultät Wissenschaftszentrum Weihenstephan für Ernährung, Landnutzung und Umwelt der Technischen Universität München zur Erlangung des akademischen Grades eines

Doktors der Naturwissenschaften

genehmigten Dissertation.

Vorsitzender: Univ. Prof. Dr. S. Scherer
Prüfer der Dissertation:
1. Univ. Prof. Dr. W. Wurst
2. Univ. Prof. Dr. H. Lickert

Die Dissertation wurde am 28.07.2015 bei der Technischen Universität München eingereicht und durch die Fakultät Wissenschaftszentrum Weihenstephan für Ernährung, Landnutzung und Umwelt am 12.11.2015 angenommen.

Für meinen Großvater

1 CONTENT

2 SUMMARY

In the mature central nervous system (CNS), neurons using ɣ-aminobutyric acid (GABA) as their neurotransmitter are the main inhibitory neurons and disturbation in their development and function are implicated with severe neurological conditions. The midbrain (MB) is an important integration center where GABAergic neurons (GABAn) control several aspects of behavior, sensory-motor and motivational processes. Thus, marked dysfunction of GABAergic interneurons in the MB is associated with psychiatric diseases such as schizophrenia, bipolar disorder, epilepsy and attention deficit hyperactivity disorder (ADHD). Moreover, MB GABAergic interneurons are also important targets of medical treatments as well as drugs of abuse. To understand how a finite number of genes gives rise to complex behavior, the specific codes of genes, their protein interactions and the mechanisms used by each brain region have become increasingly crucial for understanding the basic steps of GABAergic neuronal specification. By the use of a mouse model I aimed to further decipher such mechanistic codes particularly for GABAergic neurogenesis in the MB.

In the present study, I provide molecular, genetic and phenotypic evidence for the unique, overlapping and synergistic interaction between the *hairy/Enhancer of split*-related [*h/E(spl)*] transcription factor (TF) MEGANE (MGN, HELT, HESLIKE) and the proneural TF MASH1 (ASCL1) for the acquisition of MB GABAergic identity. The combination of gain- and loss-of-function experiments in the developing MB led us to the discovery of a novel dorsal/ventral specification mechanism by which MGN and MASH1 induce MB GABAergic identity. Protein–protein interactions are intrinsic in eliciting the function of virtually all basic helix-loop-helix (bHLH) factors. Yet, TFs belonging to the [*h/E(spl)*] and proneural families were always believed to counterpart each other's function. My results suggest a new concept regarding these two critical families of bHLH factors and provide a novel paradigm for how they cooperate for the acquisition of MB GABAergic neuronal identity.

We determined the *in vivo* relevance of their interaction by phenotypic analysis of the *Mgn*/*Mash1* double knockout (dblKO; *Mgn-/-/Mash1-/-*) and compound mice: single mutants (sglMut; *Mgn-/-/Mash1*+/+ or *Mgn*+/+/*Mash1-/-*), double heterozygous mutants (dblHet; *Mgn*+/-/*Mash1*+/-) and mutants with only one active allele of either *Mash1* or *Mgn* (a compound homozygous, heterozygous mutant combination; *Mgn*+/-/*Mash1-/-, Mgn-/-/Mash1*+/-). In this way I show that MB GABAergic neurogenesis depends essentially on these two genes and three mechanisms for the acquisition of MB-GABA fate during the distinct phases of development: i) in the dorsal MB, where the levels of *Mgn* and *Mash1* expression are lower than in the ventrolateral MB, MGN/MASH1 heterodimers formation is a *conditio sine qua non*

condition for GABAergic neurogenesis, ii) in the ventrolateral MB, MGN/MASH1 heterodimers are not essential as GABAergic neurogenesis occurs indistinctly in the presence of MGN and/or MASH1 homodimers in a dose-dependent manner and iii) the GABAn of the SN and VTA in the most ventral MB are independent of either MGN/MASH1 heterodimers or homodimers for their specification.

Additionally, we found that homo- and heterodimers activate essentially the same downstream targets, which are involved in MB GABAergic neurogenesis. Nevertheless, these requirements appear highly region specific: heterodimers can trigger GABAergic markers not only more efficiently than homodimers in the dMB but heterodimers are also required in the ventrolateral MB for the expression of *Tal2* (m5), *Lim1* (m3-4) and *Sox14* (m3-5). This suggests that different GABAergic markers are more sensitive and activated by homodimers (GAD67, GATA2 and TAL1 in the ventrolateral MB) whereas some downstream targets (SOX14, TAL2, GAD67, GATA2 and TAL1) in specific areas require heterodimers.

Similarities and differences in the molecular regulatory mechanistic actions revealed the basis of the GABAergic neurogenesis. Thus, this research not only provides new insights into the molecular generation of GABAn but also about the vast diversity in their development, depending on their origin in the neural tube. Further, it may shed light on GABAn development in other brain areas, when transferring and integrating the mechanism we discovered into known and newly discovered pathways. In summary, it will allow to better understand the development and function of GABAn, thus, providing novel insights into the molecular etiology underlying neurological and psychiatric disorders in which the GABAergic system is disturbed.

3 ZUSAMMENFASSUNG

Neurone mit dem Neurotransmitter Gamma-Aminobuttersäure (GABA) sind die wichtigsten inhibitorischen Neurone des Zentralnervensystems. Auf Störungen in ihrer Entwicklung und Funktion lassen sich schwere neurologische Erkrankungen zurückführen. Um nachvollziehen zu können, wie sich komplexes Verhalten aus einer letztlich begrenzten Anzahl von Genen bedingt, sind Analyse und Verständnis der spezifischen Codes einzelner Gene, deren Proteininteraktionen und die auf Neurotransmitter-Aktionen basierenden Mechanismen einzelner Hirnregionen unerlässlich. Daher ist die Ergründung grundlegender Schritte zu GABA-erger neuronaler Spezifikation essentiell. Das Mittelhirn (im Folgenden mit der englischen Abkürzung MB für midbrain bezeichnet) ist ein wichtiges Integrationszentrum, von dem aus GABA-erge Neurone verschiedenste Aspekte des Verhaltens sowie sensomotorischer und motivatorischer Prozesse steuern. Symptome einer Disfunktion des GABA-ergen Systems im MB manifestieren sich in schweren psychischen Erkrankungen wie Schizophrenie, bipolarer Störung, Epilepsie oder Aufmerksamkeits-Defizit-Hyperaktivitäts-Störung (ADHS). Gleichzeitig sind diese GABA-ergen Interneuronen des MB aber wichtige Angriffspunkte medizinischer Behandlung mit Psychopharmaka und auch Andockstation bewusstseinserweiternder Drogen. In früheren Studien konnten die beiden Helix-Loop-Helix-Transkriptionsfaktoren (bHLH TF) MASH1 (auch bekannt als ACHAETE SCUTE 1; ASCL) und MEGANE (MGN auch bekannt als HELT, HESLIKE) als Schlüsselfaktoren für die Spezifikation von GABA-ergen Neuronen (GABAn) des MB identifiziert werden, da beide Einzel-Mutanten einen sehr ähnlichen Phänotyp für GABAn im MB zeigen. In den Hirnen beider Mutanten produzieren die Neurone im dorsalen Bereich des MB kein GABA, während im ventrolateralen MB, die GABA-erge Neurogenese unverändert bleibt.

Diese Studie belegt die einzigartige, überlappende und synergistische Wechselwirkung zwischen dem *hairy/Enhancer-of-split (*[*h/E(spl)*]) zugehörigen TF MGN und dem proneuralen TF MASH1. Protein-Protein-Wechselwirkungen sind immanent und essentiell für die Auslösung von Funktionen nahezu aller bHLH Faktoren. Die Kombination von *gain-and-loss-of-function* Experimenten während der Entwicklung des MB zeigte kooperierende Rollen der beiden Gene *Mgn* und *Mash1* für die Spezifikation GABA-erger Identität und führte zu der Entdeckung eines neuen dorsal/ventralen Spezifikationsmechanismus, dem GABA-erge Identität zu Grunde liegt. Die Ergebnisse stellen ein neues Konzept auf, in dem die zwei entscheidenden Familien neurogener bHLH Faktoren synergetisch die GABA-erge Neurogenese im MB regulieren. Die *in vivo* Relevanz der Interaktion wurde anhand phänotypischer Analyse jener unterschiedlichen Mausgenotypen aufgezeigt: *Mgn*/*Mash1* Doppel-Knockout Mutanten (dblKO; *Mgn -/- /Mash1-/-*), *Mgn*/*Mash1* Einzelmutanten (sglMut; *Mgn -/- /Mash1+/+* oder *Mgn+/+/Mash1-/-*),

Mgn/*Mash1* doppel-heterozygote Mutanten (dblHet; *Mgn+/-/Mash1+/-*) und Mutanten mit nur einem aktiven Allel von entweder *Mash1* oder *Mgn* (*Mgn+/-/Mash1-/-* oder *Mgn-/-/Mash1+/-*). So konnte ermittelt werden, dass GABA-erge Neurogenese im MB im Wesentlichen von den oben genannten Genen und ihrer Allel-Kombination abhängt. Beide Proteine sind in der Lage, MGN/MASH1 Hetero- / und MGN/MGN bzw. MASH1/MASH1 Homodimere zu bilden, die wiederum verschiedene dorso/ventrale Prozesse zur Induktion von MB GABAn beeinflussen: Im dorsalen MB sind MGN/MASH1 Heterodimere *conditio sine qua non* für die Entstehung von GABAn. Im Gegensatz dazu besteht im ventralen MB keine Notwendigkeit für das Vorhandensein von MGN/MASH1 Heterodimeren, da die GABAn Neurogenese durch Homodimere bzw. in Dosisabhängigkeit der vorhandenen Proteine von MGN oder MASH1 induziert werden kann.

Außerdem wurde festgestellt, dass Homo- und Heterodimere von MGN und MASH1 im Wesentlichen identische an GABA-erger Neurogenese im MB beteiligte Marker-Gene aktivieren: Heterodimere induzieren nicht nur GABA-erge Marker effizienter als Homodimere im dorsalen MB, sondern sind auch im ventralen MB für die Expression von *Tal2* (m5) , *Lim1* (m3-4) und *Sox14* (m3-5) notwendig. Dies deutet darauf hin, dass bestimmte GABA-erge Marker-Gene leichter auf Homodimere reagieren und von diesen aktiviert werden (*Gad65/67, Gata2* und *Tal1* im ventralen MB), während wiederum andere Marker-Gene (*Sox14, Tal2, Gad67*, *Gata2* und *Tal1*) in partiellen Bereichen Heterodimere erfordern. Nichtsdestotrotz sind diese Abhängigkeiten äußerst ortsspezifisch.

TF, die den *Enhancer-of-split* verwandten und proneuralen Familien zugewiesen werden, galten lange als Gegenspieler. Diese Arbeit beweist jedoch, dass diese beiden Familien auch zusammenwirken können und stellt ein neues Paradigma auf, wie TF dieser Familien für die Entstehung von GABA-erger neuronaler Identität kooperieren. Gemeinsamkeiten sowie Unterschiede in molekular-regulatorischen mechanistischen Vorgängen zeigen sowohl die Gemeinsamkeiten in GABA-erger Neurogenese in einzelnen Gehirnregionen als auch die enorme Diversität dieser Neurone. Diese Ergebnisse tragen dazu bei, die mechanistischen Vorgänge der Neurogenese auf andere Hirnbereiche übertragen zu können. Zudem ermöglichen sie es uns, GABAerge Neurogenese im Allgemeinen besser zu verstehen und somit auch ein besseres Verständnis der Ätiologie psychiatrischer Störungen auf Basis misregulierter GABA-erger Systeme zu schaffen.

4 REVIEW OF LITERATURE

4.1 THE NEUROTRANSMITTER γ-AMINOBUTYRIC ACID

Already in the early 1950s, gamma-aminobutyric acid (γ-Aminobutyric acid; GABA) was identified in studies of free amino acids by paper chromatography in various neural and neoplastic tissues in several species of animals (Awapara *et al.*, 1950) and it was shown that nearly all organisms, ranging from bacteria to humans can synthesize GABA (Elliott and Jasper, 1959). During the next decade, GABA was discovered to act as an inhibitory neurotransmitter since extracts from mammalian brains were able to block impulse generation in crayfish stretch receptor neurons (Elliott and Florey, 1956) and topically applied solutions of GABA exerted inhibitory effects on electrical activity in the brain (Hayashi and Nagai, 1956). Along research, GABA was identified as the main inhibitory neurotransmitter in the adult mammalian central nervous system (CNS) and to comprise about 1/3 of the entire neurotransmitter content. GABAergic neurotransmission plays a pivotal role in the CNS as it regulates and balances excitatory network activity and is involved in diverse neural functions ranging from development and neural plasticity to the control of motor behavior and emotions. The high specificity of GABA function in the nervous system (NS) is achieved, in part, by structural and neurochemical heterogeneity of GABAergic neurons (GABAn) and a variety of GABA receptors (GABA-R). Due to the ubiquity and crucial function of GABA and its receptors in the immature as well as in the mature brain, perturbations in GABAergic transmission have the potential to result in severe psychiatric and neurological disturbances, like bipolar disorders, attention deficit hyperactivity disorder (ADHD), autism as well as addiction and anxiety. Additionally, various commercially available pharmaceuticals and addictive drugs, such as sedatives, anxiolytics, benzodiazepines and alcohol exert their function via the GABAergic system.

4.1.1 Two enzymes for the synthesis of GABA

GABA is synthesized from glutamate in a reaction catalyzed by two isoforms of glutamic acid decarboxylase (GAD); GAD1 (GAD67) and GAD2 (GAD65) (Roberts and Frankel, 1950). Their name derive from their approximate molecular weights of 65.4 kilo Dalton (kDA) for GAD65 and 66.6 kDA for GAD67 (Erlander *et al*., 1991). Despite their common function, they are encoded by two genes and differ in their amino acid sequence, cellular and subcellular location and interaction with the GAD cofactor pyridoxl-5'-phosphate (Soghomonian and Martin, 1998). Further, the *Gad67* gene is extensively regulated at the level of transcription: ten alternatively spliced isoforms were identified. Isoforms 1/2 that are translated into the full length, enzymatically active Gad67 protein, while isoforms 3-10 are responsible for

the production of a short, enzymatically inactive peptide with unknown function and molecular weight of 25kDa (GAD25-1 and GAD25-2) (Szabo *et al.,* 1994, Bond *et al*., 1990). Although the majority of GABA-containing neurons in the brain coexpress the two genes expressing *Gad65/67* isoforms, and both enzymes are found in membrane and soluble fractions of the brain (Dirkx *et al.,* 1995), each *Gad* mRNA isoform is very heterogeneous at both, the regional and cellular level. These differences in subcellular localization imply that the spatial segregation of both enzymes in different intracellular compartments has functional different purposes: the preferential distribution of GAD65 in axon terminals, its association with membranes and apparent vesicular localization suggest an involvement preferentially in the synthesis and release of vesicular GABA. The cytoplasmic localization of GAD67 in contrast, indicates that GAD67 is involved mainly in non-vesicular GABA release and therefore in the synthesis of GABA, readily available for metabolism and for general metabolic activity (Esclapez *et al*., 1994). There is evidence, that GAD67 is responsible for the major synthesis of GABA although GAD65 appears to be at least as abundant as GAD67; GABA and GAD67 levels show a reduction of 13% in *Gad65* knockout mice, whereas in *Gad67* knockout mice, total GABA activity and GABA contents are significantly reduced down to 7%, - although GAD65 levels are normal (Asada *et al.*, 1996, Asada *et al.*, 1997). This indicates that GAD65 cannot fully compensate for the loss of GAD67. Further, GABA provided by GAD67 may additionally be able to support normal intercellular signaling, including synaptic transmission, as *Gad65* mutant mice do not show major behavioral deficits (Asada *et al*., 1996).

Their contrasting role in major GABA synthesis may be explained by their different responsiveness to their cofactor pyridoxal-5′-phosphate (pyridoxal-P), which regulates the activation of the holoenzyme GAD, regulating the short-term regulation of GAD activity (Battaglioli *et al.*, 2003, Porter *et al.*, 1985). Pyridoxal-5'-phospate activates apoGAD in a two-step process involving a rapid, reversible association of the co-factor with the enzyme. This apoenzyme is produced by an alternative-transamination reaction catalyzed by GAD by which the normally bound pyridoxal-phosphate is catalyzed to pyridoxamine-5′-phosphate, which subsequently dissociates leaving inactive apoGAD. In turn, ApoGAD can re-form holoGAD by combining with free pyridoxal-P in case of presence. At least 50% of GAD is present in brain as apoenzyme (GAD without bound cofactor; apoGAD), serving as reservoir of inactive GAD for eventual GABA synthesis. HoloGAD65 is converted to apoenzyme about 15 times faster than is holoGAD67, and apoGAD65 can be activated by pyridoxal-P more than 10 times faster than GAD67 (Battaglioli *et al.*, 2003). ApoGAD65 accounts a substantial majority in the brain in neurons. Further, GAD65 is found mainly in synaptic endings while GAD67 is more evenly distributed all over the cell (Esclapez *et al.*, 1994). This suggests, that GAD65 is specialized to respond to short-term changes in demand for transmitter while GAD67 accounts for constant levels of GABA in GABAn (Martin and Rimvall, 1993).

4.1.2 GABAergic signaling

GABAn are found in all regions of the CNS, although, depending on their location, they differ extensively in morphology, neurochemical composition, synaptic connectivity and gene expression profile (Kawaguchi and Kubota, 1997). In general, information processing in the NS occurs along signaling junctions (synapses) between two neurons by the passage of an electrical or chemical signal from the presynapse (the nerve ending that releases signaling molecules) to the postsynapse (the nerve ending that contains receptors for the signaling molecules). Synapses can be distinguished into two fundamentally different types: chemical synapses and electrical synapses. In a chemical synapse, electrical activity and following activation of voltage-gated calcium (Ca^{2+}) channels in the presynaptic neuron is converted into the release of chemical signaling molecules (neurotransmitters), which either excite or inhibit the postsynaptic neuron. By binding to postsynaptic receptors, the neurotransmitter initiates an electrical response - either directly (ionotropic; ligand-gated ion channels) or via a secondary messenger pathway (metabotropic; G-protein-coupled receptors) - and excites or inhibits the postsynaptic neuron. Electrical synapses consist of presynaptic and postsynaptic cell membranes connected by gab junctions, capable to pass the electrical stimulus directly and thereby act much faster than chemical synapses. Notably, neuromodulators as monoamines and peptides as DOPAMIN (TH), SEROTONIN (5-HT), ACETYLCHOLINE (ACh), ENDORPHINES, SUBSTANCE P, etc. can also exert a transmission modulating function via chemical synapses. Thereby they influence larger areas simultaneously as they act more diffusely on more than one synapse. Neuromodulators act on the postsynapse mostly via G-protein coupled receptors and act on a much longer time scale (LeVine, 1999). After synthesis of GABA in the neuron, GABA is loaded into synaptic vesicles by a vesicular neurotransmitter transporter VGAT (Fon and Edwards, 2001). Upon nerve stimulation, GABA is liberated from them by Ca^{2+}-dependent exocytosis into the synaptic cleft. Notably, non-vesicular forms of GABA secretion (for example, by reverse transporter action) have also been described and might particularly be important during development (Attwell *et al*., 1993). In principal, GABA mediated signaling lowers the electrochemical potential of the postsynaptic cell, harboring the receptor, thereby making the postsynaptic neuron less likely to “fire” and therefore inhibiting signal transduction. Postsynaptically, the effect of GABA can be mediated by the activation of both, ionotropic or metabotropic receptors, which can be localized pre- and postsynaptically (Figure 4.1). Three types of GABA-R have been identified on the basis of their pharmacological and electrophysiological properties. Fast responses are mediated by ionotropic $GABA_A$-R and their pharmacological variants $GABA_A$-rho-R, whereas slow responses are mediated by metabotropic $GABA_B$-R (Bormann, 1988, Kaila, 1994). $GABA_A$-R are activated by GABA binding, which induces conformational change in the hetero-pentameric, membrane spanning channel protein that allow a net inward or outward flow of ions through its pore - depending on the electrochemical gradient of the permeant ion (mainly chloride; Cl^-). By contrast, $GABA_B$-R couple to Ca^{2+} and potassium (K^+) channels

via G-proteins and second messenger systems (Bowery, 1989, Bowery *et al.*, 1980, Nicoll, 1988); presynaptical inhibition via $GABA_B$-R occurs through a $GABA_B$-receptor-mediated reduction in Ca^{2+} current and a subsequent reduction in transmitter release, whereas postsynaptical inhibition via $GABA_B$-R occurs by activation of K^+ currents that hyperpolarize the neuron (Bormann, 1988). Termination of GABA signaling ensues by reuptake into nerve terminals and into surrounding glial cells by four highly homologous plasma-membrane GABA transporters (GAT-1, GAT-2, GAT-3, and BGT-1; (Borden, 1996)). GAT1 (expressed in GABAergic nerve terminals) and GAT3 (mostly expressed in astrocytes) are the major GABA transporters in the brain (Melone *et al*., 2005), while GAT-2 and BGT-1 are primarily expressed in the liver and kidney. Subsequent, the catabolism of GABA, in both, neurons and glia (Parviz *et al*., 2014) - depends on the action of GABA transaminase enzyme (GABA-T) and succinate semialdehyde dehydrogenase enzyme (SSADH), which convert GABA into intermediates of the Krebs cycle and substrates for new production of glutamate. As in glia cells, GABA cannot be resynthesized due to the lack of GAD, glutamine is transferred back to the neuron where GABA is processed by GAD (Roberts and Frankel, 1950). GABA transporters further regulate GABA spillover to neighboring synapses and maintain GABA homeostasis to prevent excessive activation (Borden, 1996).

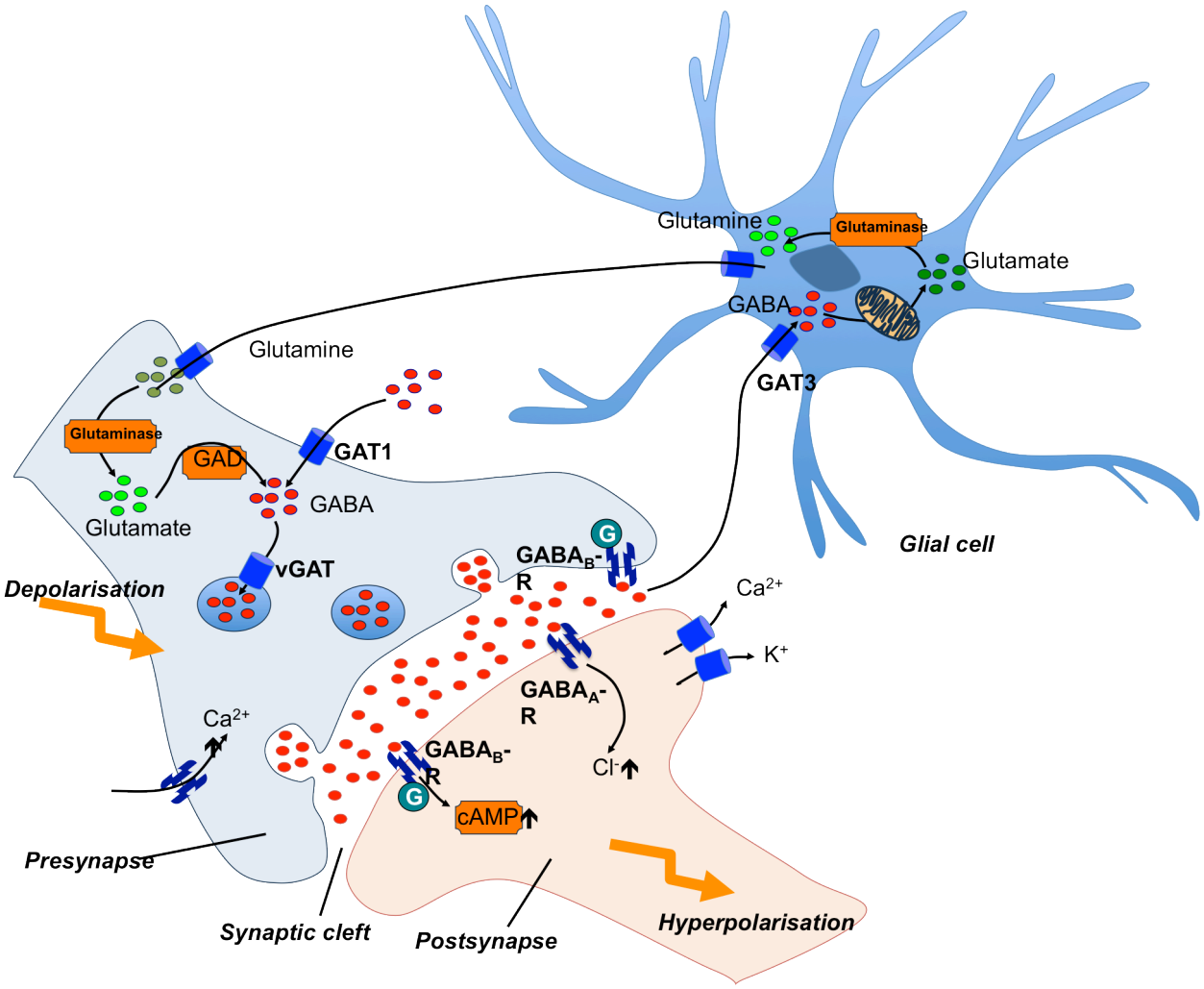

Figure 4.1: The GABAergic transmission system.
GABA is catalyzed from glutamate by GAD and transported into vesicles. Upon stimulation of the presynaptic neuron and subsequent Ca^{2+} influx, the vesicles merge with the presynaptic membrane and GABA is liberated into the synaptic cleft. GABA binds to $GABA_A$-R or $GABA_B$-R which are located post- and presynaptically. $GABA_A$-R stimulation increases its permeability for Cl^-, and Cl^- influx hyperpolarizes the postsynapse. This is supported by postsynaptical Ca^{2+} and K^+ efflux through voltage gated channels. $GABA_B$-R are G-protein coupled; postsynaptically, they trigger K^+ efflux and inhibit Ca^{2+} influx which provokes hyperpolarisation, while located at the presynapse, they inhibit Ca^{2+} influx which reduces transmitter liberation. Exceeding GABA is taken up either back into the presynapse by GAT1 or into glial cells mainly by GAT3, where it is processed via Krebs cycle to glutamate and glutamine and transported back to the GABAergic neuron. There, it is recycled to GABA by glutaminase and GAD for further metabolic activity or signal transmission. *Adopted from A&D systems*

4.1.3 GABA signaling in the immature brain

In contrast to the adult brain, GABA exerts an excitatory effect on developing neurons; over a certain period of development there is a switch of the electrophysiological (depolarization to hyperpolarization) properties. GABAergic transmission, excitatory versus inhibitory, is determined primarily by the intra- and extracellular concentrations of Cl^-, defining its electrochemical gradient along the membrane. The intracellular Cl^- concentration in the developing brain is higher than in mature neurons due to expression disparity of two membrane bound Cl^--transporters (Ben-Ari *et al*., 1989, Serafini *et al.,* 1995, Lu *et al.*, 1999); In immature neurons the Na^+-K^+-2Cl^--cotransporter 1 (NKCC1), which transports negative Cl^- ions into the cell predominates, with a yet only small amount of Cl^- extrusion by the K^+-Cl^--cotransporter 2 (KCC2) (Khirug *et al*., 2008, Lu *et al.,* 1999). This drives the membrane potential below the resting potential of mainly -65mV of adult neurons. Subsequent binding of GABA into GABA-A receptors allows efflux of Cl^- ions down their concentration gradient, leading to the depolarization of the cell (Figure 4.2). During the first two postnatal weeks (in rats), KCC2 expression increases while NKCC1 becomes downregulated (Rivera *et al.*, 1999). This results in a shift to a lower intracellular Cl^- concentration, which rises the resting potential toward ca. -65mV. As the neurons acquire more mature membrane properties, GABA-R activation leads to Cl^- influx, hyperpolarisation and inhibition of signal transduction. Further, the GABAergic depolarization acts in synergy with a transient N-methyl-d-aspartate (NMDA) receptor-mediated and voltage-gated Ca^{2+} currents: this enhances intracellular Ca^{2+} (Connor *et al*., 1987, Yuste and Katz, 1991) exerting widespread trophic effects on maturation of the NS, as promoting neuronal survival and differentiation (LoTurco *et al.*, 1995, Ikeda *et al*., 1997) well as forming, stabilizing, and strengthening synaptic connections (LoTurco *et al.*, 1995, Nguyen *et al.*, 2003, Kneussel and Betz, 2000). Further, GABA has a motogenic effect as chemo-attractant in the cortex for tangentially migrating interneurons (Behar *et al.,* 1996) and regulates synaptogenesis in immature neurons, activity dependent glutamatergic synapse and dendritic spine formation, and also final circuit formation (Ben-Ari *et al.*, 1989, Ben-Ari *et al.*, 2007, Wang and Kriegstein, 2009, Huang, 2009).

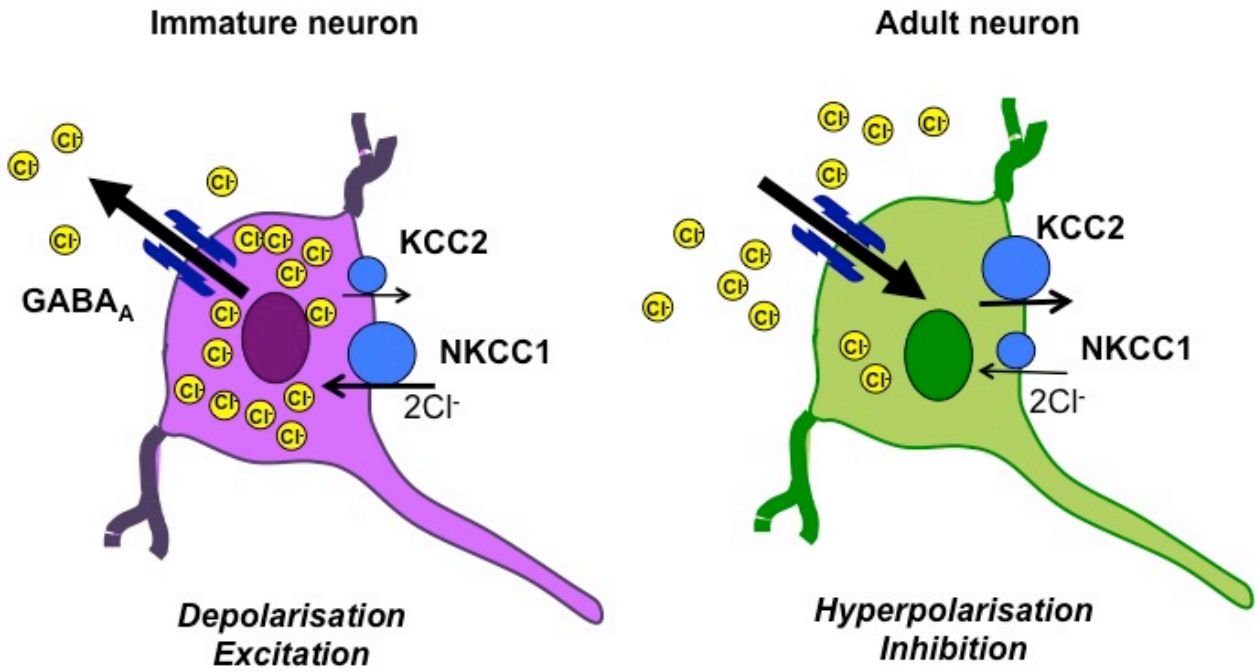

Figure 4.2: Immature GABAn are excitatory while adult GABAn are inhibitory.
Schematic diagram of the alterations of Cl^- concentration levels during development, due to opposite actions of Cl^- co-transporters, which alters the polarity of the actions of GABA. In immature neurons the intracellular Cl^- levels are higher than adult neurons, due to the initially poorly active Cl^- exporter KCC2 and the higly active NKCC1 importer. This leads to a high intracellular Cl^- concentration: GABA-R activation provokes Cl^- efflux, which depolarizes and excites the immature neuron. In adult neurons the Cl^- exporter KCC2 is more active and intracellular Cl^- decreases. Therefore, GABA activation provokes Cl^- influx down to the concentration gradient and inhibits adult neurons. Adopted from (Ben-Ari, 2014).

4.2 DEVELOPMENT OF THE VERTEBRATE CNS

The CNS is one of the first systems to develop during embryogenesis and the last to be completed. It is the most complex system of all organ systems in the animal embryo and consists of an enormous amount and variety of neurons and glial cells, creating the neural network that makes up the functioning NS and body. Despite the differences in morphology, expression pattern, electrical and chemical properties of distinct neural subtypes and the complexity of the CNS itself, all cells of it derive from one primordial neuroepithelium. The formation of the CNS is initiated at a very early stage of development, the gastrula stage; in complex and precisely timed and coordinated series of events a group of ectodermal cells allocates as precursors of the entire NS. Further, this process is orchestrated by the expression of thousands of genes (Hemmati-Brivanlou and Melton, 1997). Functional or structural abnormalities during the early phase of development lead to severe neurological disorders as paralysis, muscle weakness, poor coordination, loss of sensation, seizures, confusion, pain and altered levels of consciousness or even premature death.

4.2.1 Neural induction

Development of the brain starts during gastrulation when the bilaminar embryonic disc undergoes an epithelial-mesenchymal transformation and reorganization to form a trilamiar disc, containing the three primary germ layers. The bilaminar disc is formed during blastula stage and consists of two layers of different cell types (Dyce *et al.*, 1987, Fleming, 1987). The upper layer, called the epiblast and the lower layer, called the hypoblast. The appearance of the so called primitive streak marks the beginning of gastrulation the first antero-posterior (A/P) axis of the mammalian embryo: the primitive streak is formed as epiblast cells converge on the posterior end of the disc, move under the surface and condense. Proliferating cells of the epiblast migrate through the streak to spread out laterally and anteriorly between epiblast and surface below, to give a layer of prospective mesoderm. The migrating cells of the epiblast, detach from their neighbors, and migrate forward through the streak as individual cells (Burdsal *et al.,* 1993) but also spread laterally. This induces the formation of the three germ layers - the ectoderm, the mesoderm, and the endoderm (Figure 4.3). Endoderm, the most internal germ layer, gives rise to the lining of the gut and other internal organs. Ectoderm, the most exterior germ layer, forms skin, brain, the NS, and other external tissues. Mesoderm, the middle germ layer, forms muscle, the skeletal system, and the circulatory system. Some migrating cells give rise to the notochord, which is a temporary, rod-like structure that develops along the dorsal surface of the embryo. It is the defining structure of chordates and of the early embryo of vertebrates. With its positions centrally in the embryo, the notochord maintains the dorsal-ventral (D/V) polarity by induction of specific D/V patterns of gene expression in the surrounding

tissue (Lee and Anderson, 2008, Meinhardt, 2001, Gerhart, 2001, Cleaver and Krieg, 2001). These signals from the notochord and the mesoderm induce the ectodermal cells above them to elongate into columnar neural plate cells (Smith and Schoenwolf, 1989, Keller *et al.*, 1992). The ectoderm of the plate is called neuroectoderm and will give rise to the brain and spinal cord by a process called neurulation: as the neural plate lengthens along the A/P axis, it deepens at the center creating the neuronal groove, bends on both sides by neuronal fold, and fuses at the dorsal midline to create a cylindrical-shaped neural tube (reviewed by (Stern, 2005, Vieira *et al*., 2010, Saxen, 1989). Closure begins in the middle of the embryo and progresses toward both cephalic and caudal ends. As the neural tube seals dorsally completely, the posterior end of the neural tube closes and the tube starts growing in size and length. Neuroectodermal cells at the lateral edges of the neural plate do not become part of the tube. They form the neural crest cells over the neural tube (Nichols, 1981), which give rise to a wide variety of cell types including peripheral and enteric neurons and glia, craniofacial cartilage and bone, smooth muscle, and pigment cells (reviewed in (Huang and Saint-Jeannet, 2004).

4.2.1.1 Patterning of the neural tube

During and after gastrulation, the vertebrate embryo becomes pattered along the A/P and the D/V axes. Combinatorial graded signals from various regions of the embryo induce regionally restricted expression of specific TFs that give the cells unique identities depending on their exact position in the neural tube. It further gives local competence to the cells to form secondary organizers further defining the A/P specification of different neural territories. These signaling centers contain specific cells and typically border two different brain compartments and instruct the regional differentiation of the flanking tissue (Echevarria *et al*., 2003). The regional patterning thereby is determined by morphogenic activity and the subsequent combinatorial expression of TFs triggering positive and negative feedback loops (Echevarria *et al*., 2003), refining the A/P specification of three main domains in the brain primordium; the prosencephalon also called forebrain (FB), the mesencephalon also called midbrain (MB) and the rhombencephalon also called hindbrain (HB) (Rubenstein *et al*., 1998). Further, this morphogenetic activity of secondary organizers controls polarity and generation of neural sub-regions inside these main regions (Crossley *et al*., 1996, Martinez and Puelles, 2000, Shimamura *et al*., 1995, Vieira *et al.,* 2010).

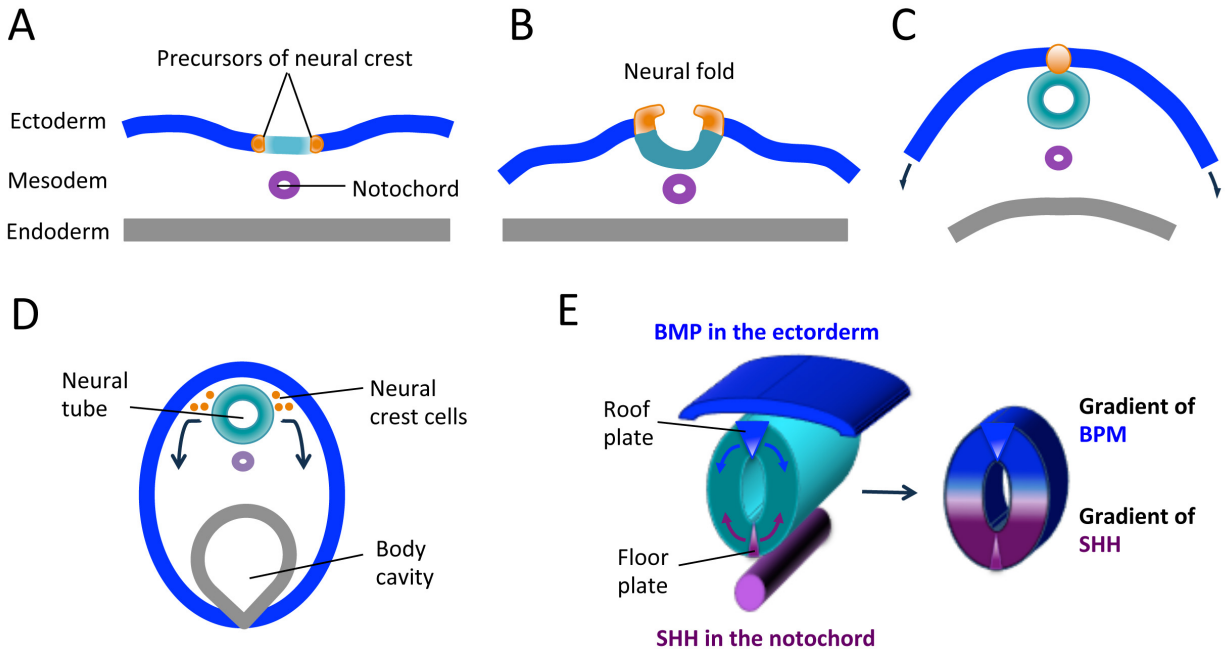

Figure 4.3: Neurulation and induction of the floor plate (FP) and roof plate (RP).
(A) Cells within the mesoderm form the notochord. Sonic hedgehog (SHH) signaling from the notochord triggers neuroectodermal tissue above it to differentiate from the ectoderm and to thicken into the neural plate. Precursors of the neural crest at the plate border separate the ectoderm from the neural plate. **(B)** The neural plate folds inward, forming neural folds. The folds gradually become elevated forming the neural groove. **(C)** The grove coalesces in the middle line, forming the neural tube. **(D)** Neural crest cells undergo an epithelial to mesenchymal transition, separate from the neural tube and migrate to become a variety of different cells like melanozytes, craniofacial cartilage and bone, smooth muscle, peripheral and enteric neurons and glia. **(E)** SHH signaling from the notochord induces the FP, which then secretes SHH as essential ventral morphogen. The dorsal epidermal ectoderm is a source of BONE MORPHOGENIC PROTEINS (BMPs) that induce the formation of the RP in the neural tube, secreting dorsalizing morphogens as BMPs, DORSALIN and ACTIVIN.

4.2.1.2 A/P patterning of the brain

The A/P axis of CNS is generated in the early neural plate stage during gastrulation by morphogenic gradients from adjacent non-neuronal tissue. The molecular graded interplay of FIBROBLAST GROW FACTORS (FGFs), WINGLESS-RELATED (WNT) and BONE MORPHOGENIC PROTEINS (BMPs) inhibitors instruct cells of the neural tube to adopt specific identities along the A/P axis which is the first to define head and tail structures (Vieira *et al.*, 2010, Nordstrom *et al.*, 2002). Further specification and region specificity of neural precursors at distinct transverse domains at different axial positions is acquired by the secondary organizers (reviewed in (Vieira *et al.*, 2010). Such three signaling centers in the developing neural tube can be found: anterior neural ridge (ANR), Zona Limitans Intrathalamica (ZLI) and Isthmic Organizer (IsO). The ANR lies where the most anterior neural tissue meets the non neural ectoderm forming a smile-shaped junction marked by FGF8. It secretes signaling molecules (mainly WNT

inhibitors and FGF (Nordstrom *et al*., 2002, Houart *et al*., 2002) that generate the A/P patterning of the presumptive FB. The FB is transversally divided into two segments; secondary prosencephalon including telencephalon and diencephalon. Latter is subdivided into three segments called prosomeres, (p1: pretectum; p2: thalamus and p3: prethalamus (Puelles *et al*., 2013). Between p2 and p3, the ZLI further regulates patterning of both segments by secretion of SHH, FGF and WNTS (Garcia-Lopez *et al.*, 2004, Scholpp and Lumsden, 2010, Martinez and Puelles, 2000). Already during gastrulation, the early epiblast region is separated into anterior and posterior by the expression domains of the homeodomain (HD) TFs OTX2 and GBX2; *Otx2* is expressed in the anterior region of the mouse embryo in all three germ layers while Gbx2 is expressed throughout all germ layers in the posterior part of the embryo. This pattern defines the MB and the HB; subsequently approach of the posterior and anterior expression borders of *Otx2* and *Gbx2* ultimately defines the mid-hindbrain boundary (MHB) (Acampora *et al.*, 2001). After neural induction, *Otx2* defines the MB and *Gbx2* the anterior HB (rhombomer 1; r1 (Garda et al., 2001, Millet *et al.,* 1999): The repressive interaction between them creates a sharp boundary at the MHB and positions the IsO responsible for encoding MB and HB fate (Hidalgo-Sanchez *et al*., 1999, Millet *et al*., 1999, Acampora *et al*., 2001, Broccoli *et al.,* 1999). Along maturation, the MB is further defined into M1 and M2 and the HB into the isthmus and seven rhombomeres (r1-r7) and three pseudorohombomeres (r8-11); the IsO secretes multiple intercellular signaling molecules, such as WNT and FGF8, which are expressed in the adjacent regions of posterior MB and anterior HB, respectively. The graded signaling controls the expression of several HD TFs defining MB and HB; the neural tube region where *Otx2, Pax2*, and *En1* are expressed, acquires MB identity and *Pax3/7* forces the MB to further differentiate into the tectum. FGF8 signal from the isthmus activates a RAS-ERK signaling pathway to organize the cerebellum (Figure 4.4) (Nakamura *et al.,* 2005, Prakash and Wurst, 2004, Crossley *et al.,* 1996, Hidalgo-Sanchez *et al.*, 2005, Scholpp *et al*., 2003, Wurst and Bally-Cuif, 2001).

4.2.1.3 D/V patterning of the developing brain

D/V patterning begins during neurulation. The notochord is a source of *sonic hedgehog* (*Shh*) that induces a floor plate (FP) at the ventral midline of the neural tube. The FP as a secondary signaling center subsequently secretes SHH that is the essential ventral morphogen. The dorsal epidermal ectoderm (initially at the lateral edge of the neural plate) is a source of BMPs that induce the formation of the roof plate (RF) in the neural tube. Dorsalizing morphogens that includes several members of the TGFβ family of growth factors (BMPs, DORSALIN, ACTIVIN) counteract the ventral morphogen gradient of SHH. This creates different domains along the V/D axis of neural tube: the ventral FP, basal plate (BP) and alar plate (AP) and dorsal RF. In these domains, the counteracting of ventral and dorsal morphogenic signaling

is translated into a HD TF code that defines, specifies and positions distinct progenitor populations (Briscoe *et al.,* 2000, Nakatani *et al*., 2007, Balaskas *et al.*, 2012, Wurst and Bally-Cuif, 2001).

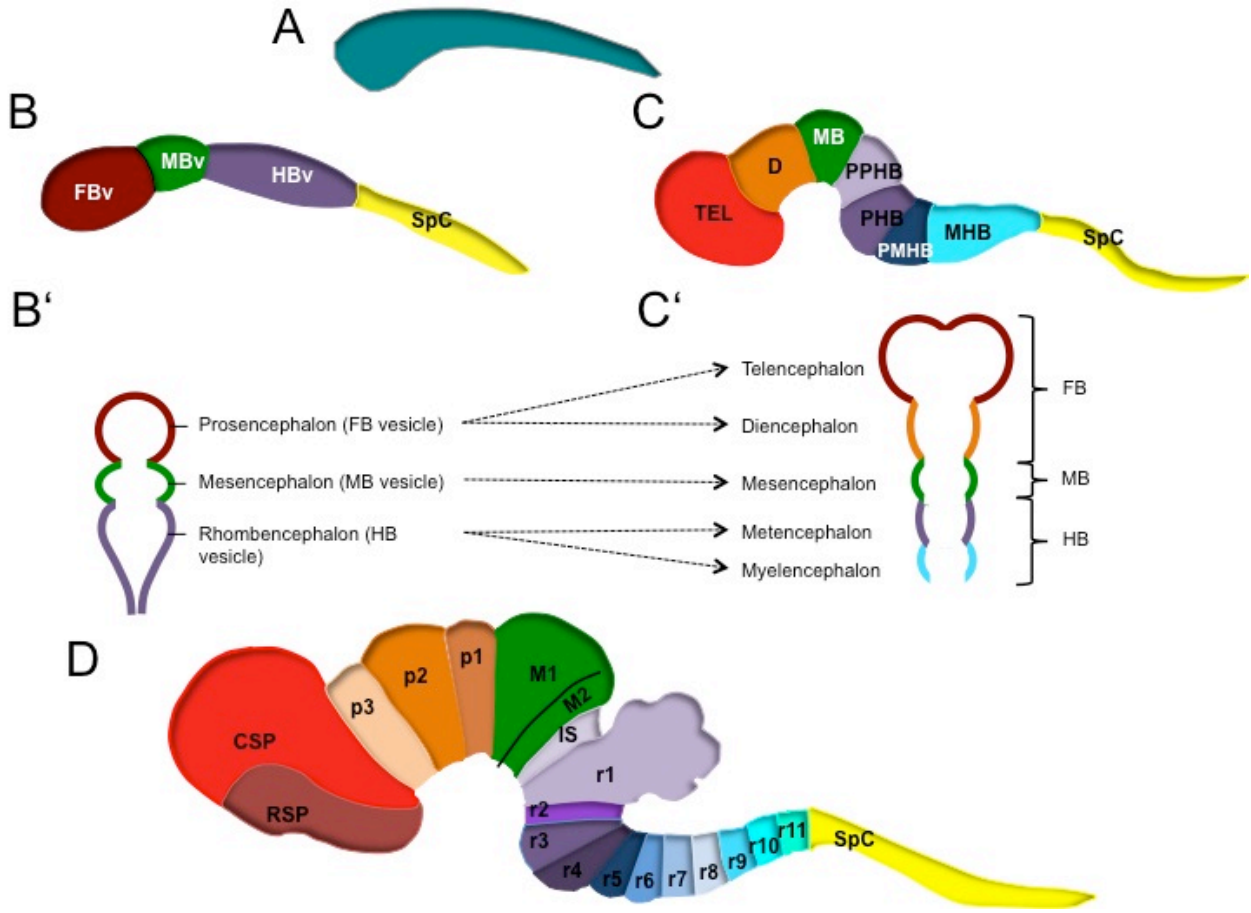

Figure 4.4: Development of the mouse brain.
(A) The neural tube has no subdivisions and bulges into **(B)** the vesicles (v) of the rostral FB (prosencephalon; FBv), the MB (mesencephalon; MBv) and HB (rhomben-cephalon; HBv), with the developing spinal cord (SpC). **(C)** The FBv divides into two divisions, the telencephalon (TEL) and the diencephalon **(D)**, the HBv is divided into four regions: prepontine hindbrain (PPH), pontine hindbrain (PH), the pontomedullary hindbrain (PMH), and the medullary hindbrain (MH). **(B`, C')** The three earliest brain vesicles give rise to the adult brain structures: telencephalon, diencephalon, mesencephalon, metencephalon and myelincephalon comprising forebrain (FB), midbrain (MB), and hindbrain (HB)**. (D)** The FB is further subdivided into caudal (CSP) and rostral (RSP) secondary prosencephalon and prosomeres 1–3 of the diencephalon (p1, p2, p3). The MB is divided into mesomere 1 and 2 (M1 and M2), the HB into isthmus (IS) and rhombomeres 1–11 (r1 to r11). Adopted from (Puelles *et al.*, 2013)

4.3 DIFFERENTIATION OF NEURONS IN THE BRAIN

During the development of the NS, neural precursors proliferate and give rise to neurons and glial cells through processes known as neurogenesis and gliogenesis, respectively. During neurogenesis, the generation of distinct brain parts and functional nuclei depends on the proliferation of progenitor cells and their subsequent differentiation into diverse neuronal cell types. This precisely timed process determines choice of cell fate, leading to the genesis of neuronal subpopulations and CNS with the correct size, shape and cell composition. Subsequent to the patterning process, division of the neural primordium into distinct domains and allocation of positional identity - essentially by HD, generation of neuronal progenitors and development of neural lineages is initiated mainly by two families: the *hairy*/*Enhancer of split*-related [*h/E(spl)*] and proneural genes, which both encode TFs of the basic helix-loop-helix (bHLH) class.

4.3.1 Coordination of neuronal fate: regulation of neurogenesis

The number of times which neuroepithelial cells in the wall of the neuronal tube re-enter the cell cycle and the precise control of the cell number generated during neurogenesis ensure correct organization, size and function of the mature brain later on. The number of generated cells depends on the type of progenitor domains during brain development and their regional position along the neural tube. Multipotent progenitors residing in the ventricular zone (VZ) predominantly undergo symmetrical and assymetrical proliferative divisions. Symmetrical proliferative divisions generate two identical self-renewing progenitor cells. By following asymmetric neurogenic division, the cell creates a copy of the earlier divided progenitor and a progeny of a more differentiated, postmitotic precursor which fraction increases as neurogenesis proceeds (Caviness *et al.*, 2000). As development advances, neuroepithelial cells gradually change to radial glial cells, which display similar properties to embryonic neuronal stem cells and have their cell body in the ventricular zone (VZ) and the radial fiber reaching the pial surface. Radial glial cells lead to many different types of neurons. Repeated asymmetric cell division generates one new radial glial cell and one neuron or neural precursor, which will migrate along the radial fibers to the outer layers. Simultaneously, radial glial cells differentiate into astrocytes (Hatakeyama *et al.*, 2004). During development, the neuroepithelium turns into a multilayered (in the MB one-two layers) structure where different cell types can be distinguished according to their specific molecular and cellular expression markers. When postmitotic precursors move out of the VZ towards the mantle zone (MZ), they undergo terminal differentiation and subsequently migrate to their final positions where they establish contacts with their targets.

4.3.2 NOTCH-signaling and lateral inhibition

The balance between self-renewal and differentiation is under stringent control to allow proper development and avoid uncontrolled growth. The process of neurogenesis implies the production of different neuronal types of cells in adequate number and position and the simultaneous maintenance of the stem cell pool. This is acquired by [*h/E(spl)*], proneural genes and the DELTA-NOTCH signaling pathway, which actively participate to determine and to coordinate the accuracy of the neurogenesis process (Kageyama and Nakanishi, 1997).

Neuronal progenitors equivalently express proneural genes, which, while driving neuronal differentiation, also activate the NOTCH signaling pathway in neighboring progenitors. This process is called lateral inhibition, which allows only subsets of cells to differentiate into neurons while keeping others as neural stem cells (Louvi and Artavanis-Tsakonas, 2006). Proneural factors directly activate the transcription of NOTCH ligands such as DELTA-like (DLL1 and JAGGED in mammals) (Castro *et al*., 2006). The NOTCH receptor and its ligands are transmembrane proteins with large extracellular domains. Ligand binding of DLL on NOTCH on neighboring cells triggers proteolytic cleavages of NOTCH which result in the release of the NOTCH intracellular domain (NICD) and its translocation to the nucleus (Weinmaster, 2000). In the nucleus, NICD forms a complex with the DNA (desoxyribonucleic acid)-binding protein RBPj and additional coactivators (Honjo, 1996). The major direct targets of this complex include the bHLH transcriptional repressors of the *Hes* family members *Hes1* and *Hes5* (Ohtsuka *et al.*, 1999). Latters bind directly to the promoters of proneural genes. Thus, these cells, which express higher levels of HES, downregulate the expression of the proneural genes *Mash1* (*Achaete-Scute homolog 1*; *Ascl1*) and *Neurogenin 1-3 (Ngn1-3)* and *Dll1* which inhibit neuronal differentiation and keep the cell in a "stem cell" state (Bertrand *et al*., 2002, Kageyama *et al*., 2007). HES1 and HES5 also repress the expression of DLL1. Consequently, the surrounding cells are less affected by NOTCH signaling. Consequently these cells express less HES and again upregulate the expression of proneural genes (Castro *et al.*, 2006, Henrique *et al*., 1997), which in turn enhance expression of DLL1 (Kunisch *et al*., 1994). By this loop, lateral inhibition amplifies the variations in progenitor state between the neighboring cells until subsets of cells express proneural genes and *Dll1* genes at such high levels that they start to differentiate into postmitotic neurons. Concurrently, the surrounding cells display strong expression of NOTCH and upregulated expression of *Hes* genes and remain as neural progenitors. Thus, proneural genes are both, regulators and regulated by the NOTCH signaling pathway. The looping signaling pathway with the major targets, the *Hes* genes, creates a network, which functions parallel to the differentiation program to keep adjacent cells undifferentiated and prevents simultaneous differentiation of all progenitors, ensuring that an appropriate number is maintained during embryonic development (Figure 4.5).

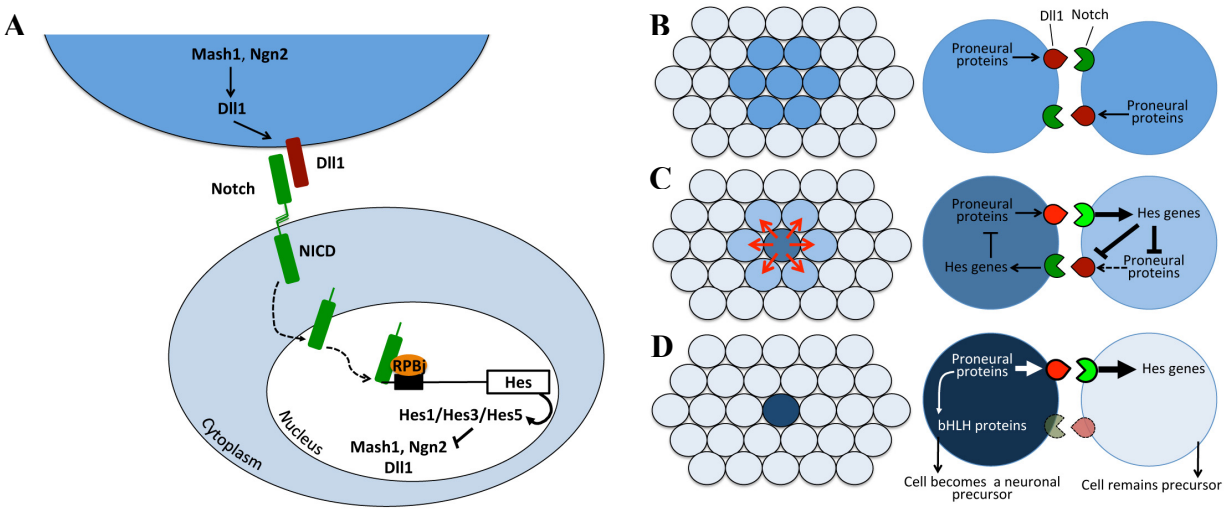

Figure 4.5: (A) The core pathway of *Notch* signaling.
Proneural genes as *Mash1* and *Ngn2* activate the neuronal differentiation program and are direct activators of DLL1, resulting in mutual activation of NOTCH signaling in neighboring progenitors. Upon activation of Notch, the intracellular domain (NICD) is released from the transmembrane portion and transferred to the nucleus, where the NICD forms a complex with the DNA-binding protein RBPj. This NICD-RBPj complex induces expression of transcriptional repressor genes as *Hes1* and *Hes5*. HES1 and HES5 then repress expression of proneural genes and DLL1. Adopted from (Kageyama *et al*., 2009)
(B-D) Lateral inhibition. **(B)** Proneural gene expression and NOTCH signaling between cells is initially similar in the proneural region of the ectoderm. **(C)** Proneural factors in one cell (left cells) directly activate the transcription of the NOTCH ligand. DLL1 thus activates NOTCH to a higher level in the neighboring cell (right cell), which represses the expression of proneural genes and DLL1 via the expression of the major targets of the NOTCH signaling pathway – the *Hes* genes. **(D)** This creates a feedback pathway, which results in a rapidly amplified imbalance of the expression level of proneural proteins between the cells. When subsets of cells express proneural genes and DLL1 at high levels, they start to differentiate into neuroblast precursors (left cell), while cells highly affected by NOTCH signaling, expressing *Hes* genes, remain precursors (right cell).

4.3.3 bHLH-TFs

Hes genes and proneural genes belong to the group of the bHLH protein family. bHLH proteins are found in almost all eukaryotes and are transcriptional regulatory proteins, which act as key players in a wide array of developmental processes (Atchley and Fitch, 1997). In animals, they are important regulators of embryonic development, particularly in neurogenesis but also myogenesis, heart development and hematopoiesis (reviewed in Massari and Murre, 2000, Imayoshi and Kageyama, 2014, Murre *et al*., 1994). Their capacity to implement such divers function is founded in their capacity to form heterodimers with other proteins. The members of the bHLH superfamily have two highly conserved and functionally distinct domains, which together comprise a region of about 60 amino-acid residues. These domains comprise a basic region (b) and two long α-helices connected by a short loop (HLH). The amino-terminal end of the HLH structure contains the basic domain, which makes contact with the major groove of the DNA at a consensus hexanucleotide sequence known as the E-box (Figure 4.6) (Ephrussi *et al*., 1985, Murre *et al.*, 1989). Different E-box consensus sequences are recognized by different families of bHLH proteins. The carboxy-terminal end contains aditional HLH domains, which facilitate interactions with other protein subunits to form homo- and hetero-dimeric complexes. Different combinations of dimeric structures are possible and lead to different binding affinities between homo- and heterodimers. Thus, heterogeneity in the recognized E-box sequence and the dimers formed by different bHLH proteins determine the way of transcriptional regulation of diverse developmental functions (Fairman *et al.,* 1993) and their role of being activators and/or repressors take place in a context-dependent manner and very often, the crosstalk among them follows a not yet uncovered complex transcriptional network. In the mouse, bHLH proteins are classified into four groups (A, B, C, and D; which are very similar to human's group) according to E-box binding, conservation of residues in other parts of the motif, and the presence or absence of additional domains (Skinner *et al*., 2010).

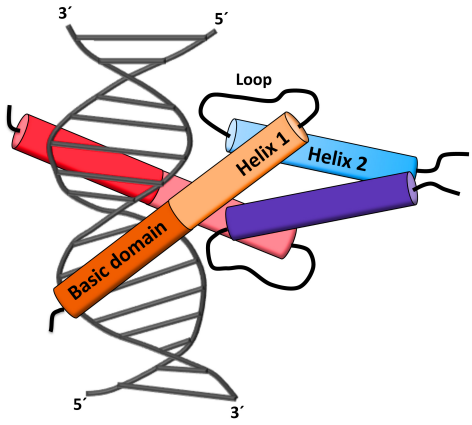

Figure 4.6: bHLH TFs
The motif of these TFs is characterized by two α-helices (helix 1 and 2) connected by a loop and one helix containing basic amino acid residues that facilitate DNA binding. Helix 2 at the carboxy terminal allows dimerization by folding and packing against the helix of another bHLH TF. The basic region at the amino-terminal is involved in connecting to the major groove of the DNA. bHLH TFs mostly act as homo- and/or hetero-dimeric complexes.

4.3.4 *Hes* genes

Hes genes encode a family of bHLH transcriptional repressors and are mammalian homologs of the *Drosophila* genes [*h/E(spl)*]. They are grouped in class C as they are designated to the bHLH-O TFs (Davis and Turner, 2001). Many of the bHLH-O TF proteins are effectors of the NOTCH signaling pathway and involved in regulating neurogenesis (Artavanis-Tsakonas *et al*., 1999). These bHLH TFs have 3 conserved domains: a bHLH-, an Orange- and a WRPW-domain. The Orange domain of *Hes* is a 30-residue sequence that is located at the carboxy-terminal to the bHLH region and responsible for the selection of partners during heterodimer formation. The carboxy-terminal tetrapeptide WRPW motif (Trp-Arg-Pro-Trp) allows direct repression by binding the transcriptional co-repressor, *Groucho* (Paroush *et al.*, 1994). Of the seven members of *Hes* family, *Hes1, Hes3, Hes5* and *Hes6* are expressed in the mouse neuronal progenitors during embryogenesis. Already during neural plate stage, *Hes1, Hes3* and *Hes5* are expressed along the entire neuraxis in neuroepithelial cells and positively influenced by regional patterning factors as FGF SHH, WNT and BMPs but yet NOTCH independently (Hatakeyama *et al.*, 2004, Kageyama *et al.*, 2008). Later, particularly *Hes1* and *Hes5* expression is restricted to the cell bodies of radial glia in the VZ and involved in lateral inhibition (Akazawa et al., 1992, Ohtsuka et al., 1999). The antagonistic effect between *Hes* and proneural genes is achieved in part as *Hes1* can actively repress *Mash1* by binding to its promoter region or directly inhibit MASH1-E-protein interactions (Chen et al., 1997, Kageyama *et al*., 2005). Inactivation of *Hes* genes leads to upregulation of proneural genes, acceleration of neuronal differentiation, premature depletion of neural stem cells and severe defects in several brain structures (Kageyama *et al*., 2008, Hatakeyama *et al.*, 2004, Ishibashi *et al*., 1995). Conversely, overexpression of *Hes* genes leads to inhibition of neurogenesis and maintenance of neural stem cells (Kageyama *et al*., 2008). An exception is *Hes6* that is expressed by both, undifferentiated and differentiated cells. This is in contrast to *Hes1* or *Hes3*. *Hes6* suppresses *Hes1* at a post-transcriptional level from inhibiting MASH1-E47-heterodimers, which in turn enables upregulation of *Mash1* in the presence of HES1 (Bae *et al.*, 2000). In addition, lateral inhibition can be influenced by the autoregulatory capability of *Hes1* to bind its own promoter and thereby to repress its own transcription. High levels of HES1 are able to induce degradation of unstable *Hes1* messenger ribonucleic acid *(*mRNA) and HES1 protein. This releases negative feedback regulation which enables another round for activation of *Hes* expression resulting in an oscillatory expression of *Hes1* in neural progenitors with a period of 2–3 h. *Hes1* expression exhibits an inverse correlation with *Ngn2* and *dll1* mRNA expression in neural progenitor cells and mutual activation of NOTCH signaling between neighboring cells maintains a group of cells in the undifferentiated state. It is likely that NGN2 cannot induce neuronal differentiation when its expression oscillates but induces the maintenance of progenitor cells. Although in differentiating neurons, when *Hes1* expression is repressed, *Ngn2* expression is sustained and induces neuronal differentiation. In contrast, cells in boundary regions such as the isthmus appear to express *Hes1* in a sustained manner

which induces dormancy. The oscillations might act as a cellular clock establishing an ability of progenitor cells to either activate or repress downstream target genes required for proliferation or differentiation (Shimojo *et al.*, 2008, Kageyama *et al*., 2009).

4.3.5 Proneural proteins

Proneural proteins belong the same family of bHLH TF that initiate the development of neuronal lineages, promote the generation of progenitors that are committed to differentiate and contribute to the specification of progenitor-cell identity. Albeit the shared bHLH motif, proneural proteins can be grouped into distinct families that are characterized by the presence of family-specific residues in their bHLH domain (Lee, 1997). Vertebrate proneural bHLH genes fall into two families, based on homology to bHLH genes that were originally identified in *Drosophila* as mutations that block neural differentiation: one, related to the *Drosophila* Achaete-Scute genes (e.g. *Mash1*) and one related to *Drosophila* atonal (comprising the subgroups of *Ngn*-like, *NeuroD-like* and *atonal*-like). Most vertebrate proneural-related genes are expressed exclusively or principally in the developing NS. Particular the genes *Mash1*, *Math1, 5*, *Ngn1-3* and *NeuroD* have been shown to be crucial for the development of neuroectodermal progenitor cells. Their expression in individual neural progenitors is transient as they are downregulated before progenitor cells exit the proliferative zone and begin to differentiate. Ectopic expression of proneural genes can lead to perturbation of differentiation by a rapid cell cycle withdrawal and a highly efficient differentiation of progenitors (Ma *et al.,* 1997, Lee, 1997, Lee *et al*., 1995). Additionally, proneural factors are able to elicit different biological responses as expressed in different cellular contexts where they participate in the ontogeny of different neuronal types (Brunet and Ghysen, 1999, Ma *et al.*, 1997). Besides their ability to promote full neuronal differentiation and to regulate the balance between proliferating and differentiating progenitor cells, they have a pivotal role in integrating positional information and the acquisition of neural lineages (migration and fate) in neural progenitor cells (Parras *et al*., 2002). In the absence of MASH1, tissue morphology, proliferation, and gene expression within FB regions is disrupted (Horton *et al.*, 1999). Further, in the knock out mice of *Mash1*, olfactory and autonomic neurons are missing and differentiation of retinal neurons is delayed (Casarosa *et al.*, 1999, Guillemot *et al.,* 1993). Single mutants of *Ngn1* or *Ngn2* lack complementary sets of cranial sensory ganglia and double mutants further lack spinal sensory ganglia and partially ventral spinal cord neurons (Ma *et al.*, 1998, Ma *et al*., 1999, Scardigli *et al*., 2001). In some cases proneural genes appear to be coupled with certain neuronal fates as in the cortex *Mash1* can drive GABAergic and *Ngn2* glutamateric neuron differentiation (Fode *et al*., 2000, Parras *et al*., 2002). In addition, they have also been shown to be involved in the neuronal-versus-glial cell-fate decision (Tomita *et al.,* 2000).

4.3.6 Neuronal subtype specification in proliferating progenitors

At the cell cycle exit, proneural genes activate pan-neural genes as well as subtype specification factors to activate both, generic and subtype-specific neuronal-differentiation programs coupling the selection of progenitor cells with specification, respectively. The capacity of proneural genes to elicit different biological responses may be reasoned in their structure, in particular their bHLH domain but also from the fact that they elicit different biological responses when expressed in different cellular contexts. The combination of their structure and different DNA-binding specificities, allows them to cooperate with regionally expressed determinants that modify the neuronal specificity. The physical interactions with region specific factors and co-factors result in the potential of proneural genes to confer regional specificity and to apply direct transcriptional control of further specification genes (Wong *et al*., 2003, Lee, 1997, Jan and Jan, 1993). For example, in the basal FB, *Mash1* together with *Dlx1/2* (Fode *et al*., 2000) can define GABAergic subtype specification. In the MB, *Megane* (*Mgn* also known as *Heslike; Helt*) acts synergistically with *Mash1* for GABAergic subtype specification (Wende *et al.*, 2015) while in the HB, *Mash1* directs noradrenergic fate through PHOX2a/b TFs and together with *Gata3, Lmx1b* and *Pet1* serotonergic fate (Bertrand *et al*., 2002, Pattyn *et al*., 2004).

4.3.7 Neuronal subtype specification in postmitotic neurons.

As the proliferating progenitors exit the cell cycle, they start to express subtype specification factors ("drivers" (Hobert *et al.*, 2010), able to solely define the ultimate function of the mature neuron. Such subtype specification factors are bimodal regulators, which act as sole activators or inhibitors, activating gene expression batteries driving neuronal precursors towards a certain cell fate while simultaneously inhibiting other cell fates. In this way, the activation of the differentiation cassettes (a set of genes that belong to the same pathway) drives the neurons to the expression of terminal differentiation genes and they acquire their ultimate mature function (Hobert *et al.*, 2010). The triggered differentiation cassette can be altered by loss or gain of a selector gene function regardless of the cell patterning history. Although, the loss of a selector gene does not necessarily imply an alteration in the number of precursor cells or the survival or migration of postmitotic neurons, the cells lose their specific neuronal identity while becoming transformed into an alternative fate (Achim *et al*., 2014). A number of such "driver" genes have been described for the control of GABA identity versus glutamatergic fate in the mammalian brain (Eisenstat *et al*., 1999, Glasgow *et al*., 2005, Muroyama *et al.,* 2005, Cheng *et al.*, 2005). GATA Binding Protein 2 (GATA2*)* is a driver of MB GABAn (Kala *et al*., 2009) and *Ptf1a* drives GABAn in the cerebellum (Hoshino *et al*., 2005) and dorsal spinal cord (Glasgow *et al.*, 2005), while *Tlx1* and *Tlx2* homeobox genes drive glutamatergic fate in the dorsal spinal cord (Cheng *et al*., 2004) and the TF T-CELL ACUTE LYMPHOCYTIC LEUKEMIA 1 (TAL1, SCL) drives GABAn induction in the ventral spinal cord

(Muroyama *et al*., 2005). This multi-step progress of the generation of individual neuron types terminates in the expression of neuron specific terminal differentiation genes (terminal markers). These genes encode for proteins that determine the functional properties of the adult neuron throughout its lifetime. A mature neuron is defined by a molecular unique signature of genetic markers whose functions allow the neuron´s individual correct morphology, composition of ion channels, transporting proteins, cell surface receptors functional composition and synthesis of neurotransmitter (in case of neurons with chemical synapses) (For GABAn terminal marker (see chapter 4.1.2 GABAergic siganlling). Only the correct composition of such proteins will allow the neuron to exert its proper function.

4.4 SPECIFICATION OF GABAN IN DIFFERENT BRAIN AREAS

In the early neuroepithelium, the progenitor domains are patterned by various TFs and regulated by extracellular signals. Despite some of these TFs, are shared by many GABAergic domains, none of them is present in all of the GABAergic progenitor domains. Instead, each domain has adopted an individual set of genes either exclusively or in spatially coherent groups, which trigger gene cascades leading to GABAn which are specific for the respective region. Likewise, the contribution of the three proneural genes Mash1 and Ngn1/2 to the specification of neuronal fates varies greatly in different lineages: it includes various neurotransmitter identities like noradrenergic, Ach+, 5-HT+, and TH+ lineages, as well as oligodendrocytes and astrocytes (Kim *et al*., 2008, Guillemot *et al*., 1993, Pattyn *et al*., 2004, Parras *et al.*, 2002), presumably depending on the presence of other determinants of neuronal identity (Parras *et al.*, 2002). Simultaneous generation of multiple cell types correlates with the overlapping expression of both in these regions and their function in GABA versus glutamatergic fate. Despite the complexity of generation of GABAn, *Mash1* has been shown to be involved particularly in GABAn specification. *Mash1* directs GABAergic neuron differentiation ventrally in the ganglionic eminences (Roybon *et al.*, 2010), in the telencephalon, (Fode *et al.*, 2000) and ectopic expression of *Mash1* results in the induction of GABAergic neurons in the telencephalon and V2 interneurons in the spinal cord (Parras *et al*., 2002).

Rationed by the selector gene for GABAergic fate, so far three regions of the developing brain were identified: the Dlx-type (telencephalon-anterior diencephalon), the *Gata2*-type (posterior diencephalon-MB) and the *Ptf1a* and *Tal1*-Type (the HB-spinal cord) (Achim *et al*., 2012).

4.5 GABAERGIC NEUROGENESIS IN THE MB

Despite the important functions of GABAergic MB nuclei, the regulation of their development is only beginning to be understood. Although MB-GABAn development share similarities with adjacent brain parts in the expression of GABA-fate associated factors appears to have specific gene cascades regulating GABAergic neurogenesis. They are highly divergent in terms of their location, morphology, connection patterns and functions. Further, GABAn in the MB are highly divergent in terms of their developmental origins and molecular regulatory mechanisms. As most of the MB GABAn nuclei are functionally associated with other neurotransmitter circuits, like the dopaminergic, many of the MB GABAn subpopulations are highly relevant for neurological and psychiatric disease.

4.5.1 Subpopulation of GABAn in the mature MB and their function

MB GABAn comprise diverse interneurons, which can be distributed over three major subdomains of the MB neuroepithelium (further assigned into seven molecular subdomains, m1-m7; see chapter 4.5.2 Patterning of the embryonic MB neuroepithelium; Figure 4.8): i) the dorsal MB (dMB) GABAn, ii) the ventrolateral MB (vlMB) GABAn and ii) the ventral-most MB (vmMB) GABAn.

The dMB GABAn comprise the interneurons of the superior and inferior colliculus (SC and IC, respectively) and the one of the latero-dorsal part of the periaqueductal gray (PAG). The neurons of the SC and IC mostly act as inhibitory neurons between the layers of the SC and are thereby involved in the integration of visual and auditory information into topographic maps and the generation of goal-directed orienting behavior in response to sensory stimuli (Felsen and Mainen, 2008). More than 25% of the interneurons in the IC are GABAergic (Oliver *et al.*, 1994). In contrast to the laterodorsal part of the periaqueductal gray (PAG), which is also attributed to the dMB, the ventral part of the PAG already accounts to the vlMB together with the interneurons of the reticular formation (MRF) area. GABAn in the PAG nuclei are involved in the control of fear and anxiety and pain processing (Behbehani, 1995), and GABAn of the MRF, which are co-distributed with excitatory glutamatergic neurons are found to regulate sleep-wake state (Brischoux *et al.*, 2008, Luppi *et al.*, 2011). The vmMB GABAn correspond to the neurons of the ventral tegmental area (VTA) and substantia nigra (SN). Theses neurons are associated with voluntary movements, regulation of mood, motivation and reward (Grillner *et al.*, 2005). These vmMB-GABAn are intimately associated with the dopaminergic neurons (DAn) exerting activity regulation on the TH system. In the substantia nigra pars reticulata (SNpr) the vast majority of neurons are GABAergic but also the substantia nigra pars compacta (SNpc), which lies more caudally, contains intermingled GABAn. Thus, by their intimate association they highly influence the DA output of the basal ganglia (BG). Furhter, the GABAn of the VTA, (20-35% of the neurons are GABAergic (Nair-Roberts *et*

al., 2008, Olson and Nestler, 2007)), at least partially project to limbic areas in the FB and cortex and thereby regulate reward prediction and behavioral control as well the development of addiction (Figure 4.7) (Cohen *et al.*, 2012, Sanchez-Catalan *et al.*, 2014).

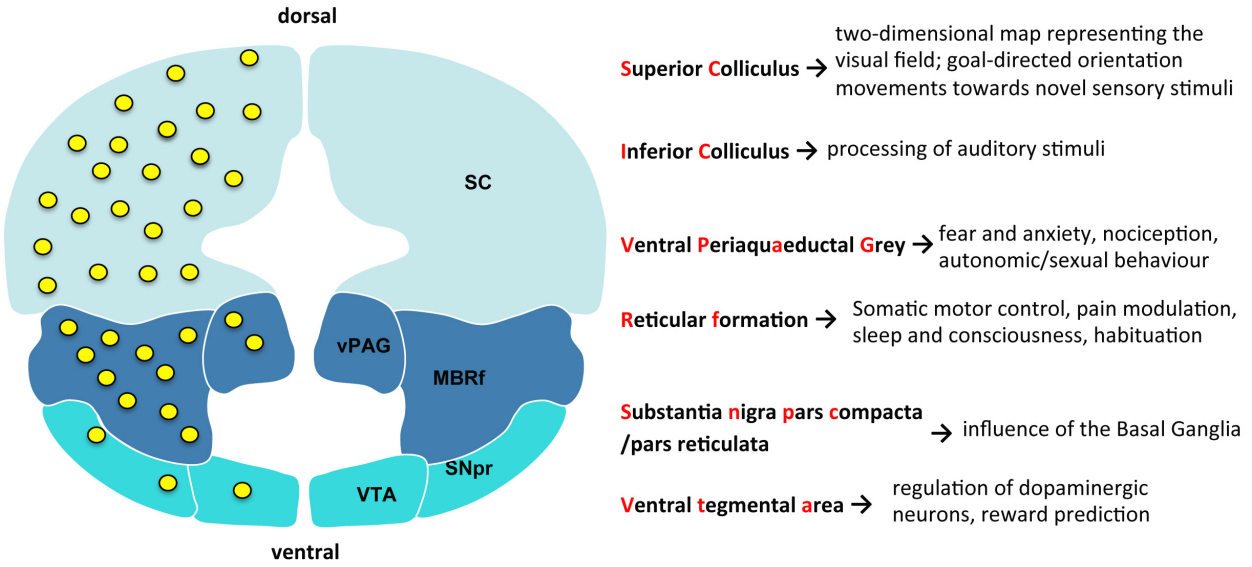

Figure 4.7: Schematic view of an E15.5 MB coronal section, depicting GABAergic nuclei and their function.
The nuclei of the IC and the SNpc are not depicted in this section because of their more caudal and more rostral location, respectively.

4.5.2 Patterning of the embryonic MB neuroepithelium

The D/V patterning by SHH signals from the FP and BMP/WNT signals from the RP (see chapter 4.2 Development of the vertebrate CNS) results in a D/V division into seven subdivisions of the MB, termed m1-7. These subdomains are characterized by the expression of specific TF as e.g. NKX2.2, NKX6.1, NKX6.2, PAX6 (AN2), MASH1 and MGN, giving rise to specific neuronal differentiated subtypes (Figure 4.8). Domains m1-3 comprise the RP and AP, domains m4-m6 the BP and domain m7 the FP. The AP gives rise to the d/vlMB GABAn but also glutamatergic neurons. Subdivisions m3, m5 and the dorsal half of m4 are generating solely GABAn while the ventral half of m4 generates mainly glutamatergic neurons. Thus, in the mouse MB, m1-5 are able to produce GABAn. From m6 cholinergic neurons intermingled with glutamatergic neurons are generated and DAn arise exclusively in m7 (Kala *et al.*, 2009, Nakatani *et al.,* 2007).

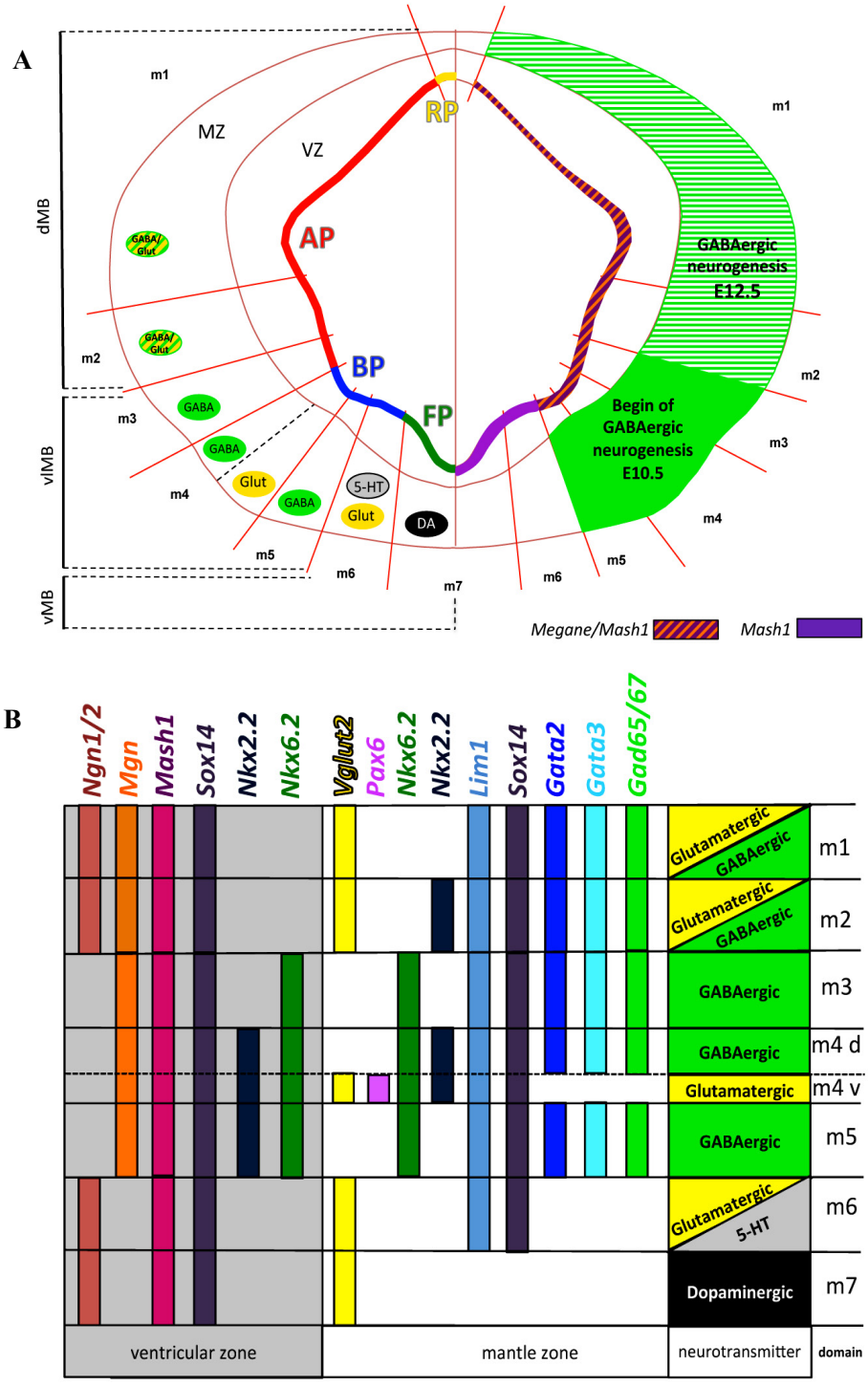

Figure 4.8 (A) Schematic view of a coronal section of an E12.5 MB.
The MB is divided in seven subdomains that give rise to all main neurotransmitter phenotypes. m1-5 give rise to GABAn. *Mash1* is expressed in m1-7 and overlaps with *Mgn* expression in the VZ of m1-5. First MB GABAn are generated in vlMB (m3-5 region of the AP/BP) at E11.5. At E12.5 GABA markers can be detected in the dMB (m1-2).
(B) The MB is subdivided into 7 subdomains defined by particular expression pattern of TFs giving rise to particular transmitter phenotypes. Adopted from (Kala *et al.*, 2009).

4.5.3 Migration of different MB GABA populations

In addition to the high diversity of function of MB GABAn, recent work revealed that these neurons to also differ in their developmental origin. GABAn of the d/vlMB (m1-m5) are born in the neuroepithelium of the MB itself and migrate radially towards the MZ, showing only very little tangential migration subsequently (Tan *et al*., 2002) – which is in contrast to the mouse FB. GABA specific markers are first detected in the m3-5 domain at embryonic day E10.5 and one day later also in the dorsal aspect of the MB (m1-2) where neurogenesis subsequently continues longer (Achim *et al.,* 2012). On the contrary, recent birth-dating studies reported that the vmMB GABAn, associated with DAn (MRF, PAG and SNpr), are populated by tangentially migrating cells during midgestation: these DAn-associated neurons are suggested to be composed of developmentally different subgroups: i) one group of GABAn deriving from the HB r1, giving rise to neurons in VTA and caudal part of SNpr, ii) one group which derives from the MB itself and iii) one group which is suggested to migrate from the diencephalon, additionally contributing to the anterior part of SNpr located in the mature diencephalon. The majority of SNpr and VTA GABAn was seen to be born by E12.5 in the HB, then to migrate towards the vmMB, likely guided by MB DAn (Vasudevan *et al*., 2012), and appear in the MB at E14.5 (Kala *et al.,* 2009, Achim *et al*., 2012). The SNpr is not a homogeneous population and the origins of these GABAn are distributed in two opposite rostrocaudal gradients: the contribution of r1 GABAn to the SNpr displays a distribution along the rostrocaudal axis, being more abundant in the caudal SNpr and almost absent in the rostral part (Achim *et al*., 2013). The more rostrally located GABAn derive from a NKX6.2+ domain in the ventricular zone of the vlMB and these neurons are distributed in a rostrocaudal gradient along the SNpr, opposed and complementary to the r1 derived GABAn (Madrigal *et al*., 2015). Thus this nucleus is composed by two neuronal populations distributed in opposite gradients with different origins, one from r1 (marked by *Tal1* expression), caudal to rostral, and the other from the MB (marked by *Six3* downstream of *Nkx6.2*), rostral to caudal. The GABAn reaching from the diencephalon are thought to be guided by DA receptors D1 and D2 (Crandall *et al.,* 2007).

4.5.4 MGN and MASH1*:* two key factors for the early specification of MB GABAn

In the last decade, more and more key factors have been discovered to play a role in GABAergic neurogenesis. Particularly the proneural gene *Mash1* has been shown to contribute to the specification of various neural fates in different lineage, including manifold neurotransmitter identities as noradrenergic, acetyl cholinergic, serotonergic, and glutamatergic lineages, as well as oligodendrocytes and astrocytes (Kim *et al*., 2008, Guillemot *et al*., 1993, Pattyn *et al.,* 2004, Parras *et al*., 2002), which presumably depends on the presence of other determinants of neuronal identity (Parras *et al*., 2002). Nevertheless, *Mash1* has been shown to be involved particularly in GABAn specification. More in particular in the MB,

the two bHLH TFs MASH1 as well as MGN, both expressed in progenitors of the MB VZ, have been described to function as early key cell fate determinants for MB GABAn (Nakatani *et al.,* 2007, Guimera *et al*., 2006b, Peltopuro *et al.*, 2010).

4.5.4.1 *Megane*

Mgn is a single copy gene on mouse chromosome 8 that encodes a 27 kDa protein functioning in the nucleus. MGN protein shares structural homology in the bHLH region with other members of the [*h/E(spl)*] family including *Hes, Sharp* and *Hey* (Miyoshi *et al*., 2004, Nakatani, 2004, Guimera *et al.*, 2006a). Despite this structural similarity, MGN displays critical divergences in several characteristic residues that distinguish it from other subfamilies related to the [*h/E(spl)*] family, including the mammalian HES, HEY, SHARP and DEC1 subfamilies in 3 distinguishing features; i) MGN has a novel lysine residue instead of the conserved proline residue within the DNA-binding basic domain that is known to provide subfamily-specific functions, ii) the absence of the conserved tetrapeptide WPRW groucho/TLE binding motif at the carboxy-terminus, a landmark of the [*h/E(spl)*]/HES proteins (see chapter 4.3.4. *Hes* genes) and iii) its divergence in several critical and conserved amino acid positions within the bHLH domain, characteristic of the DEC1/SHARP, HEY/HRT and HES/HER subfamilies; instead of the alanine-rich domain, present in the *Hey/Her* subfamily, and the glutamine-rich domain of hairy, MGN protein has a proline-rich portion between the bHLH-O domain and the carboxy-terminal region, involved in protein–protein interactions. These facts argue that *Mgn* constitutes a new subclass of bHLH TFs (Guimera *et al.,* 2006a). Promoter binding analysis performed *in vitro* suggest MGN homodimers act as a transcriptional repressor by binding to E-box class B and C1 sequences, which are typical recognition sequences for bHLH repressors, but with a different preference for the core sequence when compared with other bHLH-O repressors (Nakatani *et al.,* 2007). Thus, whether MGN activates neurogenesis *in vivo* by binding to E-box class A or represses repressors of neurogenesis needs to be formally probed.

4.5.4.2 Expression pattern of *Mgn*

Expression of *Mgn* mRNA shows a specific and dynamic pattern in the embryonic CNS, which is developmentally controlled in a tissue-specific manner: tissue distribution and the ontogenetic expression pattern of *Mgn* show a spatio-temporal correlation with that of GABAergic markers (*Gad65/67*). At E9.5, *Mgn* expression is first detected bilaterally restricted to the ventral domain of most rostral mesencephalic region. At E10.5 its expression domain expands caudally towards the isthmus, while rostral, the bilateral expression domains split into dorsal and ventral stripes: the ventral stripes are extended rostrally and delineate the caudal ZLI where it overlaps with the longitudinal *Nkx2.2* expression from the caudal part of

isthmus up to the ZLI domain adjacent to that of *Shh*. *Mgn* expression stops at the dorsal tip of the ZLI, while *Nkx2.2* expression continues within the prethalamus into the secondary prosencephalon. The dorsal stripes end in the pretectum and demark this domain, colocalizing with *Pax6.* At this stage, further weak expression can be detected in the lateral ganglionic eminence (LGE), the caudal ganglionic eminences (CGE), prethalamus and olfactory placode, which intensifies along maturation. At E11.5, *Mgn* expression expands dorsally in the pretectum and the MB. At E12.5, the dorsal expression of *Mgn* in the MB becomes more intense at E12.5 and is maintained at E13.5. From E14.5 onwards, *Mgn* expression in the MB, the pretectum as well as in the ZLI gets gradually downregulated and disappears by E17.5. *Mgn* expression is not controlled by *En1* or *Wnt1* and never expressed in the regions caudal to the isthmus (Guimera *et al.,* 2006a). From E15.5 onwards, *Mgn* is also expressed in the rostral migratory stream but not in the olfactory bulb and from E18.5 onwards in the cortical sub-plate as well as layer VI of the cortex and the striatal sub-VZ. In the adult CNS is found in single cells in the sub-VZ surrounding the lateral ventricles and the olfactory ventricles and in testis (Guimera *et al*., 2006a).

4.5.4.3 MGN is a cell fate determinant for MB GABAn

Mgn is expressed in neural progenitors but decreases rapidly as neuronal differentiation proceeds and is never detected in the MZ of the developing brain. Its early mosaic (most likely cyclic) expression pattern at E9.5 in the vlMB, and at E12.5 in the dorsal aspect corresponds with the onset of the first vlMB and dMB GABAn, respectively. Therefore in the MB, *Mgn* expression shows a spatiotemporal expression with GABAn by expression analysis of *Gad65* and *Gad67* in adjacent but never overlapping regions. Early expression of *Mgn* at E9.5 in the vlMB (m3-5) corresponds with the onset of the first wave of appearence of mature GABAn as well as for the second wave in the dMB (m1-2) at E12.5. *Mgn* expression is turned off in all GABAn immediately after they became postmitotic. This suggests that in the MB, *Mgn* is expressed in a population of progenitor cells, which will later differentiate into GABAn when migrating out towards the MZ. By loss-of-function studies, MGN was identified as a cell fate determinant for MB GABAn particularly in the dMB (Guimera *et al.*, 2006b): in the absence of MGN, induction of dMB GABAn does not take place at any time during development although precursor cells are generated at proper numbers. The defective GABAn are kept and do not enter into apoptotic programs nor do the mutant brain reveal any morphological alteration although the mutant mice die of postnatal lethality between the 2nd and 5th week and display seizures (Guimera *et al*., 2006b). In contrast, GABAn in the vlMB remained unchanged at E15.5. Similarly, *Mgn* is strictly required for *Gad67* expression in a small area of the rostral population of thalamic progenitors (pTHr) (Delogu *et al*., 2012). Further it was reported that *Mgn* can promote the GABAergic fate by repressing glutamatergic fate (Nakatani *et al*., 2007, Delogu *et al*., 2012). Later on is was in the MB, MGN can repress the proneural genes *Ngn1/2*,

which are associated with glutamatergic neurogenesis. In the absence of MGN, *Ngn1/2* are seen ectopically expressed and cells in the MB expressed ectopic glutamatergic markers (Nakatani *et al*., 2007). Yet, MGN is unlikely to directly form dimers with the NGN proteins 1, 2, 3 (Wende *et al*., 2015). Further, *Mgn* overexpression can induce GABAergic fate, in the MB as well as in the FB, particular in the rostral thalamic region (Nakatani *et al*., 2007, Sellers *et al*., 2014). In summary, *Mgn* plays a key role as a primary selector of GABAergic neuronal identity in distinct progenitor domains.

4.5.5 The bHLH TFs MASH1 and MGN have a similar function regarding specification of MB GABAn

Whereas *Mgn* is the earliest GABAergic marker, expressed specifically in mitotic GABAn precursors, expression of *Mash1* is maintained in many postmitotic cells of the basal and alar MB neuroepithelium. Yet it overlaps with the expression of *Mgn* in the VZ of the MB, expressed in a manner similar to *Mgn*. Both genes reveal an expression pattern with high levels of expression in the vlMB area (at E10.5) when compared with the low levels in the dMB at E12.5. Further, MASH1 co-localizes with MGN in the vlMB (Miyoshi *et al.*, 2004). Albeit *Mash1* has been shown to have a pivotal role also for the fate specification of neurons that release neurotransmitters other than GABA in the entire CNS (Kim *et al*., 2008), and in the MB, it also regulates glutamatergic neurogenesis, *Mash1* has a highly region-specific function in the development of the MB GABAn (Peltopuro *et al*., 2010). Analysis of *Mash1* knockout mice revealed a GABAergic phenotype very similar to that of *Mgn* knockout mice as shown by the complete depletion of GABAn in the SC at any time during development but induction of vlMB GABAn. In addition, *Mash1* appears to have dual and region-specific roles in supporting neural progenitor cell state and promoting cell cycle exit as in *Mash1* knockout mice neurogenesis is initially delayed in m3 and m5 while post-mitotic neuronal differentiation is precociously activated in m4. A puzzling phenotypic feature of *Mgn* and *Mash1* single mutants is that the GABAergic phenotype is circumscribed to the dMB domains where *Mgn* and *Mash1* are expressed at low levels compared with their vlMB expression. Another key point is that MGN and MASH1 factors were identified to interact with each other as determined by yeast two hybrid system (Y2H) studies and their binding specificity was confirmed in mammalian cells by Co-Immunoprecipitation (Co-IP) assays using MGN and MASH1 epitope-tagged fusion proteins (Wende *et al*., 2015). Thus MGN can form both homodimers (MGN/MGN), as previously reported by *in vitro* experiments in 293E cells (Nakatani, 2004) and heterodimers with MASH1 (MGN/MASH1).

Notably, upon *Mgn* misexpression in the presence of MASH1, premature GABAn were generated at E10.5 in the dMB, despite GABAergic neurogenesis in this area starts only at E11.5-12.5, dependent on the expression level of *Mgn* (see 4.5.4.2 Expression pattern of *Mgn*). Similarly, ectopic GABAn were generated in the vmMB, which normally expresses *Mash1* only and does not give rise to GABAn at any

stages (Miyoshi *et al.*, 2004). Additionally, in cultured cells, co-transfection of *Mgn* and *Mash1* potentiated GABAergic differentiation (Miyoshi *et al.*, 2004). These facts suggest, that MGN and MASH1 are two critical bHLH factors, which have parallel and marked roles during MB GABAergic neurogenesis.

4.6 SUBTYPE SPECIFICATION AND MAINTENANCE IN POSTMITOTIC MB GABAN PRECURSORS

Once early specification of MB GABAergic fate is performed by MGN and MASH1, a gene cascade is initiated to ensure final expression of terminal GABAergic markers (GAD65/67; GABA). Along this cascade several downstream genes and genes destined particularly for MB GABAn have been identified so far.

4.6.1 GATA and TAL TFs

The zinc finger TF GATA2 plays important roles in the hematopoietic system but also functions essentially in the CNS as loss of GATA2 function leads to neurodevelopmental defects including abnormal axon pathfinding, fasciculation and arborization. Moreover, *Gata2* is required for V2b spinal interneuron subtype identity (Zhou *et al.*, 2000, Karunaratne *et al*., 2002), drives precocious neuronal differentiation in chick spinal cord (El Wakil *et al.*, 2006), and is sufficient for ectopic serotonergic neuron specification in lateral hindbrain (Craven *et al.*, 2004). In the MB and posterior diencephalon, all GABAergic precursors express *Gata2*, which controls their differentiation (Lakshmanan *et al.*, 1999, Kala *et al.*, 2009, Bell *et al.*, 1999, Nardelli *et al.,* 1999). The expression of *Gata2* in the MB begins at E10.5 in GABAn precursors as they exit the cell cycle and is gradually downregulated during development (Kala *et al*., 2009). It is partially co-expressed with *Mgn* and downstream of *Mgn* (Kala *et al*., 2009). Conditional inactivation of *Gata2* in the MB was seen to transform GABAn precursors in the m1-5 domain into glutamatergic neurons (shown by a robust increase in the glutamatergic neuron marker VGLUT2), while not affecting cell cycle exit. Further, overexpression of *Gata2* in the chick dMB generated ectopic GABAn (Kala *et al*., 2009). During hematopoietic differentiation, GATA factors are able to interact with different cell specific cofactors and to form multi-protein transcription complexes with other proteins that promote commitment to maturated fate (Wadman *et al.,* 1997). The bHLH TF TAL1 and T-CELL ACUTE LYMPHOCYTIC LEUKEMIA 2 (TAL2) were reported to be such interactors. Mice lacking TAL factors or GATA2 show similar phenotypes by early embryonic lethality due to failure in hematopoietic development (Cantor and Orkin, 2002, Shivdasani *et al.,* 1995). Similar to *Gata2*, *Tal1* is expressed during brain development in the intermediate and marginal zone of diencephalon, MB and HB

(van Eekelen *et al*., 2003). *Tal1* is also implicated in brain development as conditional inactivation of *Tal1* in *Nestin-Cre;Tal1 Flox/Flox* mice show growth-retarded and hyperactive mutant mice, displaying altered motor coordination and premature dying. Although TAL1 was seen to be downstream of GATA2 (and MGN) in the MB (Kala *et al*., 2009), in contrast to *Gata2*, it has only a minor impact on directing GABAergic fate in this brain area. By contrast, *Tal1* regulates GABAergic neurogenesis in the HB, where it is required for the population of mvMB GABAn, which migrate into the MB from the HB (Achim *et al.*, 2012, Achim *et al*., 2013). Inactivation of *Tal1* in r1 of the HB leads to GABAergic to glutamatergic neuron fate change already at early stages of development and this transformation is persistent until birth (Achim *et al*., 2013). Thus, the defect in GABAergic neurogenesis in r1 correlates with a loss of vmMB GABAn of the VTA-SN. Albeit *Mash1* is widely expressed in the HB, it has no regulatory effect on *Tal1* and therefore neither on these population of GABAn (Peltopuro *et al.*, 2010). In the MB, *Tal1* expression is preceded by the expression of *Tal2* in overlapping domains (Mori *et al.*, 1999) and acts downstream of *Tal2. Tal2* is activated very early during GABAn differentiation, similar to *Gata2*, and its function is important for correct anatomical formation of SC and IC (Bucher *et al*., 2000). Moreover, *Tal2* knockout and *Gata2* knockout mice show a very similar phenotype regarding MB GABAergic neurogenesis: the majority of MB GABAn switch to a glutamatergic-like phenotype (except for some remaining cells in the m5 domain). Nevertheless, the *Tal2* and *Gata2* genes are activated independently (Achim *et al.*, 2013) and the phenotype of both mutants is different in detail. In *Tal2* mutants only the m4v domain transforms to *Pax6* expressing glutamatergic neurons and the m3 domain starts expressing m1–m2 glutamatergic marker POU DOMAIN, class 4, TF 1 (POU4F1) also known as BRAIN-SPECIFIC HOMEOBOX/POU DOMAIN PROTEIN 3A (BRN3A) (Kala *et al.*, 2009). On the contrary, in *Tal2* mutants the switch to glutamatergic fate appears by extensive ectopic Pax6 positive cells in m3-4 (Achim et al., 2013). However, in contrast to the *Gata2* mutant, GABAn in the m5 domain still retain some of their GABAergic characteristics without *Tal2.* Studies of the *Tal1/2* double knockout (dblKO) mutants suggest that this can partly explained by redundancy between *Tal2* and *Tal1*. Parallely, the MB GABAn appeared in the *Tal1* mutant may be controlled by the coincident expression of *Gata2* and *Tal2* that leads to formation of a terminal selector complex triggering GABAergic identity. Additionally, both factors may also have functions independent of each other or/and their absence can be differentially compensated by other associating factors (Achim *et al.*, 2013). As *Gata2* and *Tal2* are downregulated along maturation of GABAn and required for their downstream target *Tal1* - which has no impact on GABAn fate - they may be involved in postmitotic selection of GABAergic fate, while *Tal1* is rather involved in the maintenance of GABA fate (Achim *et al.*, 2013). Besides, TAL1 together with SOX14 (member of the Sex-Determining-Region-related HMG box class of TF) is further important for pTHr GABA subtype identity where it acts downstream of MGN (Delogu *et al*., 2012). Interestingly, these GABAn are characterized by their sequential activation of three lineage-restricted TFs: MGN, TAL1 and SOX14 (Sellers *et al.*, 2014),

resembling highly the MB in their expression order. Nevertheless, TAL and GATA factors are clearly implicated in MB GABAergic neurogenesis, as *Tal1/Tal2* dblKO brains show a total lack of GABAergic markers concomitant with the loss of *Sox14* (and *Six3*) expression, although some residual cells expressing *Gata3* can be found in the m5 domain of the MB (Achim *et al.,* 2013).

4.6.2 *Lim homeobox1* and *Brn3a*

Two additional genes involved in either GABAergic or glutamatergic neurons are *Lim homeobox 1 (Lim1; Lhx1*) and *Brn3a*, respectively. LIM HD TFs have been associated with subtype-specific identities and their expression may be required for maintenance of GABAergic identity by controlling sets of genes, leading to possible GABA neurotransmission (Hobert and Westphal, 2000). Just as *Gata2* and *Tal2, Lim1* is also expressed in the MB intermediate zone (IZ) in GABAergic precursors (Nakatani *et al*., 2007), pretectum, and pTHr (Moreno *et al.*, 2004). Further, LIM1 was shown to define MB GABAn (by colocalization with GAD67) in contrast to BRN3A, which specifically marks glutamatergic neurons. At E12.5 in the MB, *Lim1* and *Brn3a* expression are defined to m1-6 expression. Both factors show mutually exclusive expression patterns in the MB (Nakatani *et al.*, 2007), albeit they are coexpressed in m6 - which gives rise to the glutamatergic neurons of the red nucleus (Agarwala and Ragsdale, 2002). These two factors have been shown to be controlled by *Mgn* expression (Nakatani *et al.*, 2007). In the *Mgn* knockout, *Lim1* expression at E12.5 was seen down regulated from the dMB (m1-2) but not in m3-5, where *Gad67* expression was retained. Instead, ectopic *Brn3a* expression was observed in the m2-4 and virtually all neurons of m1 domain expressed *Brn3a* instead of *Lim1*. *Lim1* can further be attributed to the GABAergic lineage as it is coexpressed with *Gata2* in m3-5 and also requires GATA2 function in m3 and m5 (Kala *et al*., 2009).

4.7 SIMILARITIES OF GENETIC CASCADES TO THE MB

In the early neuroepithelium, the progenitor domains are regulated by extracellular signals. Despite some of these TFs, are shared by many GABAergic domains, none of them is present in all of the GABAergic progenitor domains specific for the GABAergic phenotype. Instead, each domain has adopted an individual set of genes either exclusively or in spatially coherent groups leading to GABAn specific for the respective region. Similar to the MB, GATA2, TAL1, TAL2 and SOX14 are also found in the diencephalic region, where they are not only implicated in GABAergic neurogenesis but also share similarities with the MB in their expression sequences. Each of the three diencephalic prosomeres (p1, p2, p3) of the developing diencephalon gives rise to several diencephalic GABAn and glutamatergic neurons.

While the progenitors of the pTH or caudal region of the thalamus (cTH) give rise to glutamatergic neurons, and contribute to all thalamic nuclei that project to the neocortex via thalamocortical axons, the pTHr positioned between cTH and the ZLI and the pretectum generate GABAn that contribute to the nuclei of the ventrolateral geniculate nucleus (vLG) and the intergeniculate leaflet (IGL) (Delogu *et al.,* 2012). rTH GABAergic progenitors arise from MASH1+ domain and can be defined by the hierarchical and sequential expression of *Mgn, Gata2, Tal2, Tal1* and *Sox14* and *Six3* (Delogu *et al*., 2012, Sellers *et al.,* 2014), which resembles greatly the MB. *Mash1* promotes cell cycle exit and GABAergic fate in the pretectum and prethalamus but prevents it in the rTH (Peltopuro *et al*., 2010). In the absence of *Mgn* or *Mash1,* the hierarchical expressed genes *Sox14, Tal2, Tal1, Gata2, Gata3, Six3* and *Gad67* in the pretectum are downregulated but not affected in the rTH albeit they changed slightly as they started to express specific GABAergic markers of the adjacent prethalamus (Kala *et al.*, 2009). Likewise ectopic expression of *Mgn* in the cTH progenitor domain was sufficient to divert the fate of the cTH progenitors from glutamatergic to rTH GABAergic fate (Sellers *et al*., 2014) underlining *Mgn* cell fate function in GABAergic neurogenesis. The loss of *Mash1* or *Mgn* disrupted neuronal specification in the pretectum, accompanied by a GABAergic to glutamatergic neuronal fate switch, and this alteration appeared to result from de-repression of *Ngn2* (Virolainen *et al.*, 2012, Delogu *et al.*, 2012). This is similar to what was observed in the MB upon *Mgn* ablation (Nakatani *et al.,* 2007). Interestingly, ablation of both, *Mgn* and *Mash1,* leads to an almost complete abrogation of TH-R GABA identity. Although the GABAergic markers TAL2 and GAD67 were strongly downregulated, *Ngn2* was not de-repressed as observed in single mutants and accompanied with a loss of the rTH specific markers TAL1, GATA2, (GATA3, SIX3), and SOX14, they acquired a fate of prethalamic progenitos. Similar to the MB, *Gata2* is downstream of *Mgn* in the diencephalon and in its absence, rTH neurons adopt a fate of prethalamic progenitors (Virolainen *et al.*, 2012), resembling the phenotype of *Mgn/Mash1* double mutants and implicating a role for *Gata2* as a downstream effector of combined *Mgn/Mash1* activity (Song *et al.*, 2014). Thus, similar transcription cascades and the similar expression of *Mgn* and *Mash1* and downstream factors in the diencephalon and MB make it reasonable to speculate that particular these two factors play an essential role in shaping up the full transcriptional profile GABAn also in functionally distinct anatomical regions.

5 AIM OF THE STUDY

Particularly in the MB, the two bHLH-TF MASH1 and MGN have been proved to function as key factors for the early specification of dMB GABAn. Although it is still poorly understood, how MGN and MASH1 regulate GABAn induction in the entire MB, the phenotypes of *Mgn* and *Mash1* single mutants indicate an apparent similarity of their gene function - specifically operating during MB neurogenesis. Further, both proteins are able to interact *in vitro*, which makes it likely also to interact *in vivo* - exerting a mutual function.

The focus of this present study is to show by molecular, genetic and phenotypic evidence that the protein-protein interaction between MGN, a member of the [*h/E(spl)*] family and the proneural bHLH TF MASH1 takes place *in vivo* and plays a crucial role in neuronal GABAergic fate specification in the MB.

Further aim of this study is to investigate the interactions among MASH1 and MGN as well as the mechanisms for MB GABAergic neurogenesis.

Another specific objective is to describe the expression of downstream factors of the combinatorial expression of *Mgn/Mash1* among known MB GABAergic markers (GATA2, TAL1, TAL2, SOX14, LIM1) and glutamatergic markers (BRN3A, VGLUT2) to refine possible postmitotic changes along the specification of MB GABAergic neurogenesis

Lastly, this study represents an attempt to establish a model for the determination of the MB-GABAergic identity.

6 MATERIALS

6.1 CHEMICALS & SUBSTANCES

Chemicals	Company
100 basepare (bp) DNA ladder	Fermentas
1kilobase (kb)+ DNA ladder	Invitrogen
20x NuPAGE® Running buffer	Invitrogen
20x NuPAGE® Transfer buffer	Invitrogen
5x sample loading buffer	Invitrogen
AB-dilution-solution	DCS-LabLine Innovative Diagnostic-System
acetic acid (CH_3COOH)	Merck
acetic anhydride	Sigma
agarose	Biozym
ammonium Acetate (NH_4Oac)	Merck
ampicillin	Sigma
ampuwa	Fresenius
bacto agar	Difco
bicinchoninic acid (BCA)	Pierce
bisodium- trishydroxymethyl-aminoethane (bis-tris)	Sigma
boric acid	Merck
bovine serum albumin (BSA)	Sigma
bromhenol blue	Sigma
carrier DNA	Roche
complete protease inhibitor	Roche
Complete® mini phosphatase inhibitor	Roche
Count-off® liquid concentrate	Perkin Elmer

cresyl violet acetate	Sigma
DAB 2 component kit	DCS-LabLine Innovative Diagnostic-System
DAPI (4',6-diamidino-2-phenylindole)	Life technologies
DEPC-H_2O	Fresenius
dextran sulphate	Sigma
dimethylformamide	Sigma
disodium phosphate (Na2HPO4)	Sigma
dithiotreitol (DTT)	Roche
dNTP (100mM dATP, dTTP, dCTP, dGTP) **ribonucleoside tri-phosphate Solution Mix containing adenine (A), cytosine (C) thymidine (T) and guanine (G), as different bases (rATP; rCTP; dTTP; rGTP)**	Fermentas
ethanol (denatured)	Applichem
ethanol absolute	Merck
ethidium bromide	Fluka
ethylenediaminetetraacetic acid, (EDTA)	Sigma
Ficoll 400	Sigma
formaldehyde	Sigma
formamide	Sigma
glucose	Sigma
glycine	Sigma
goat serum	Millipore
hematoxylin	Roth
hydrochloric acid (HCL)	Merck
hydrogen peroxide (H_2O_2) 30%	Sigma
isopropanol	Merck
kanamycin	Sigma
KPL-Streptavidine-Peroxidase	DCS-LabLine Innovative Diagnostic-System
magnesium chloride	Merck

methanol	Merck
monopotassium phosphate (KH_2PO_4)	Roth
Nonidet P40 (NP-40)	Fluka
paraffin	Polyscience
paraformaldehyde	Sigma
Pertex® mounting medium	MEDITE
potassium chloride (KCl)	Sigma
potassium hydroxide (KOH)	Sigma
protein ladder IV	Aplichem
PVP40	Sigma
saline sodium citrate (SSC)	Sigma
scintillation liquid Aquasafe 300Plus	Zinser Analytic
skim milk powder	BD Biosciences
sodium acetate (NaOAc)	Merck
sodium choride	Merck
sodium citrate	Sigma
sodium cloride (NaCl)	Merck
sodium dodecylsulfate (SDS)	Merck
sodium hydroxide	Roth
sodium phosphate ($NaHPO_4$)	Sigma
triethanolamine (TEA)	Sigma; Merck
tris (Trizma-Base)	Sigma
trisodium citrate buffer (Na-Citrate buffer) (10x)	DCS-LabLine Innovative Diagnostic-System
Triton-X 100	Biorad
tRNA	Roche
tryptone	Sigma
Tween-20	Sigma
xylol	Roth

yeast extract	Difco
β-mercaptoethanol	Sigma

6.2 INSTRUMENTS

Instrument	Type	Company
autoclave	667-1ST	Aigner
balances	LC6201S, LC220-S	Sartorius
betacounter	Thriathler	Bioscan
binocular	MZ 2.5	Leica
blades	Sec35	Microm
centrifuges	Evolution RC	Roth
	5417 R, 5424 R	Eppendorf
chambers for electrophoresis	PerfectBlue™ Mini Gel	Peqlab
confocal laser-scanning microscope	Olympus IX81-Fluoview FV100	Olympus
developing machine	Curix 60	Agfa
digital camera	Axiocam MRs	Zeiss
freezer (-20°C)		Liebherr
freezer (-80°C)		Heraeus
fridge (4°C)		Liebherr
Geiger counter	LB122	Berthold
gel bloting system	XCell SureLock TM Mini Cell	Invitrogen
gel documentation system	E.A.S.Y.	Herolab
glassware		Schott
heater (radioactive)	13259-032	VWR
humid chamber radioactive		TUPPER
hybridization ovens	Model 400	MEMMERT
ice machine	AF 30	Scotsman

incubators (bacteria)	Innova 4230	New Brunswick Scientific
light source for microscopy	KL 1500	Leica
magnetic heater/stirrer	MR3001	Heidolph
microscope	Axiovert-200M	Zeiss
microtom	SM2000R	Leica
parrafin disposer	EG1166	Leica
pasteur pipettes	135038	Fortuna
Polymerase chain reaction (PCR) machine	MasterCycler Gradient	Eppendorf
pH meter	pH Level 1	InoLab
photometer	Biophotometer 6131	Eppendorf
pipettes	Ergo One	Starlab
	Pipetman	Eppendorf
power supplies for electrophoresis	E443	Consort
	EC250-90, EC3000-90	Thermo
	EPS200	Pharmacia Biotech
printer for gel documentation	P95	Mitsubishi
red light		Deitenbach/Philips
repetitive pipette	Multipette® plus	Eppendorf
shaker	Polymax 1040	Heidolph
slide holders (radioactive)	Peel-A-Way	Polyscience
slide warmer	BV SW 85	Adamas instrument
software microscope	Axiovision	Zeiss
spectrophotometer/microplate reader	SIAFR	Synergy HT
thermomixer	comfort	Eppendorf
UV-lamp	N-36	Benda
water bath	U3 AQUAline AL 12	Julabo LAUDA
water bath for tissue	HI 1210	Leica

water conditioning system (for DEPC-H_2O)	**MilliQ biocel**	**Millipore**
waterbath (radioactive)	WB14, W200	MEMMERT

6.3 CONSUMABLES & OTHERS

Consumables	Company
adsorbent silica pearls	Solvay catalytics
cassettes, lids for embedding molds	MICROM
coverslips 24x60, #1	Roth
filter paper	Whatman3 mm
filter tips	Starlab
gloves	Meditrade
gloves, nitrile	Kimtech Science
high performance X-ray film	BioMa MR; Kodak
hyperfilm	Amersham
KODAK D 19 developer	Kodak
KODAK fixer	Kodak
multiwell plates	Nunc
one way needles	Terumo
one way syringes	Terumo
pasteur pipettes	Brand
PCR reaction tubes	Biozym
photographic emulsion NTB2	Integra Biosciences, Kodak
pipette tips	Starlab
plastic pipettes	Greiner bio-one
plates for bacterial culture	Greiner bio-one
PRC reaction lids	Biozym
PVDF membrane	Millipore

reaction tubes (0.1 ml, 1.5 ml, 2 ml)	Eppendorf
tissue cassettes	Merck Polyscience
transfer pipettes	Sarstedt
wipes	Kimtech Science

6.4 STOCK SOLUTIONS AND BUFFERS

Solution	Ingrediens
"Quick and dirty" buffer	5 mM KCl 10 mM Tris 0.5% NP-40 0.5% Tween-20
Blocking solution (IHC)	3% goat serum in PBS
Blocking solution (WB)	5% skim milk powder in 1x TBS-T
Cresyl violet solution (Nissl staining)	0.5% cresyl violet 2.5 mM sodium acetate 0.31% acetic acid Add 500 ml DPEC-H_2O filter before use
DAPI stock solution (histology)	5 mg/ml DAPI in Dimethylformamide store at -20°C use 1:25000 in PBS
DTT/DEPC-H_2O	1 M DTT 0.5 M DTT
EDTA/DEPC-H_2O stock solution; pH 8.0	0.5 M EDTA Adjust pH with NaOH autoclaved

Hybridization Chamber Fluid	50% formamide 10% 20x SSC 10% hybridmix in DEPC-H_2O
Hybridmix	Do not outoclave so handle with care, use DEPC-trated buffers, store hypridization mix in 1-5 ml aliquots at -80°C until max. 1 year 20 mM Tris-HCl pH 8.0 300 mM NaCl 5 mM EDTA pH 8.0 10 % dextran sulphate 0.02 % Ficoll 400 0,02 % PVP40 0.02 % BSA 0,5 mg/ml e 0,2 mg/ml carrier DNA 200 mM DTT
Ionic strength buffer	120 mM NaCl
Loading buffer 5x for WB	5x sample loading buffer (Invitrogen) 4% β-mercaptoethanol
Loading buffer for agarose gels	0.25% bromophenol blue 0.2% Xylene cyanol 40% Sucrose in H_2O
Mildly acidic buffer; pH 2.5	100 mM glycine-HCL
NH_4Oac/DEPC-H_2O stock solution	3M Autoclaved

NTE/DEPC-H_2O (5x) stock solution	**2.5 M NaCl** **50 mM Tris-HCl pH 8.0** **25 mM EDTA**
PBS; pH 7.4	171 mM NaCl 3.4 mM KCl 10 mM Na2HPO4 1.8 mM KH2PO4 autoclaved
PBS; pH 7.4	136 mM NaCl 2.7 mM KCl 10 mM $NaHPO_4$ 1.8 mM KH_2PO_4 autoclaved
PFA, 4%	4% PFA in PBS
Proteinase K/DEPC-H_2O stock solution; pH 8.0	0.5 M Tris-HCL; pH 7.5 50 mM EDTA; pH 8.0
RIPA buffer (protein lysis buffer)	50 mM Tris-HCl 150 mM NaCl 3 mM EDTA 1% Triton-X 100 0.5% SDS 0.5% sodium desoxycholate 1 tablet complete protease inhibitor 1 tablet phosphatase inhibitor
Running buffer (1x) WB	5% 20x NuPAGE® Running buffer in DEPC-H_2O

SSC/DEPC-H_2O (20x) stock solution; pH 7.4	3 M NaCl 0.3 M sodium citrate
TAE (10x)	0.4 M Tris base 0.1 M acetate 0.01 M EDTA
TAE/DEPC-H_2O (10x) stock solution; pH 8.0 (In situ hybrisation; ISH)	1M TAE Autoclaved
TBS (10x)	0.25 M Tris-HCl pH 7.5 1.37 M NaCl
TBS-T	1x TBS 0.05% Tween-20
Transfer buffer (1x)	5% 20x NuPAGE® Transfer buffer (Invitrogen) 10% methanol
Transfer buffer (1x) WB	5% 20x NuPAGE® Transfer buffer 10% methanol In DEPC-H_2O
Tris-HCL/DEPC-H_2O (10x) stock solution **pH 8.0 (for in situ-hybridisation)**	5 M Tris base Autoclaved.
Tris-HCl/DEPC-H_2O; pH 7.5 (for ISH and IHC)	1M Tris base

6.5 KITS

Kit	Company
ECL detection kit	Amersham
FuGENE-6 transfection kit;	ROCHE
G-beads and Pierce Crosslink Magnetic IP/CO-IP Kit	Thermo scientific
Pierce® BCA Protein Assay Kit	Thermo Scientific
Qiagen Plasmid Maxi Kit	QIAGEN
Qiagen Plasmid Maxi Kit	QIAGEN
RNeasy® MinElute Cleanup Kit	QIAGEN
Vectastain Elite ABC Kit	Vector Labs

6.6 OLIGONUCLEOTIDES FOR GENOTYPING

Name	Sequence	Product size
Oligos for allele-specific genotyping for wild-type (WT) *Mash1* allele:		
Oligo Mash1exon-D1 (WT-1D)	5`CTCGTCCTACTCCTCCGAC-3`	377bp
Oligo Mash1intron-R1 (WT-1R)	5`-CTCAATACGCAGGGTCTCTATG-3`	
Oligos for allele-specific genotyping for the targeted *Mash1* allele:		
Oligo PGKpolyA-D1 (Mut-1D)	5`-GATCTCTCGTGGGATCATTG-3`	303bp
Oligo Mash1intron-R1 (WT-1R)	5`CTCAATACGCAGGGTCTCTATG -3`	

The PCR reaction solution contained 3 primers, 2 of which identifies the presence of an intact *Mash1*gene (Mash1exon-D1 and Mash1intron-R1) and the other the presence of the gene-targeting vector (OligoPGKpolyA-D1 and Mash1intron-R1)

Name	Sequence	Product size
Oligos for allele-specific genotyping for WT *Mgn* allele:		
Oligo MM108	5`-GCGGAATGCAGAGCTCTGAG-3`	334bp
Oligo MM109	5`-GAACGAGCTGGGCAAGACAG-3`	
Oligos for allele-specific genotyping for the targeted *Mgn* allele:		
Oligo MM107	5`-CAGAGACTGGAAGGAGAGTCCTTG-3`	395bp
Oligo tlacZ	5`-AGCATGATCTTCCATCACGTCG-3`	

The PCR reaction solution contained 2 pairs of primers, one, which identifies the presence of an intact *Mgn* gene, the other the presence of the Tau-LacZ cassette

6.7 WORK WITH BACTERIA

6.7.1 *Escherichia coli (E. coli)* strains

Strain	Company
DH5α	Invitrogen
TOP10	Invitrogen

6.7.2 Media and Agar

Solution	Ingredients
Ampicilin selection medium	Luria-Bertani (LB) medium with 50 µg/ml ampicillin
Ampicillin selection agar	LB agar with 100 µg/ml ampicillin
Kanamycin selection agar	LB agar with 100 µg/ml kanamycin
Kanamycin selection medium	LB medium with 25 µg/ml kanamycin
LB agar	98.5% LB-Medium 1.5% Bacto Agar
LB (Luria-Bertani) medium	10 g Bacto peptone 5 g yeast extract 5 g NaCl add 1L H_2O
SOC Medium	Prepare a solution containing the first four reagents, sterilize at 121°C, then add sterile MgC_{l2} and glucose 2% tryptone 0.5% yeast extract 10 mm NaCl 2.5 mm KCl 10 mm MgC_{l2} 20 mm glucose

6.8 ENZYMES

Enzyme	Company
desoxyribonuclease 1 (DNase I)	Roche
PCR mastermix	5 PRIME
proteinase K	Roche
restriction enzymes	NEB, Roche
ribonuclease A (RNase A)	20 µg/ml, Roche
RNAse-Inhibitor (RNasin)	Promega
T7, T3, SP6 ribonucleic acid (RNA) polymerases	Roche

6.9 PLASMIDS FOR IN SITU HYBRIDIZATION

Plasmid/Probe	Anti-sense linear.	Anti-sense Polymerase	Sense linear.	Sense Polymerase	Construct from
Gad76 **bp 934-1786; NM_008077**	*Pst*I	T7	*Bam*HI	T3	Guimera *et al*. 2006
Gata2 **bp 229-946; BC107009.2**	*Xho*I	T7	*Bam*HI	T3	Guimera *et al*. 2006
***Lim1* (*Lhx1*)** **bp 1202-2453; Z27410.1**	*BamHI*	T7	*Eco*RI	Sp6	Guimera *et al*. 2006
Mash1 **bp 5-1997; NM_008553.2**	*Sma*I	T7	*Xba*I	SP6	Guimera *et al.* 2006
Megane (Helt) **bp 166-1000, DQ294234**	*Bam*HI	T7	*Sal*I	T3	Guimera *et al*. 2006
Sox14 **bp 715-4000**	*Bam*HI	T7	*EcoRV*	SP6	Guimera *et al.* 2006
Tal1 **bp 921-1472; BC063060.1**	*Bam*HI	T7	*Eco*RV	SP6	Guimera *et al.* 2006
Tal2 **bp 332-924; NM_009317.2**	*Not*I	T7	*Sal*I	T3/SP6	Guimera *et al*. 2006
vGlut2 (Slc17a6) **bp 1030-1770; NM_080853.2**	*Eco*RV	SP6	*Bam*HI	T7	Guimera *et al*. 2006

6.10 CO-IMMUNOPRECIPITATION (CO-IP) AND WESTERN BLOT (WB)

6.10.1 Primary antibodies for Co-IP and WB

Antibody	Dilution	Company
Anti-c-myc	1:8000	Dianova #9E10.3
Anti-FLAG	1:50000	Sigma #F1804
Anti-MASH1	1:300	BD-Pharmingen
Anti-MGN	1:1000	J. Guimera; Clone #1 GenBank accession no. ABB96784.1
Mouse anti-β-actin	1:5000	Abcam #ab6276

6.10.2 Secondary antibodies for Co-IP and WB

Antibody	Dilution	Company
HRP-conjugated goat mouse IgG (H+L	1:1000	Jackson #115-035-003

6.11 IMMUNOHISTOCHEMISTRY (IHC)

6.11.1 Primary antibodies for IHC

Antibody	Dilution	Company
Mouse anti-BRN3A	1:200	Santa Cruz sc-8429
Mouse anti-CALBINDIN	1:500	Swant #300
Mouse anti-MASH1 isotype IgG1	1:300	BD Pharmingen #556604
Mouse anti-MGN	1:2000	J. Guimera; Clone #1, GenBank accession no. ABB96784.1
Mouse anti-NeuN	1:1000	Chemicon #MAB377
Mouse anti-NKX2-2	1:250	DSHB #74.5A5-c
Mouse anti-TH	1:1000	Merck/Millipore #AB152

Rabbit anti-CALRETININ	1:200	Swant CR #7699/4
Rabbit anti-CLEAVED CASPASE-3	1:300	Cell Signaling/ NEB #9661
Rabbit anti-GABA	1:300	Sigma #A2052
Rabbit anti-GATA2	1:250	Abcam ab70366
Rabbit anti-PHOSPHO HISTONE 3	1:3500	Upstate Biotech #06-570
Rabbit anti-TH	1:1000	Millipore AB152
Rabbit anti-β-galactosidase	1:100	AbD Serotec #AHP1292;

6.11.2 Secondary Antibodies for IHC

Antibody	Dilution	Company
Donkey anti-mouse Cy3	1:250	Jackson Immuno 715-166-151
Donkey anti-mouse Alexa 594	1:500	Life Technologies; A21203
Donkey anti-rabbit Alexa 594	1:500	Life Technologies; A21207
Donkey-anti-mouse Alexa 488	1:500	Life Technologies; A21202
Donkey-anti-rabbit Alexa 488	1:500	Life Technologies; A21206
Goat anti-mouse IgG-1 Alexa Fluor 594	1:500	Invitrogen A21125
Goat anti-mouse IgG-2b Alexa Fluor 488	1:500	Invitrogen A21141

6.13 MOUSE STRAINS

Mouse-strain	Source
***Mash1*-mouse**	(Guillemot *et al.*, 1993)
***Mgn*-mouse**	(Guimera *et al*., 2006a)
Wild type	C57BL/6J

7 METHODS

7.1 MOUSE HUSBANDRY

All mice were kept and bred at the Helmholtz Centre Munich according to national guidelines. Five mice at maximum were house grouped in individually ventilated cages (IVC). The mice were maintained on a 12 h dark/light cycle with food and water *ad libitum*. The temperature was kept at 22 ± 2°C with a relative humidity of 55 ± 5%. To breed the mice, matings were set up. Pups were weaned with an age of 3 weeks according to their gender. For identification, earmarks were made and tail clips were taken for genotyping. Upon crossing double-heterozygous (dblHet) mice (*Mgn-/+/Mash1-/+* x *Mgn-/+/Mash1-/+* inbreed mice that had been consecutively backcrossed for eight generations to C57BL/6, a myriad of compound mutants could be found. The particular abbreviation (if applicable) of compound mutants were referred to as follows:

1. the term "double knockout" (dblKO) was reserved for *Mgn-/-/Mash1-/-* mice
2. the term "single mutant" (sglMut) was reserved for *Mgn-/-/Mash1+/+* or *Mgn+/+/Mash1-/-* mice
3. the term "double heterozygous mutant" (dblHet) was reserved for *Mgn+/-/Mash1+/-*
4. mice, carrying only one active allele of either *Mash1* or *Mgn* (compound homozygous, heterozygous mutant combination) *Mgn+/-/Mash1-/-* or *Mgn-/-/Mash+/-*

The animal experiments were conducted in accordance with the recommendations in the "*Guide for the Care and Use of Laboratory Animals of the European Union and of the Federal Republic of Germany (TierSchG)"*. The study protocol was approved by the *"HMGU Institutional Animal Care and Use Committee (ATV)"*.

7.2 MOLECULAR BIOLOGY METHODS

7.2.1 Transformation of chemically competent bacteria

To prepare the riboprobes for the hot in situ hybridization (ISH), transformation was carried out using chemically competent *Escherichia coli (E. coli)* bacteria. For each transformation an aliquot of 100 µl of bacteria was thawed on ice (20-30 min). 50 ng of plasmid were added to the bacteria suspension, flipped carefully and incubated on ice for 20-30 min. After heat shock treatment at 42°C (45 s) in a water bath, to permeabilize the plasma membrane, the suspension was chilled on ice for 2 minutes. Next, 500 µl of SOC medium was added and incubated for 1 h at 37°C. The suspension with the transformants were plated on LB agar plates containing the appropriate antibiotic for selection (100 µg ampicillin or 50 µg kanamycin) respectively and placed in a 37°C incubator o/n.

7.2.2 Preparation of plasmid DNA – Maxiprep

Selected colonies from the transformation were picked and transferred into glassware containing 3 ml hand warm LB medium dosed with the appropriate antibiotic and incubated 8h - o/n at 37°C. Next day, 1 ml of this suspension was added to 200 ml hand warm LB medium with the respective antibiotic and again incubated o/n at 37°C, shaking. To extract the plasmid DNA produced by the transformed bacteria, a QIAGEN Maxi Prep Kit used and carried out following the manufacturer`s instruction.

7.2.3 Restriction digest of plasmid DNA

To digest the plasmid DNA, DNA, enzymes and buffers were mixed following manufacturer`s instructions. For 1 µg of DNA, 2 units (U) of restriction enzyme and the appropriate buffer were added and incubated for minimum 3 h - o/n at 37°C. 20 µg of a plasmid containing the target gene were linearized with the suitable restriction enzyme and the digested DNA fragments were proven of linearization by gel electrophoresis.

7.2.4 Agarose gel electrophoresis

Gel electrophoresis was performed to check complete digestion. Linerized probes were mixed with loading buffer and loaded on agarose gels of different concentrations of agarose (polymerase chain reaction (PCR): 2.5%, proof of linearization of plasmids: 1-2%). The gels contained 1 µg/ml ethidium bromide. The run was performed in 1xTAE buffer at 100V for 30-60 min, depending on the size of the fragments. As a length standard ladder (PCR: 100bp ladder; proof of linearization of plasmids: 1kb+

ladder) was applied next to the linerazided plasmids used. DNA fragments were identified by size under UV light with a wavelength of 366 nm.

7.2.5 Purification of the linearized plasmid DNA

The DNA was purified using the Quiagen PCR purification Kit following manufacturer`s instructions and eluted in 50 µl DEPC-H_2O. The concentration of linearized DNA was determined with a spectro-photometer by measurement of the optical density (OD) at a wavelength of 260 nm (OD_{260} = 1.0 corresponds to 50 µg/ml double stranded or 33 µg/ml single stranded DNA) and stored at -20°C until use.

7.2.6 Isolation of genomic DNA

The genomic DNA from cells, mouse tails and embryonic tissue was isolated as follows: The tissue was incubated shaking at 56°C for 5 h – o/n 400 µl lysis buffer containing proteinase K (0.1 mg/ml). Following, proteinase K was inactivated at 90°C for 30 min. Samples were centrifuged at 12,000 rpm (radius: 8.4; RCF: 13523; 5 min) at RT and processed for PCR analysis. For PCR analysis 1 µl of isolated DNA was used. The remaining isolated DNA was stored at 4°C for eventual re-genotyping.

7.2.7 Genotyping of mice by PCR

For amplification of DNA fragments from genomic DNA, PCR analysis was performed.

Set up:

1 µl of isolated DNA
1 µl of 10 µg forward primer for the WT allele
1 µl of 10 µg reverse primer for the WT allele
1 µl of 10 µg forward primer for the mutant allele
1 µl of 10 µg reverse primer for the mutant allele
10 µl 5x MasterMix

Add up to 25 µl with H_2O DPEC

The following program was used for every PCR:

94°C	4 min		
94°C	30 sec	}	35-40 cycles:
57°C	30 sec		
72°C	30 sec		
72°C	10 min		
4°C	∞		

PCR amplification products were electophoretically (long run; 2-2.5% agarose gel) identified by size (see. 6.6 Oligonucleotides for Genotyping).

7.3 HOT IN SITU HYBRIDISATION

To ensure an RNAse free working environment, solutions and glassware were autoclaved and disposable gloves were used during the entire protocol.

Labeling (day 1)

Riboprobes were generated by transcription of linearized plasmid DNA templates with the respective RNA polymerase following this protocol.

3 µl 10x transcriptions buffer
3 µl NTP-mix (rATP/rCTP/rGTP 10 mM each)
1 µl 0,5 M DTT
1 µl RNasin 40 U/µl
8 µl ^{35}S-thio-rUTP from Perkin Elmer; 12,5 mCi/mM
1 µl T7, T3 or SP6 RNA polymerase (20 units/µl)
17 µl total
x µl H_2O-DEPC
x µl (1.5 µg DNA) linearized plasmid DNA template
13 µl total

30 µl total volume

All reaction solutions were mixed at RT and incubated at 37°C for 3 h in total in the radioactive laboratory. After 1 h, 0.5 µl of RNA polymerase was added again. Subsequent, 2 µl RNase-free DNase I was added to digest template DNA for 15 min at 37°C and riboprobes were purified using RNeasy MinElute Cleanup Kit according to the supplied protocol. 1 µl of riboprobe in 2 ml scintillation liquid was used to measure radioactivity in counts per minute (cpm) in a beta-counter. Minimum threshold for used labeled riboprobes was 0.5 million cpm. Riboprobes were stored at -20°C. Preferentially, riboprobes, were used the next day. Storage up to 3 days should not be exceeded to ensure proper results.

Pretreatment of paraffin sections

Paraffin sections were transferred to racks (20 slides per rack) and processed according to the following protocol. Each rack was started 10 min after the former.

Step	Solution	Time	Remarks
Dewax	Xylol	15 min	Fresh Xylol
Dewax	Xylol	15 min	Fresh Xylol
Dewax	Xylol	15 min	Check dewaxing, time can be elongated
Rehydration	100% ethanol	2 x 5 min	
Rehydration	70% ethanol	5 min	
Wash	DEPC-H_20	3 min	
Wash	0.01 PBS/DEPC-H_2O	3 min	
Fixation	4% PFA/0.01 PBS	20 min	On ice
Wash	0.01 PBS/DEPC-H_2O	2 x 5 min	
	20 µg/ml Proteinase K in Proteinase-K-buffer	7 min	Add 200 µl of proteinase K (20 mg/ml)
Wash	0.01 PBS/DEPC-H_2O	5 min	
Fixation	4% PFA/0.01 PBS	20 min	On ice (same solution from step 6)
Wash	0.01 PBS/DEPC-H_2O	5 min	
	200 ml of rapidly stirring TEA	10 min	Add 600 µl acetic anhydride (for the 2nd rack no buffer change but add another 600 µl acetic anhydrid)
	2xSSC	2 x 5 min	
Dehydration	60% ethanol/DEPC-H_2O	1 min	
Dehydration	70% ethanol/DEPC-H_2O	1 min	
Dehydration	95% ethanol/DEPC-H_2O	1 min	
Dehydration	100% ethanol	1 min	
Drying (dust free)			

Prehybridization

Pretreated slides were immediately used for hybridization according to procedure, or stored at –80°C in box with desiccant for 1 – 2 days. Air-dried sections were prehybridized with thawed hybridization buffer (90 µl per slide) cover slipped for 1 h at 58°C in a humid chamber containing chamber fluid.

Hybridization

Hybridization mix containing ^{35}S - labelled-riboprobe (35000000 to 70000000 cpm/slide) was mixed with 100 µl hybridization buffer per slide, then heated to 90°C (2 min), chilled shortly on ice and kept for further processing at RT. Coverslips were removed from the slides and as much as possible liquid was removed without destroying the tissue. After application of the hybridization mix to the slides, they were covered with coverslips and again incubated in the mentioned humid chamber at around 58°C o/n - 20h. Hybridization temperature was about 25°C under the melting temperature of the probe, the higher the temperature was chosen, the less background resulted.

Wash (day 2)

Step	Solution	Time	Remarks
1	4xSSC	4 x 5 min	
2	NTE (20µg/ml RNaseA)	20 min	Add 500 µl RNaseA(10mg/ml) to 250 ml of NTE
3	2xSSC/1 mM DTT	2 x 5 min	50 µl of 5 M DTT/250 ml
4	1xSSC/1 mM DTT	10 min	50 µl of 5 M DTT/250 ml
5	0,5xSSC/1mM DTT	10 min	50 µl of 5 M DTT/250 ml
6	0,1xSSC/1 mM DTT	2 x 30 min	50 µl of 5 M DTT/250 ml
7	0,1xSSC	2 x 10 min	
8	30% ethanol in 300 mM NH_4OAc	1 min	
9	50% ethanol in 300 mM NH_4OAc	1 min	
10	70% ethanol in 300 mM NH_4OAc	1 min	
11	95% ethanol	1 min	
12	100% ethanol	2 x 1 min	
Air dry in dust free area			

Autoradiography of slides (day 3)

Dried sections were exposed to a high performance X-ray film to check hybridization performance and signal strength. After 3 days, the film was developed and kept to estimate exposure time of dipped slides while slides where transferred to dipping holders and stored at RT.

Dipping of Slides

Photographic emulsion NTB2 was melted in a water bath at 42°C for at least 1 h. Its sensitivity against light, metal and movement demanded a dipping of slides into the solution (15 s per holder) with slow movements under red safety light only. Dipped slides were dried at RT in absolute darkness o/n. Next day the slides were stored in light-tight boxes with silica gel at 4°C for 4-6 weeks depending on the strength of signal observed on the mentioned film.

Development of Slides

After the long-time exposure, boxes with slides were equilibrated at RT for at least 1 h. Next, slides were developed in KODAK D 19 developer (4 min), washed in tap water (30 sec), fixed in KODAK fixer (6 min), and rinsed in running tap water for 20 min. Remaining emulsion on the back side of slides was scratched off with razor blades. Slides were either stored at 4°C until processing or immediately counterstained with Cresyl violet (see 7.5.3 Counterstaining Nissl/Cresyl violet).

7.4 ANALYSIS OF PROTEIN SAMPLES

The analysis of protein samples was performed in collaboration with Dr. Jordi Guimera, according to the following protocol.

7.4.1 Isolation of protein

The day, on which a vaginal plug was detected early-day (between 7 – 9 o`clock), was considered E0.5. Additionally, embryos were staged precisely by counting somites. Embryos were dissected from Carbon dioxide (CO_2) asphyxiated pregnant dams, put immediately into pre-cooled 4°C PBS. For the MGN/MASH1 heterodimer and homodimer Co-IP assays, dMB, vl/vMB, and the rest of the body from E12.5 WT embryos as well MB tissue from E12.5 *Mgn-/-* and *Mash1-/-* mutant embryos were dissected and collected. Brains were dissected in pre-cooled PBS and immediately stored on dry ice. For the 2-protein Co-IP validation assays in mammalian cell culture, mouse embryonic stem cells were transiently co-transfected with the coding region of *Mgn* or *Mash1* (N-terminal FLAGtagged) and *Mash1* or *Mgn* (N-terminal myc-tagged) subcloned into pcDNA3.1 vectors according to the described protocol in (Wende *et al.*, 2015).

The tissue was homogenized with a 6mm needle syringe in RIPA buffer containing protease inhibitor cocktail with DNases and RNases (1 tablet/10ml buffer). Protein suspensions was incubated for 20 min on ice and then centrifuged at 12,000 rpm (radius: 8.3; RCF: 13362; 20 min) at 4°C. The supernatant was transferred into a new tube and further used for quantification of protein concentration as the soluble protein fraction.

The protein concentration of the soluble protein fractions was determined by BCA essay. Protein supernatant was diluted in suspensions of 1:5 and 1:10. According to the manufacturer`s protocol, the reagents of the Kit were mixed and applied to a 96-well plate. Protein dilutions were added. Further, for precise concentration measurements, mixtures of decreasing concentrations of standard BCA were set up according to the manufacturer`s protocol and also with reagents of the Kit in wells next to the protein dilutions of interest. After incubation of 30 min at 37°C, the absorption was measured at a wavelength of 562 nm with a photometer. From the values of the decreasing concentrations of standard BCA, the standard curve was established with Microsoft Office Excel. Based on the standard curve, protein concentration was determined.

7.4.2 Co-Immunoprecipitation

The tissue obtained (step 2.2.1) was incubated with MASH1 or MGN antibodies covalently coupled and cross-linked with G-beads following the manufactor`s protocol. The protein lysate was incubated o/n rotating at 4°C. Next day, the mix was washed with low ionic strength buffer and eluted with mildly acidic buffer for 10 min each. The products were verified by classical WB analysis using anti-MGN antibody, anti-MASH1 antibody, and peroxidase-conjugated antibodies. Mouse anti-β-ACTIN antibody was used as a quality control prior to Co-IP.

7.4.3 Western Blot (WB) analysis

Proteins were separated according to their size on SDS polyacrylamide gel electrophoresis using the NuPage® Novex gel system from Invitrogen. 20 µg of total protein per sample was mixed with 5x loading buffer containing 1:25 β-mercaptoethanol. Mixtures were flipped, shortly centrifuged, then denatured at 95°C for 5 min and chilled on ice. The samples were loaded on precast gels in running buffer. SDS-PAGE was performed at 120 V for 1 h. The transferred gel was blotted at 30 V for 70 min on a methanol-activated PVDF membrane in transfer buffer containing ethanol. The blotted membrane was blocked with 4% skim milk in TBS-T for 1 h at RT and incubated with primary antibody diluted in blocking solution (4% skim milk in TBS-T) at 4°C overnight (o/n). Next day, the membrane was washed 3 times (10 min each) with TBS-T and incubated with secondary, horseradish-peroxidase-conjugated antibody in the respective blocking solution for 1 h at RT. After washing again three times with TBS-T (10 min each), the protein-blotted side of membrane was covered with ECL detection reagent and incubated for 1 min in the dark. The membrane was exposed to a chemiluminescent film for seconds to several minutes, depending on the signal intensity. Exposed films were developed using a developing machine.

7.5 HISTOLOGY

All analyses were confirmed using 3 embryos of wild type and mutant mice, each from different litters.

7.5.1 Collection and Dissection of embryos

Noon on the day when a vaginal plug was detected was considered E0.5. Embryos were staged precisely by counting somites. Embryos were dissected from CO_2-asphyxiated pregnant dams, put immediately into pre-cooled 4°C PBS, dissected and transferred to 4% PFA. Embryos from E10.5-E15.5 were kept intact, while for embryos older than E15.5, the brain was taken out of the scull before they were processed as described. For post-fixation, the tissue was kept rotating in 4% PFA at 4°C. Parts of each embryo body were kept for genotyping analysis.

7.5.2 Dehydration and Paraffin embedding

Embryos and dissected brains from different stages (E9.5 - E18.5) were post-fixed in 4% PFA o/n at 4°C, washed in PBS, dehydrated in an ascending ethanol series (30%, 60%, 70%, 85%, 95%, 100%, 1 h each), kept o/n in 100% ethanol at 4°C, rotating. Next day, the tissue was cleared in xylol (10 min for E10.5 - E13.5; 20 min for E14.5 - E18.4), transferred to paraffin wax (56-58ºC; 3 changes, open lid, 3 h each) and then paraffin embedded. Embryos were cut coronal or sagittal on a microtome at 4–6 µm, depending to the stage of embryos, flattened in a 39°C water bath and then mounted on slides in series of 4-8. After drying o/n at 37°C, they were stored at 4°C in storage cassettes until use.

7.5.3 Counterstaining with Cresyl violet

To counterstain the tissue, Nissl (Cresyl violet) staining was performed. Slides were stained in Cresyl violet staining solution (1-5 min, depending on the tissue) and exceeding Cresyl violet was washed away by rinsing in purified water until water became clear. After 2 short washes in 70% ethanol (1 min each), slides where bleached in 96% ethanol with 0.5% acetic acid until the desired staining intensity was reached. Then, 2 washes in 96% ethanol (1 min each) were followed by 2 washes in 100% ethanol (2 min each) and 2 washes in xylol (5 min each). To mount the stained tissue on slides small amounts of pertex were applied and covered with coverslips. Then slides were dried o/n at RT.

7.6 IMMUNOHISTOCHEMISTRY

7.6.1 3-3´Diaminobenzidine (DAB) staining

DAB is a commonly used compound for immunohistochemical staining of proteins. TBS-T contained 0.1% Tween-20. The staining was performed according to the following protocol:

Step	Solution	Time	Remarks
1. Dewaxing	Xylol	30 min	
2. Rehydration	100% ethanol	2x 5 min	
3. Rehydration	96% ethanol	2x 5 min	
4. Rehydration	70% ethanol	2x 5 min	
5. Rehydration	50% ethanol	5 min	
6. Rinse	DM-H_2O	3 min	Floating until all streaks are gone
7. Antigen retrieval	1x Na-Citrat buffer	3 min	
8. Antigen retrieval	1x Na-Citrat	30 min	Slow cooker, Microwave 900W
9. Antigen retrieval	1x Na-Citrat	10 min	Cool down
10. Wash	TBS-T	10 min	Cool down
11. Quenching	methanol + H_2O_2	5 min	Destruction of endogenous peroxidases
12. Wash	DM-H_2O	10 min	Floating until all streaks are gone
13. Blocking	3% goat serum/TBS-T	1 h	
14. 1st antibody	antibody dilution solution	o/n	Coverslips, humid chamber, 4°C o/n
15. Wash	TBS-T	3x 5 min	
16. 2nd antibody	antibody dilution solution		Coverslips, humid chamber, RT 1 h

17. Intensifying	KPL Streptavidin-Peroxidase	30 min	
18. Intensifying	DAB 2 Component Kit		Prepare 20 min before, drop on, no coverslips, check until signal is strong enough
19. Stopping	tab H_2O		
20. Wash	tab H_2O	3 min	Floating
21. Equilibrate	DM H_2O	3 min	
22. Hämatoxylin staining	Hämatoxylin solution	minimum 1 s	
23. Dehydration	50% ethanol	5 min	
24. Dehydration	70% ethanol	5 min	
25. Dehydration	96% ethanol	5 min	
26. Dehydration	100% ethanol	5 min	
27. Dehydration	Xylol	5 min	
28. Embedding	Pertex		Work quick
29. Drying		o/n	In the hood,
30. Storage			RT

7.6.2 Immunoflourescence

For Immunoflourescence stainings, step 1-14 was performed as for DAB staining, leaving out the destruction of endogenous peroxidases (step 11 and 12), as follows:

Step	Solution	Time	Remarks
Dewaxing	Xylol	2 x 10 min	
Rehydration	100% Ethanol	2x5 min	
Rehydration	96% Ethanol	2x5 min	
Rehydration	70% Ethanol	2x5 min	
Rehydration	50% Ethanol	5 min	
Rinse	DM H_2O		Floating until all streaks are gone
Antigen retrieval	0.01M Na-Citrat buffer	3 min	
Antigen retrieval	0.01M Na-Citrat buffer	30 min	Slow cooker, Microwave 900W
Antigen retrieval	0.01M Na-Citrat buffer	20 min	Cool down
Wash	TBS-T	2 x 5 min	
Blocking	10% goat serum/ TBS-T	1h	
1st antibody	Antibody dilution solution	o/n	Coverslips, humid chamber, dark, 4°C
Wash	TBS-T	3 x 5 min	
2nd antibody	Antibody dilution solution	1h	Coverslips, humid chamber, dark, RT
Wash	PBS	3 x 5 min	
DAPI staining	DAPI solution	1 min	Coverslips
Wash	PBS	3 x 5 min	
Embedding	Aqua Polymount		Work quick
Drying		o/n	In the hood, covered
Storage			4°C, dark

8 RESULTS

8.1 MGN AND MASH1 COLOCALIZE IN THE VZ OF THE MB AND FORM HETERODIMERS *IN VIVO*

Both proteins, MGN and MASH1, were able to form homo- as well heterodimers in yeast cells and in mammalian cell culture (Wende *et al.,* 2015). This prompted us to prove if the 2 proteins also interact *in vivo*. Since 2 proteins may never be in close proximity to each other within the cell even though they are otherwise able to interact, colocalization studies were mandatory. Indeed, previous studies report MGN and MASH1 to colocalize in most vlMB cells at E11.5 (Miyoshi *et al.*, 2004). But as the GABAergic phenotype of both single KO mice is circumscribed in the dMB at the onset of dMB GABAergic neurogenesis, we studied colocalization particularly in that area at E12.5: the MGN+ domain was detected in the VZ of the E12.5 MB (m1-m5) restricted exclusively to mitotic neurons, at high levels in the vlMB compared with lower levels in the dMB. Although MASH1 expression domain was broader, as also found in postmitotic neurons, all MGN+ cells were positive for MASH1 in the VZ of the dMB at E12.5 (Fig. 8.1). This colocalization not only detected precise colocalization of the molecules of interest in the dMB but also further proved the possibility of their interaction *in vivo.*

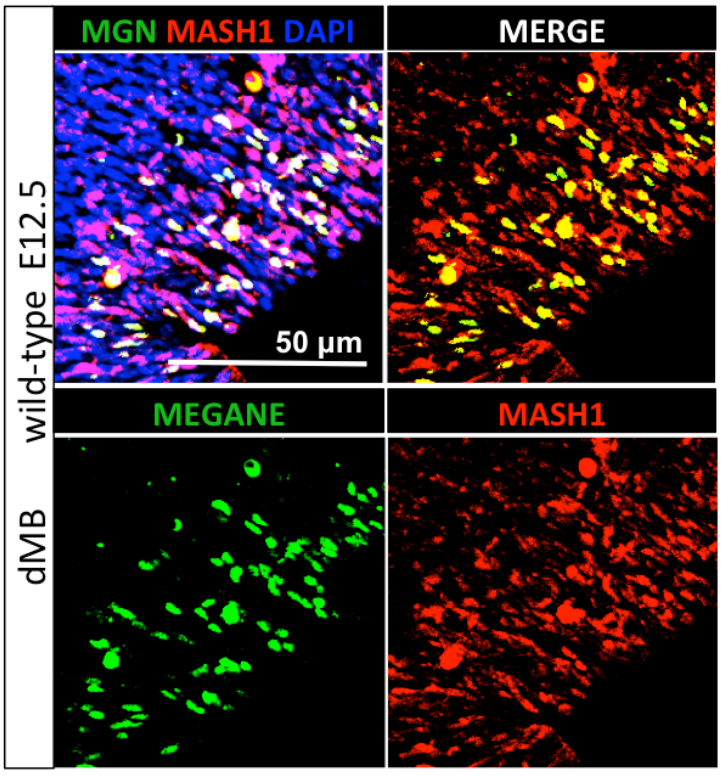

Figure 8.1: MGN and MASH1 colocalize in the dMB.
DAPI counterstain and IHC against MGN, and MASH1 on a coronal section of E12.5 dMB. All MGN expressing cells in the dMB express MASH1 at the onset of dMB GABAergic neurogenesis. The MASH1+ domain is broader since it is also expressed in postmitotic neurons.

To further visualize heterodimerization of MGN and MASH1 *in vivo* we performed Co-IPs of endogenous protein extracts from E12.5 wild-type (WT) and single mutants using specific antibodies recognizing each protein; Co-IP with anti-MASH1 antibody and subsequent WB with anti-MGN antibody, and vice versa, revealed MGN and MASH1 to form heterodimers in the dorsal and ventrolateral aspect of the MB *in* vivo (Fig. 8.2) - visualized by bands at the estimated size of MEGANE protein (Fig. 8.2; A) at 30kDA and for MASH1 protein at 35kDA (Fig. 8.2; B) respectively. Both proteins were ventrally higher expressed compared to dorsally, resulting in thicker bands after Co-IP of vlMB WT tissue compared to dMB WT tissue. Same experimental procedure with brain tissue of single mutants proved that this interaction did not take place in MB lacking one protein partner. As *Mgn* is not expressed in the body, tissue from E12.5 WT bodies was taken as negative control. Embryonic stem cells (ES cells) were used as additional control displaying the interaction: Only in lyzed ES cells containing both proteins, heterodimerization was visualized (kind regards to J. Guimera for providing the experimental results shown in Fig.8.2).

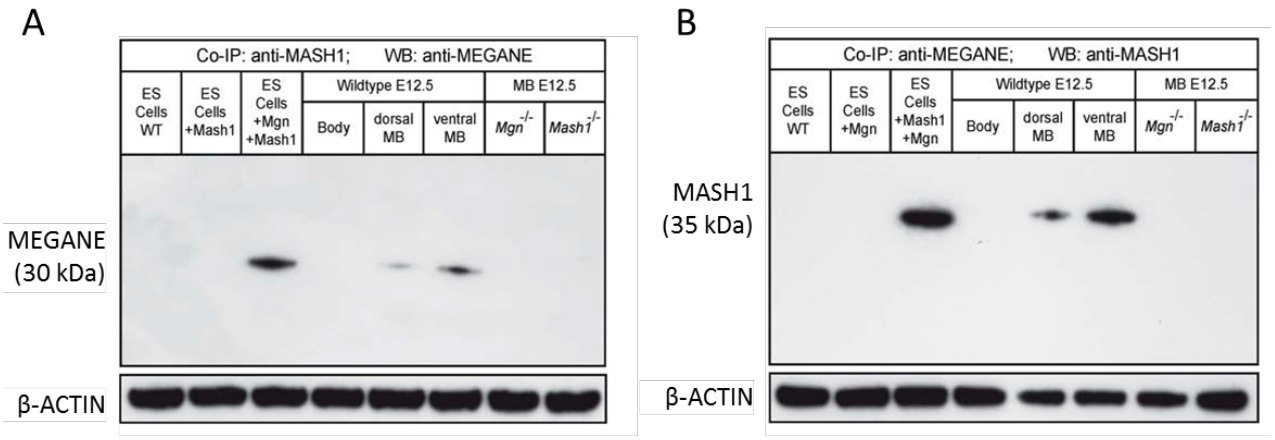

Figure 8.2: MGN and MASH1 form heterodimers in the dMB and vlMB.
(A) WB with anti-MGN-antibody after Co-IP of different protein samples with anti-MASH1-antibody and **(B)** vice versa. Tissues containing both factors (tissue of WT brains at E12.5 dorsal and ventral; embryonic stem (ES) cells transfected with MGN and MASH1) reveal heterodimerization while tissues with only one factor (non-transfected ES cells; body tissue and brain tissue from single knockout mice) do not and serve as negative control.

8.2 dMB GABAERGIC NEUROGENESIS REQUIRES HETERODIMERS OF MGN AND MASH

Remarkably, the phenotype of the single mutants is restricted to the dMB where both genes are expressed to a lower level compared to the vlMB. This raises the question if a third redundant factor takes over MGN or MASH1 function, specifying the vlMB-GABAn at the onset of GABAergic neurogenesis (E10.5) - or MB GABAergic neurogenesis depends on a different mechanism based on heterodimerization of MGN/MASH1. Thus, to identify the function and contribution of the MGN/MASH1 interaction in MB GABAergic neurogenesis, dblKO embryonic mutants of different critical ages were obtained from dblHet breedings. Concomitant loss of function of *Mgn* and *Mash1* displayed a severely compromised phenotype: most MB GABAn in both, the dMB and vlMB at E12.5, were downregulated, determined by the absence of GABAergic marker *Gad67* (and *Gad65,* data not shown; Fig. 8.3). This phenotype occurred with 100% penetrance and persisted until death (data not shown). These observations supposed no other factor being involved in MB GABAergic neurogenesis except for a small population of residual cells located in m5 (intermediate basal pate (Fig. 8.3: B, B'; F, F'; J, J'). Strikingly, this population persisted during maturation (Fig. 8.3; F, F'). As *Mgn* is not expressed in the HB, prominent expression of *Gad67* in the HB of dblKO mutant (Fig. 8.3; D, D') was unchanged compared to WT (Fig. 8.3; C, C'). Accordingly, the subpopulation of mvMB-GABAn of SNpr/VTA that reach the MB from the HB at E14.5 is independent from MGN/MASH1. These GABAergic markers in the SNpr/VTA were detected from E14.5-E15 onwards in dblKO mutants (Fig. 8.3 F-G'). Although *Mgn* and *Mash1* are also coexpressed along the ZLI, *Gad67* expression in dblKO was prominent in this region in dblKO mutants (Fig. 8.3 C-D'). As a consequence of the GAD67/65 downregulation in the dblKO mutant, no GABA transmitter was detectable in dblKO except for the residual cells in m5 (Fig. 8.3; I-J'). Simultaneously, the dopaminergic domain in the MB FP was unaltered compared to WT (Fig. 8.3; H, I). Albeit the loss of all GABAergic markers (*Gad65/67* and GABA) in prospective d/vlMB GABAn, these neurons still migrate out of the VZ zone toward the MZ, as determined by the high stability of the TAU-LACZ fusion protein expressed under the endogenous *Mgn* regulatory elements by homologous recombination in the *Mgn* locus (Guimera *et al.,* 2006b) and the neurotransmitter vesicles of GABA appeared intermingled with *tau-lacZ* expressing neurons (Fig.8.3; J, J').

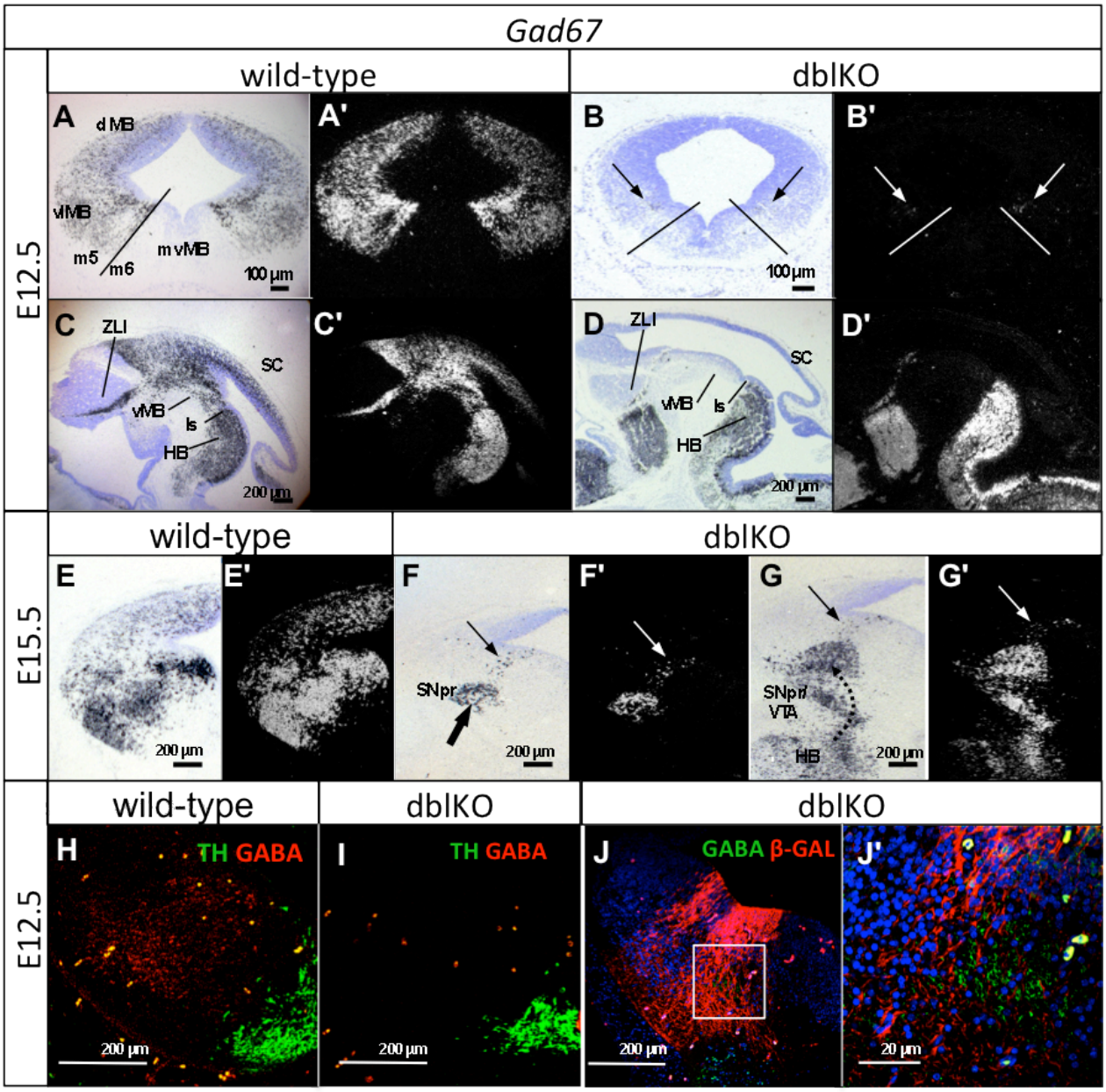

Figure 8.3: MGN and MASH1 are prerequisite for the induction of d/vlMB GABAn.
(A-G') bright- and dark field images of phenotypic analysis of the MB from WT and dblKO mice by ISH with a *Gad67* riboprobe on coronal sections at E.12.5 **(A-B`)** and at E15.5 **(E-G')** and sagittal sections at E12.5 **(C-D')**. **(H-J')** IHC against GABA, TH and β-galactosidase. *Gad67* expression and GABA transmitter is absent in dblKO mutants **(B, B', D, D', F-G', I-J')**. Thin arrows in **(B, B`; F, F``; G, G`)** indicate the presence of residual *Gad67*+ cells in the m5 domain at E12.5 and E15.5. GABAn in the mvMB migrate independently from MGN/MASH1 to the MB from the HB (visualized by dotted arrow **(G)** and appear in the MB from E14.5 onwards (indicated by thick arrow in **(F)**. No neurotransmitter GABA is detected in the MB of dblKO mutant brains at E12.5 while the TH+ domain is unchanged **(H, I)**. Defective GABAn are still present, visualized by IHC against β-galactosidase, and surround the residual GABA+ cells in m5 **(J, J')**.

8.3 MGN MASH1 HETERODIMERS ARE REQUIRED FOR DMB GABAN INDUCTION

In contrast to single mutants or dblKO mutants, where heterodimer formation cannot take place, dblHet mutants (*Mgn+/-Mash1+/-)* displayed normal GABAergic induction as the distribution of of *Gad65/67* mRNAs as well as the neurotransmitter GABA, visualized by ISH and IHC respectively, was equal to WT; dorsally and ventrolaterally, the generation of GABAn was comparable to WT (Fig. 8.4). At E12.5 a slight reduction of dMB GABAn induction was observed (Fig. 8.4; B) which was recovered one day later at E13.5 and GABA vesicles were intermingled with *tau-lacZ* expressing cells (Fig. 8.4; E, H). Along maturating, GABAn of dblHet mutants populated all MB GABAergic nuclei (Fig. 8.4; J) and the phenotype persisted with 100% penetrance. In contrast to dblKO mutants, dblHet mice were vital, reproductive and aged normally. GABAn induction in dblHet mutants suggested, that in the dMB GABAergic neurogenesis is dependent upon heterodimerization of MGN/MASH1 whereas in the vlMB, expression of either *Mash1* or *Mgn* was sufficient (as reported in single mutants).

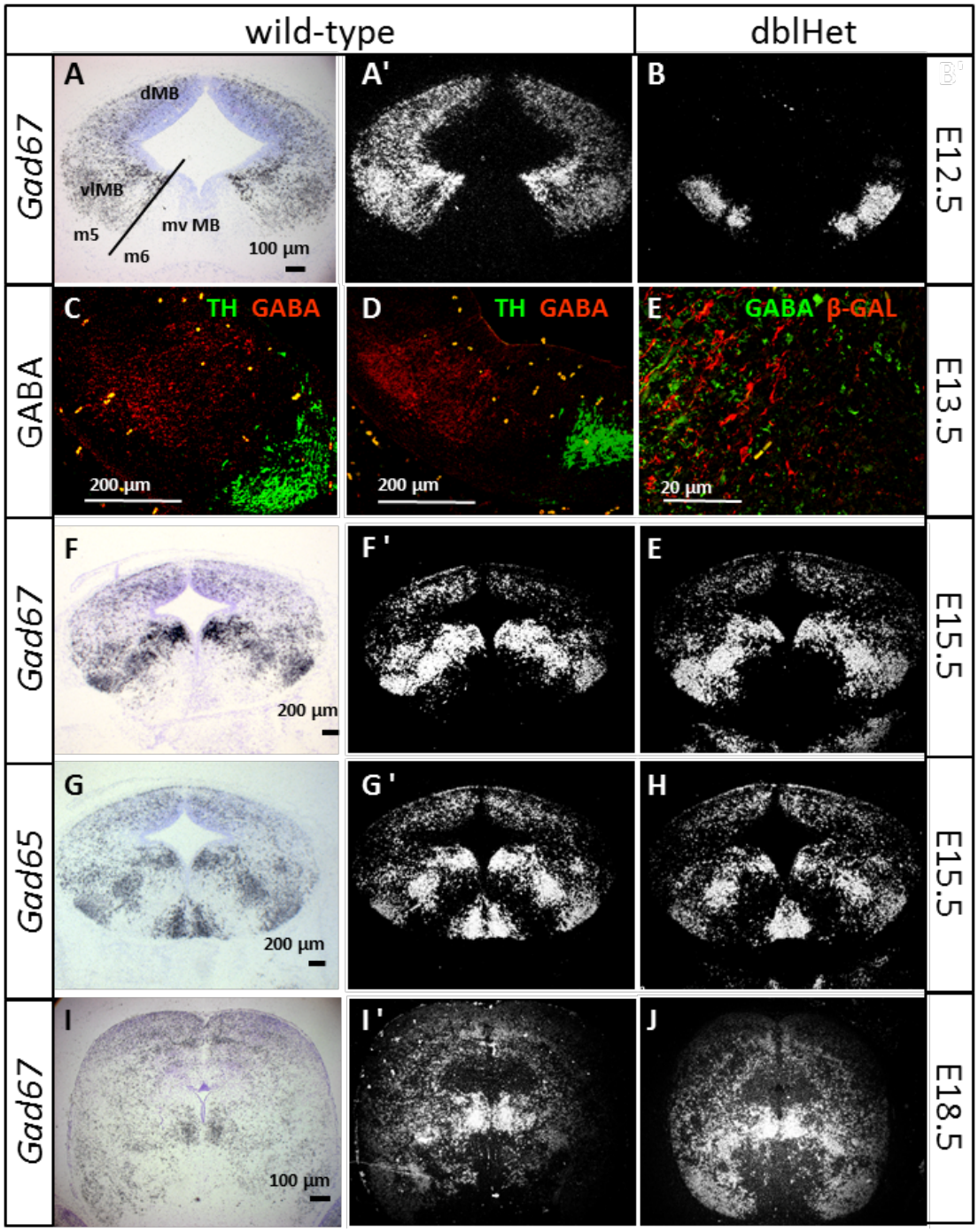

Figure 8.4: dMB GABAn induction requires heterodimers of MGN and MASH1.
Expression analysis on MB coronal sections of WT and dblHet mutants by ISH with a riboprobe for *Gad67* at E12.5 **(A-B)**, at E15.5 **(F-E)** at E18.5 **(I-J)** and a riboprobe for *Gad65* at E15.5 **(G-H)**. IHC against TH, GABA and β-galactosidase on coronal sections of MB at E13.5 **(C-E)**. **(B, D, E, F, H, J)** in dblHet mutants, *Gad65/67* expression and neurotransmitter GABA is expressed in the vlMB as well as in the dMB although with a slight reduction dorsally at E12.5 **(B)**, which is recovered along maturation **(E, H, J)**. In dblHet MB, tau-lacZ expressing neurons are generated, migrate normally and are intermingled with GABA filled vesicles **(E)**. **(F-J)** this phenotype persists during maturation. (I-J) in dblHet mutants, all GABAn of the MB at E18.5 express *Gad67* at comparable levels comparable to WT littermates.

8.4 GABAN INDUCTION IN THE VLMB IS DOSEDEPENDENT ON MGN/MASH1 DIMERS

The lack of GABAn in the dMB but not in the vlMB in the absence of heterodimers of MGN and MASH1, suggested different d/vl mechanisms depending on MGN and MASH1 hetero/homodimerization. This demanded further analysis on compound mutants (*Mgn-/-Mash1+/-*, *Mgn+/-Mash1-/-)* to unravel the intrinsic cell mechanism regulating vlMB neurogenesis.

The presence of one single allele of *Mgn* or *Mash1* was sufficient to induce vlMB GABAergic neurogenesis (Fig 8.5; E, F), although a reduction was observed, compared to single mutants (carrying two active alleles; Fig. 8.5; B, C). Likewise as in single mutants, no dMB GABAergic phenotype was observed in dblHet embryos. These observations suggested a model where vlMB GABAergic induction is dose dependent on the numbers of alleles from the *Mgn* and *Mash1* loci: one active allele of either *Mash1* or *Mgn* was sufficient to induce vlMB GABAn and the strength of induction increases with the number of active alleles. This was in contrast to the dMB where heterodimerization of MGN and MASH1 was a prerequisite to trigger GABAn induction.

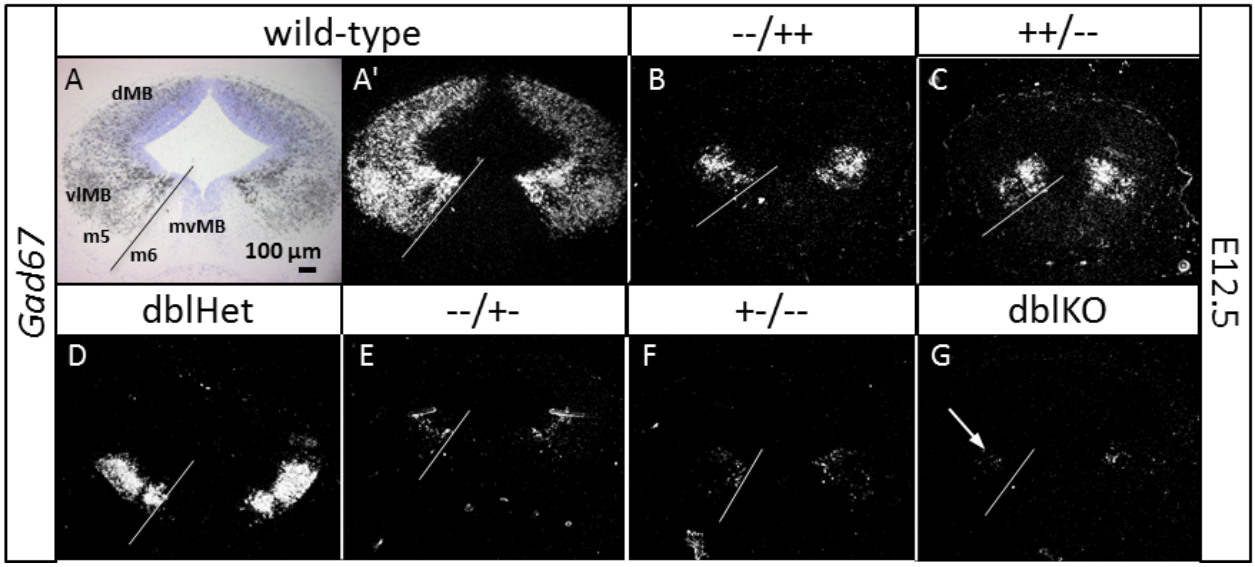

Figure 8.5: vlMB GABAn induction is governed by the amount of active alleles of *Mgn* or *Mash1*. Analysis of compound mice with a *Gad67* riboprobe on coronal sections of the MB at E12.5: **(B, C; E, F)** in the vlMB, one allele of either *Mash1* or *Mgn* is sufficient for GABAn induction. **(B, C; E; D)** GABAn induction was dose dependent on the allele frequency of *Mgn* and/or *Mash1* as two alleles of either *Mgn* **(C)** or *Mash1* **(B)** trigger stronger vlMB GABAergic neurogenesis.

8.5 IMPAIRED NEUROTRANSMITTER SPECIFICATION IN THE D/VLMB OF MGN MASH1 MICE

The lack of GABAergic markers in dblKO mutants required studies of cell proliferation, programed cell death and cytoarchitecture to elucidate if the lack of GABAergic markers is based on a defect in neurogenesis or a defect in transmitter fate specification. No increased apoptosis could be made a condition to the lack of GABAn since IHC staining of cleaved caspase3 (cCASP3), which plays a central role in the execution-phase of cell apoptosis, was comparable between WT, dblHet and dblKO (Fig. 8.6). IHC staining of PHOSPHO HISTONE 3 (pHH3) in mitotic cells surrounding the lumen of the neural tube revealed no reduction in cell proliferation nor decrease in proliferative progenitors when comparing WT embryos with dblKO or dblHet littermates (Fig. 8.7). Similar to single mutants, cytoarchitecture of dblKO mutants did not reveal any significant difference compared to WT at E12.5, when we tracked neurons, expressing tau-lacZ under the endogenous *Mgn* regulatory elements of the *tau-lacZ* knocked in the *Mgn* locus (Guimera *et al*., 2006b) at different time points. These results were consistent with previous studies in single mutants (Guimera *et al*., 2006b). In dblKO mutant brains, neurons migrated radially out of the VZ in stream-like routes towards the MZ (Fig. 8.8). As mentioned before, the residual GABA+ population in m5 was independent from MGN/MASH1 (Fig. 8.8; A, A'). At E12.5 β-galactosidase+ cells could clearly be detected also in the dMB in dblKO (Fig. 8.8; B) as well as in dblHet mutants (Fig. 8.8; C'') - albeit missing GABAergic markers in dblKO mutants (Fig. 8.5; G) and a slight reduction in *Gad65/67* expression was observed at that time in dblHet mutants, respectively (Fig. 8.5; D). Further, migrated, mature neurons appeared functional as IHC studies for Ca^{2+} binding proteins, calretinin and calbinin, indicated no differences between WT and dblKO as there was no significant difference in the amount of stained neurons between the dorsal and the ventrolateral domain (Fig. 8.9). Similarly, IHC with anti-NEURONAL NUCLEI (NEUN), which marks postmitotic neurons in vertebrates, displayed that neurons in the dblKO mutants were generated to the same extent as in WT and cell density was not significantly altered (Fig. 8.9) Summarizing, these results indicated that the MGN/MASH1 pathway controlled GABAergic neurotransmitter identity without regulating proliferation of precursor cells.

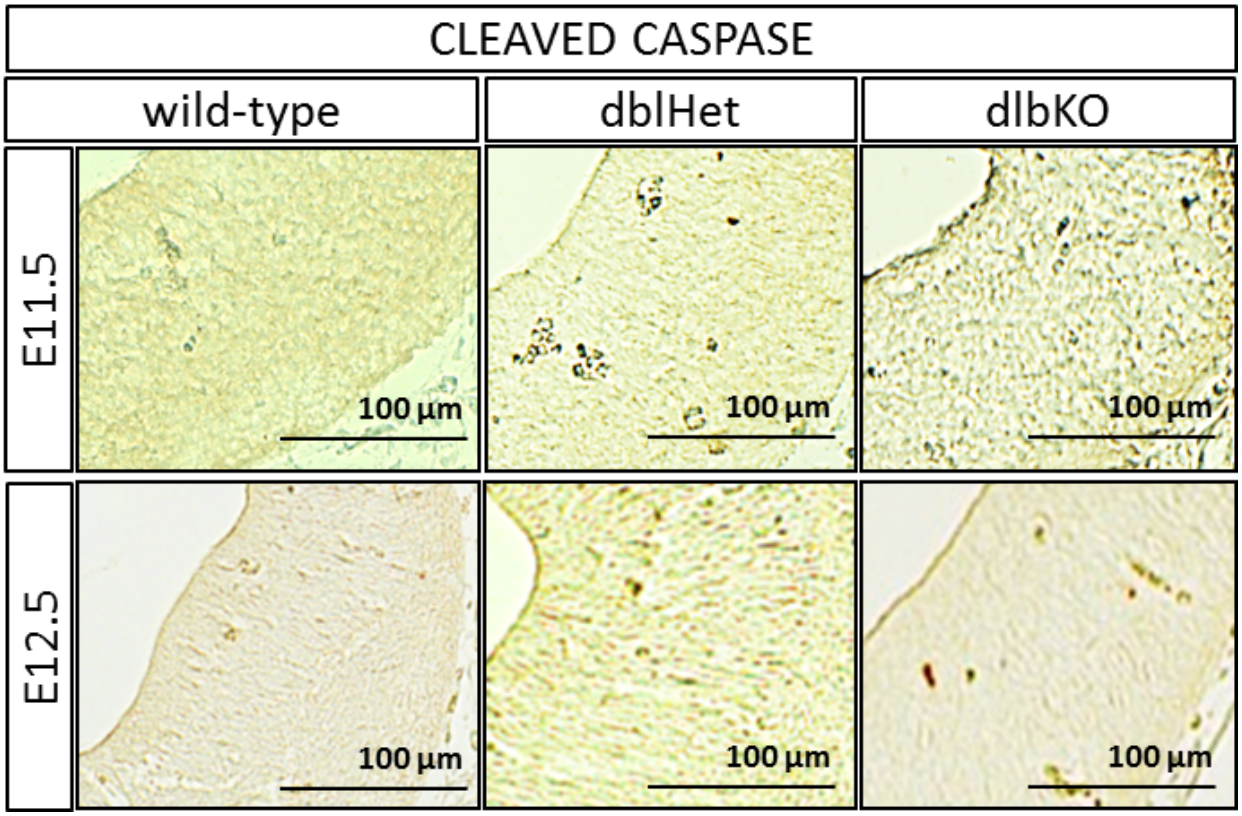

Figure 8.6: No increased apoptosis occurs neither in dblHet nor dblKO mutants.
DAB-IHC on coronal MB sections with anti-CLEAVED-CASPASE-antibody at E11.5 and E12.5

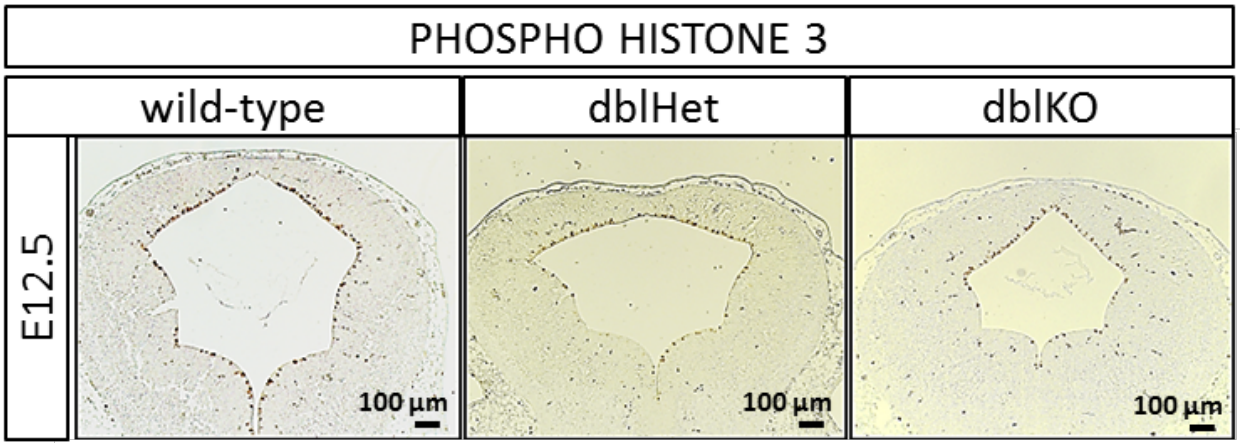

Figure 8.7: Proliferation is not altered in dblHet nor dblKO mutants.
DAB-IHC on coronal MB sections against PHOSPHO-HISTONE at E12.5.

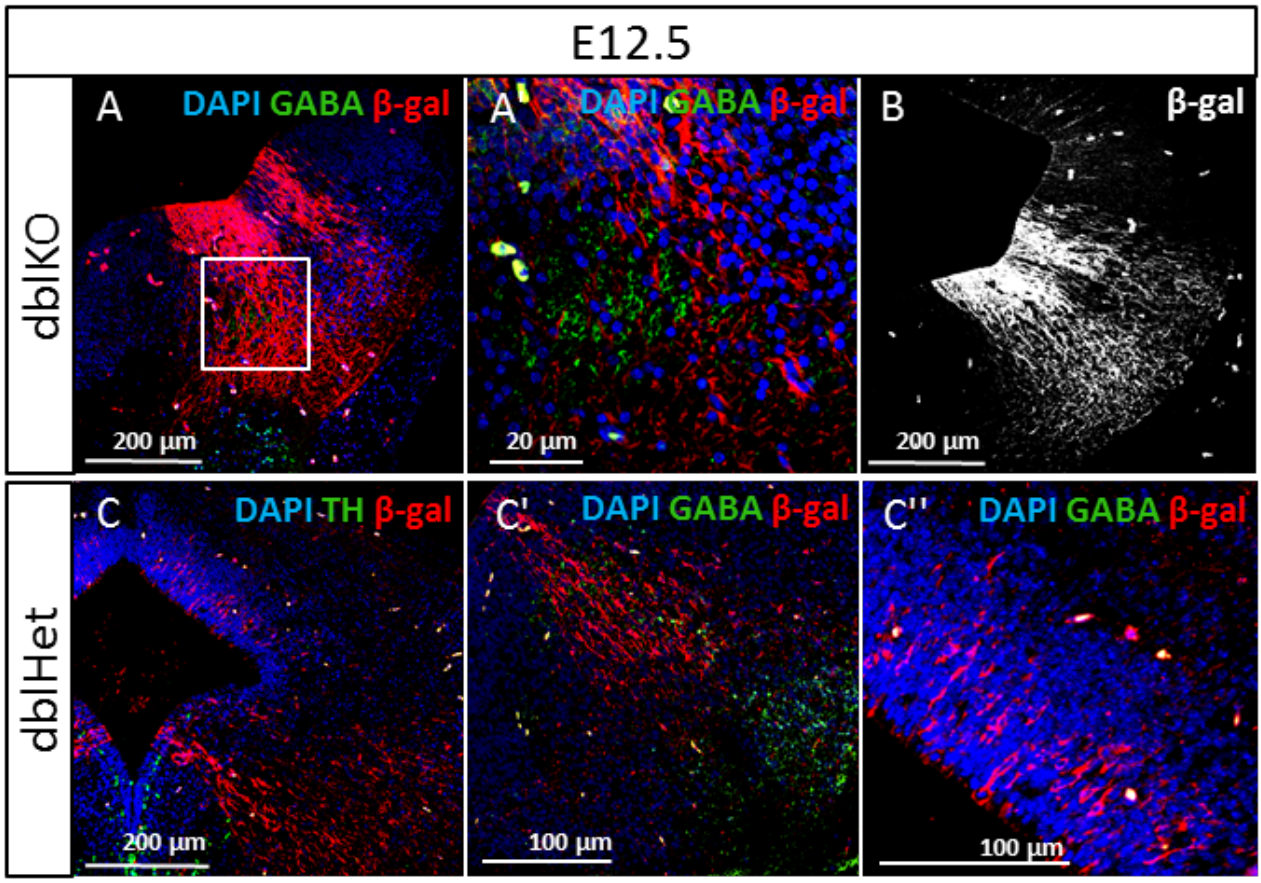

Figure 8.8: Neurons in dblHet and dblKO mutants migrate in stream-like routes from the VZ towards the MZ albeit the lack of GABA.

DAPI counterstaining on IHC with anti-GABA, anti-β-galactosidase and anti-TH antibody on coronal sections of E12.5 MB of **(A-B)** dblKO and **(C-C'')** dblHet brains. Neurons migrate in stream-like routes in both mutants **(A, A'; C, C')** ventrally and **(B; C'')** dorsally.

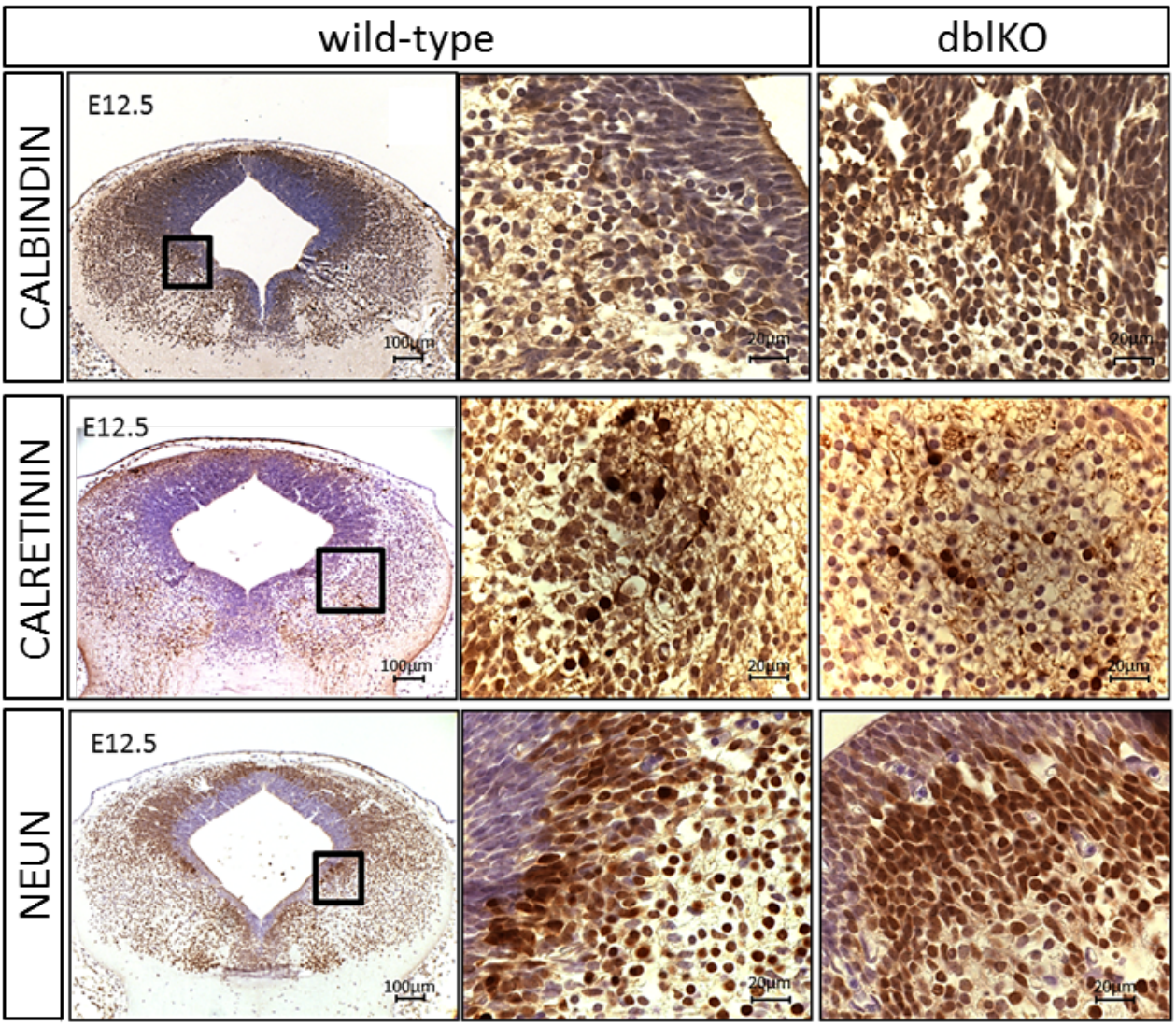

Figure 8.9: No change in the cytoarchitecture in MB of dblKO mutants.
DAB-staining used in IHC on coronal sections of WT and dblKO mutants at E12.5. Neurons are generated in mutant brains as IHC for Ca^{2+} binding proteins CALBINDIN, CALRETININ and NEUN reveal no significant change in density or numbers of neurons compared to WT in the vlMB or dMB respectively.

8.6 DIMERS OF MGN AND/OR MASH1 ACTIVATE THE DOWNSTREAM TARGETS OF THE MB GABAERGIC PATHWAY: *GATA2* AND *TAL1*

Next we proved if known downstream markers of the MB GABAergic pathway were dependent on homodimers/heterodimers of MGN and MASH1. The zink-finger *Gata2* (and *Gata3* - not shown) and the bHLH *Tal1* genes are essentially coexpressed in the MB GABAergic domain at E10.5-E12.5 and have been proven to be involved in MB GABAergic specification (Kala *et al*., 2009, Achim *et al.*, 2013, Achim *et al.*, 2012). *Gata2* is coexpressed with *Mgn* in a few cells in the VZ, just when prospective GABAn become postmitotic and *Mgn* becomes downregulated (Fig. 8.10; (A) H-H' (Kala *et al.*, 2009)). Moreover, *Gata2* has been shown to be downstream of *Mgn* (Kala *et al*., 2009) and *Tal1* to be downstream of *Gata2* (Achim *et al*., 2013).

Phenotypic analysis of *Gata2* and *Tal1* expression in sglMut and compound mice suggested that MGN/MASH dimers essentially activate the same pathway as determined by the expression of the terminal GABAn markers *Gad65/67* in the MB. In the MB, *Gata2* and *Tal1* expression followed the dorsal/ventrolateral *Gad67* phenotype of single, dblHet, dblKO and compound mutants (Fig. 8.10): in the dMB, both genes were downregulated in all genotypes where heterodimerization was not possible; single knockout (Fig. 8.10; (A): B, C and (B): B, C), dblKO mutants (Fig. 8.10; (A): G, J; C, M and (B): G, I-I', L) and compound mice (*Mgn-/-/Mash1+/-*, *Mgn+/-/Mash1-/-* (Fig. 8.10; (A): E, F and (B): E, F, I). In the vlMB downregulation was dose-dependent according to the *Mgn* and *Mash1* genotype, as *Gata2* and *Tal1* expression in compound mutants was reduced in the m4-5 domain when compared to single mutants. – Contrary, dblHet mutants (Fig. 8.10; (A): D, L and (B): D, K) showed expression pattern of *Tal1* and *Gata2* similar to WT (Fig. 8.10; (A): A, A'; I, I'; K and (B): A, A'; H, H'; J), with equivalent dorsal and ventral expression. Similar to *Gad67* expression in mutants, at E12.5 in the dMB of dblHet mutants, *Gata2* and *Tal1* expression was not as strong as in WT (Fig. 8.10; (A): D and (B): D). Nevertheless, at E15.5 strong expression was detected also in the dorsal aspect comparable to WT. When all 4 alleles from the *Mgn* and *Mash1* loci were mutated, mutants also lack expression of *Gata2* and *Tal1* in the vl and dMB. In dblKO mutants, *Gata2* and *Tal1* expression was absent - except for a small population in m5. This population correlated in position and numbers with the remaining *Gad67* expressing cells in dblKO mice (Fig. 8.10; (A): G, J and (B): G, L). Notably also the few *Gata2* and *Tal1* expressing, residual cells spread around the m5 in the MB domain were still prominent in the brains of dblKO mutants at E15.5. Although *Mgn* and *Mash1* are coexpressed in subpopulations along the ZLI, *Gata2* as well as *Tal1* were expressed in this area in dblKO brains (Fig. 8.10; (A): J and (B): I, I'). Likewise, the GABAn population migrating from the HB, which also expresses *Tal1* and *Gata2*, showed independence from *Mash1* and *Mgn* in the HB and appeared in the MB at E14.5. These results are in good agreement with the results of the expression analysis of *Gad65/67* in the dblKO mutants.

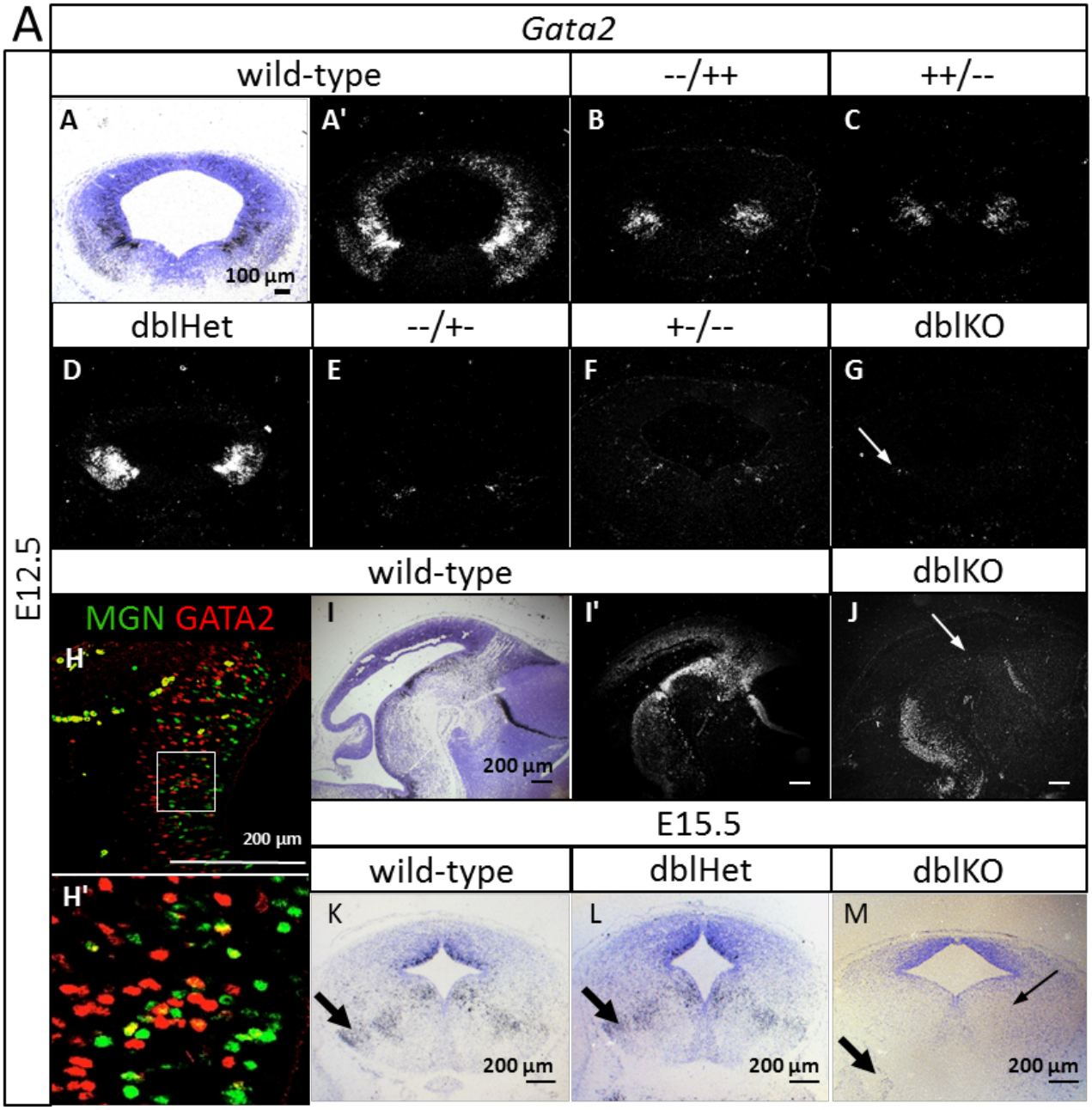

Figure 8.10: Homodimers and heterodimers of MGN and/or MASH1 activate downstream targets of the MB GABAergic pathway - *Gata2* and *Tal1*. For full description see next page

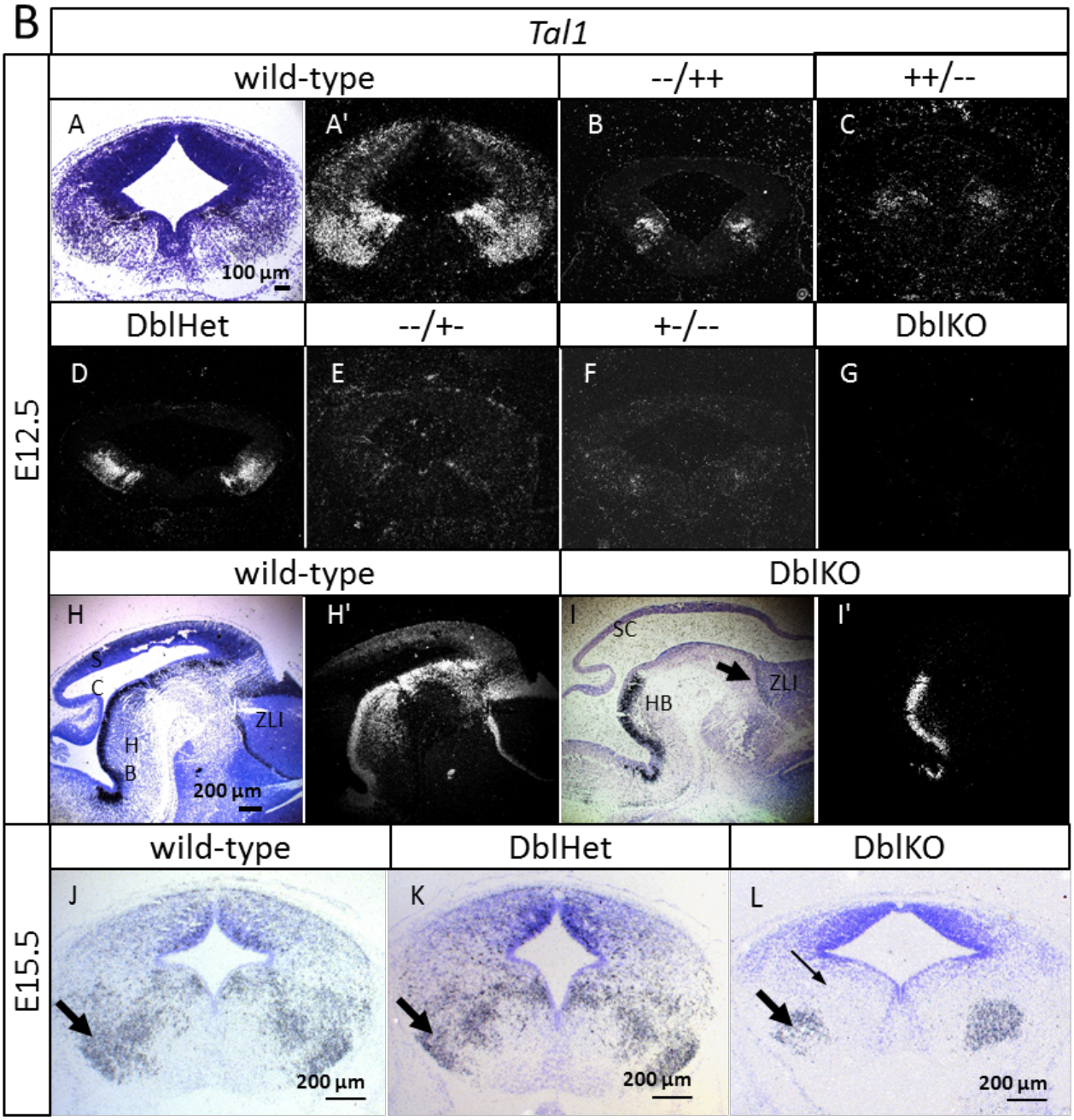

Figure 8.10: Homodimers and heterodimers of MGN and/or MASH1 activate downstream targets of the MB GABAergic pathway - *Gata2* and *Tal1*.

Phenotypic analysis of coronal and sagittal sections of WT, single knockout, dblHet, dblKO and compound mutants by ISH with riboprobes of **(A)** *Gata2* and **(B)** *Tal1*. **(A: H, H')** IHC for MGN and GATA2; MGN and GATA2 colocalize in in a few cells of the MZ. *Gata2* and *Tal1* are downstream of the MGN/MASH1 pathway and follow the phenotype of *Gad67*: **(A: G, J, M; B: G, I, I', L)** expression of both factors is completely downregulated in dblKO mutants except for a small population in m5 (indicated by arrows). Only those mutants where heterodimerization is allowed, expression of *Gata2* and *Tal1* can be detected in the dMB **(A: D; B: D).** In dblHet mutants, at E12.5, dorsal expression is delayed but is recovered only one day later as neurogenesis proceeds **(A: L; B: K).** GABAn, generated in the HB are unaltered **(A: J, M; B: I, L**; indicated by thick arrows).

8.7 MGN AND MASH1 CONTROL GABAERGIC MARKERS *TAL2 AND SOX14* INDIVIDUALLY AND BY DIFFERENT MOLECULAR CODES.

We further focused on possible downstream targets that have been seen to be implicated in GABAergic neurogenesis in other brain areas to interrogate if their expression in the MB is also governed by dimers of MGN and MASH1. As *Tal2* was reported to be a selector for postmitotic MB GABAn and inactivation of *Tal2* results in a failure of *Gad65/67* expression in the d/vLMB (except for some remaining cells in m5 domain) (Kala *et al*., 2009), we first investigated the expression of *Tal2* dependency on dimers of MGN and MASH1. *Gata2* expression at E12.5 in the WT was observed in the IZ/MZ of the d and vlMB (m1-m6; Fig. 8.11; A, A'). In contrast to *Tal1,* which was absent in dblKO mice, *Tal2* expression was dependent on MGN/MASH1 heterodimers only in the m5 domain (Fig 8.11; F), yet independent of *Mgn* and *Mash1* expression in the m1-4 domain: all compound mice – except dblHet mutants revealed a reduction of *Tal2* expression in the m5 domain (Fig. 8.11; B-E, G).

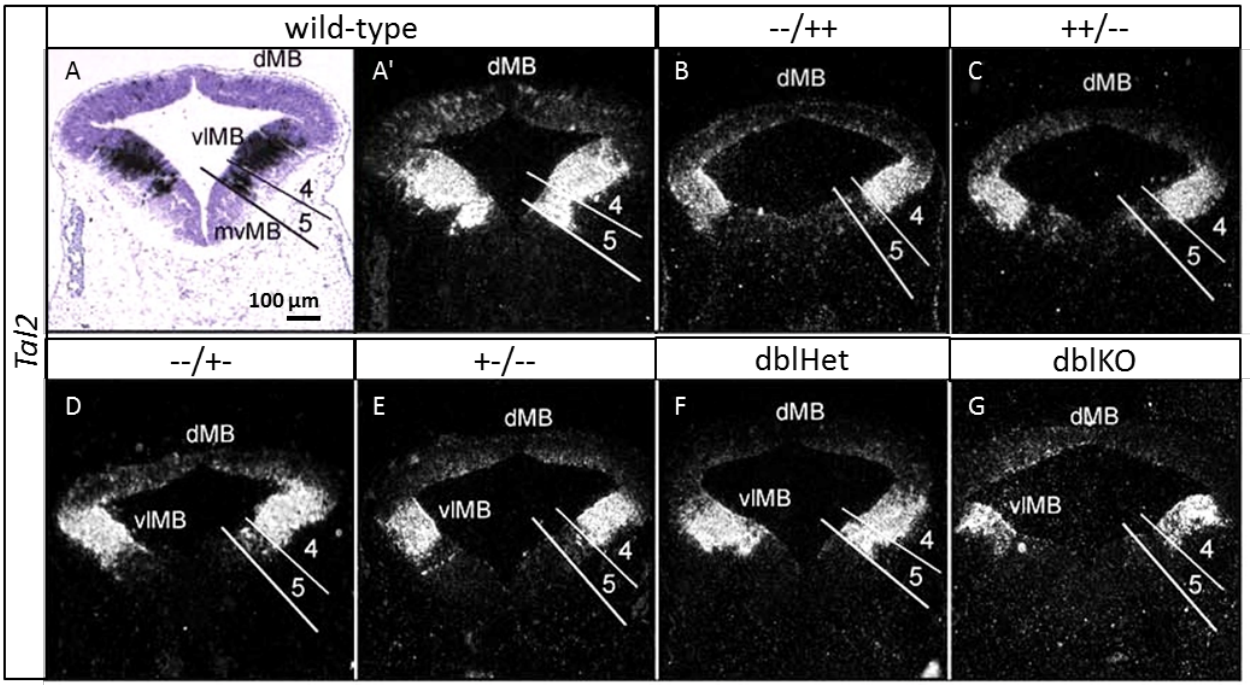

Figure 8.11: MGN/ MASH heterodimers regulate *Tal2* in the m5 domain.
Expression analysis by ISH on coronal sections of E12.5 MB of different MGN/MASH1 genotypes with a riboprobe of *Tal2*. **(F)** Only in dblHet brains, where hetero-dimerization of MGN and MASH1 is possible, *Tal2* expression in induced comparable to WT, whereas all other compound dblKO brain lack expression in m5. Bars indicate the m5 domains of the MB.

We further investigated the expression of *Sox14* in the MB, as it has been shown to be dependent on *Mgn* in a subpopulation of the FB (Delogu *et al*., 2012). *Sox14* expression analysis in the MB was clearly dependent on *Mgn/Mash1* and revealed a much stronger phenotype upon different *Mgn/Mash1* genotypes (Fig. 8.12): While S*ox14* expression in the VZ was unaltered in all different genotypes, in the MZ, mutation of the *Mgn* or *Mash1* locus resulted in a strong downregulation of *Sox14* in the entire MZ - except for some residual spread cells in the m3-5 domain. Thereby, mutation in the *Mgn* locus appeared to reveal a stronger downregulation (Fig. 8.13; B, E) compared to the phenotype after ablation of the *Mash1* locus (Fig. 8. 8.12; C, F). When only one allele (of either *Mash1* or *Mgn*) was active, *Sox14* expression in the MZ was even more downregulated to some individual cells in m4-5. Along neurogenesis, this phenotype did not change greatly in the amount of *Sox14* expressing cells when comparing E11.5 to E12.5 (Fig. 8.12; B, E; C, F; H, K; I, L). In contrast to all the genotypes, where heterodimerization was not possible, in dblHet mutants, at E12.5, expression of Sox14 was comparable to WT – albeit with a slight delay in the dorsal MZ (Fig. 8.12; G) which was recovered one day later and at E14.5, it was expressed in the entire dMB comparable to WT (Fig. 8.12; J, Q). Further, *Sox14* expression was unaltered in the HB of dblKO; there, expression of *Sox14* was prominent in the MZ, comparable to WT – in contrast to the expression pattern in the MB, where *Sox14* was mainly expressed in the MB VZ (Fig 8.12; N, O).

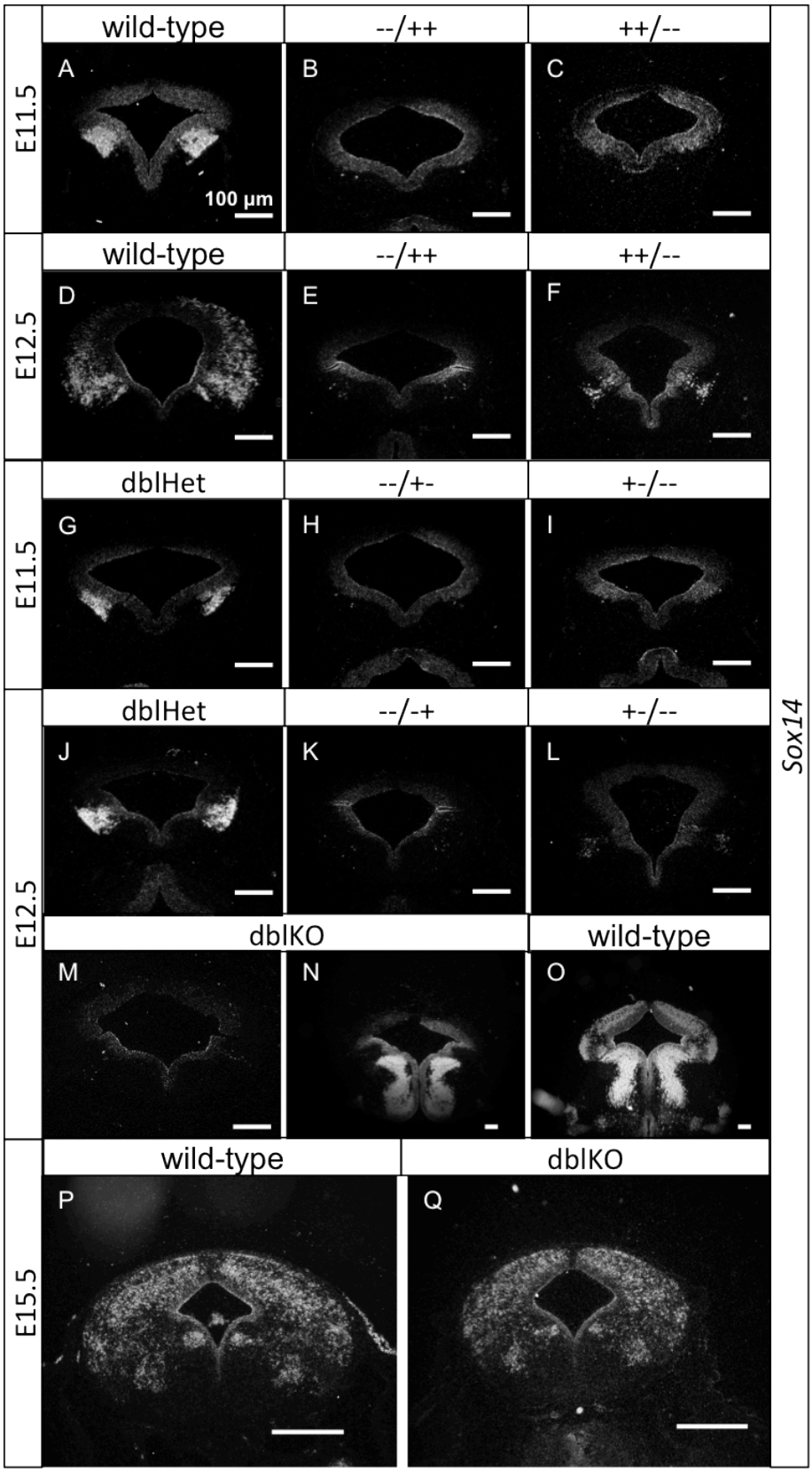

Figure 8.12: MGN/ MASH heterodimers regulate *Sox14* expression in the MZ of the MB but some cells in m3-4 are independent from *Mgn* or *Mash1*. Expression analysis by ISH on coronal sections of **(A-C, G-I)** E11.5, **(D-F, J-O)** E12.5 and **(P, Q)** E15.5 MB of different *Mgn/Mash1* genotypes with a riboprobe of *Sox14*. **(A)** in WT, *Sox14* expression at E11.5 is prominent in m3-4 and **(D)** one day later also in m1-2. **(B, C, E, F)** mutation of either *Mgn* or *Mash1* leads to a strong downregulation of *Sox14* in the entire MB MZ except for some residual spread cells (indicated by arrows) in the m3-4 domain (indicated by bars) and reveal stronger depen-dency on *Mgn* **(B, E)**. Thereby the amount of *Sox14* expressing cells does not increase greatly over time when either *Mgn* or *Mash1* is missing, as S*ox14* expression in the VZ remains unaltered in single and compound mutants. **(G, Q)** hetero-dimerization of MGN and MASH1 allows expression comparable to WT in the dMB with a slight delay, which is fully recovered at E14.5. (N) in the HB, *Sox14* expression was unaltered in the DblKO compared to WT (**O).**

8.8 HOW MGN AND MASH1 REGULATE GABA VERSUS GLUTAMATERGIC FATE IN THE MB

As inactivation of *Mgn, Mash1* and *Gata2* were reported to promote transformation of GABAergic fate into glutamatergic phenotype (Achim *et al*., 2013, Nakatani *et al*., 2007, Kala *et al.*, 2009), fate specification analysis was mandatory. Therefore, we investigated possible trans-specification of the defective GABAn into glutamatergic neurons in sglMut, dlbHet, *Mgn +/-/Mash1-/-* or *Mgn-/-/Mash1+/-* mutants and dblKO mutants.

8.8.1 MGN/MASH heterodimers regulate *Lim1* expression in m1-4 although some *Lim1* expressing cells in m3-4 and all cells in m5 are independent from *Mgn* and *Mash1*

The GABAergic marker LIM1 was also dependent on MGN/MASH1: In WT MB at E12.5, *Lim1* is expressed in the GABAergic domain m1-5 and glutamatergic domain m6. In single compound and dblKO mutants, *Lim1* expression was missing in m1-2 and reduced in m3-4 (Fig. 8.13; B, C, E-G, I, I'). The remaining cells in m3-4 were independent of *Mgn* or *Mash1* as they were still detectable in the dblKO. Domain m5 and m6 remained unaltered and therefore independent from *Mgn/Mash1* as expression was comparable to WT in the MB of the dblKO mutant MB. In dblHet mutants, heterodimerization allowed light dorsal expression of *Lim1* and the expression of *Lim1* in m3-4 was as prominent as in WT (Fig. 8.13; D). At E14.5 the delay in *Sox14* expression in the dMB recovered and it was as prominent as in WT (Fig. 8.13; J, K) - resembling the expression pattern of *Gad67, Gata2* and *Tal1*. Thus, heterodimers of MGN/MASH1 regulate *Lim1* expression in m1-4, although some *Lim1* expressing cells in m3-4 and all cells in m5 are independent from *Mgn* and *Mash1*.

8.8.2 *Mgn* prevents *Brn3a* expression in m3-4 and heterodimers of MGN and MASH1 ensure the right amount of *Brn3a* expression in the dorsal m1-2

We further examined the expression of *Brn3a*, which marks MB glutamatergic neurons in m1-2 and m6 and is regulated conversely to *Lim1*; *Mgn* was reported to indirectly repress *Brn3a* via repression of *Ngn2* in m2-4 and thereby allowing the expression of the GABAergic marker *Lim1* (Nakatani *et al*., 2007). Similar, when two alleles of *Mgn* were missing, we observed *Brn3a* ectopic expression in the m3-4 domain where it is not expressed *in vivo* (Fig. 8.14; C, E). Further, we noticed a slight upregulation of *Brn3a* in m1-2 upon *Mgn* ablation (Fig. 8.14; C, E). *Mash1* seemed not to affect *Brn3a* expression as compound mice lacking two alleles of *Mash1* showed expression pattern of *Brn3a* comparable to WT (Fig. 8.14; D). In dblHet mutants, *Brn3a* expression was not altered in the vl or dMB (Fig. 8.14; B). No ectopic expression was detectable in m3-5 neither an upregulation of *Brn3a* in m1-2. Analysis tracing

Mgn expression cells expressing tau-lacZ under the endogenous *Mgn* regulatory elements of the tau-lacZ knocked in the *Mgn* locus (Guimera *et al*., 2006b) revealed that the ectopic BRN3A+ cells are likely to be coexpressed with tau-lacZ and derive from the *Mgn* expressing pool in the VZ. Tracing these cells in dblKO mutants showed clearly that these cells are generated properly and give rise to BRN3A+ cells in m3-4 but not in m5 when two alleles of *Mgn* are missing.

In summary, *Mgn* prevented *Brn3a* expression in m3-4 and heterodimers of MGN and MASH1 ensured the right amount of *Brn3a* expression in the dorsal m1-2 (Fig. 8.14). In combination with the phenotypic analysis of *Lim1* (Fig. 8.13) our results indicated, that *Mgn* might rule GABAergic versus glutamatergic fate particularly in m4 but also that heterodimers of MGN and MASH1 regulate their expression in the dMB.

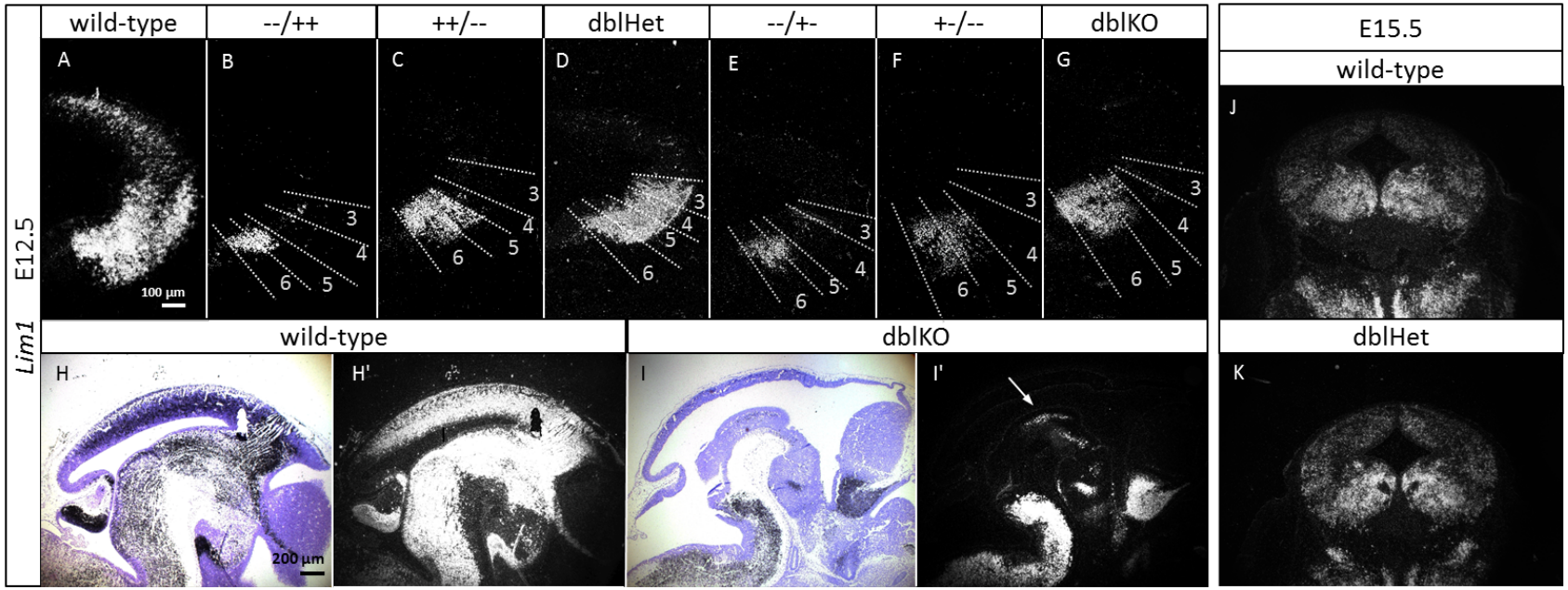

Figure 8.13:. MGN/MASH heterodimers regulate *Lim1* expression in m1-4 although some *Lim1* expressing cells in m3-4 and all cells in m5 are independent from *Mgn* and *Mash1*.

Expression analysis by ISH on **(A-G)** coronal sections of E12.5 and **(J, K)** E15.5 MB and **(H-I')** sagittal section at E12.5 of different MGN/MASH1 genotypes with a riboprobe of *Lim1*. *Lim1* expression is downregulated in all genotypes that do not allow heterodimerization and LIM+ cells in m3-4 are independent from *Mgn/Mash1* **(B, C, E-G, I, I')**. Presence of heterodimers allows strong expression in m3-4 – comparable to WT and light dorsal expression of *Lim1* already at E12.5 **(D). (K)** at E15.5, dorsal expression in dblHet mutants is prominent as in WT. Arrows in **(I')** indicate *Lim1* independent expression in m5-6.

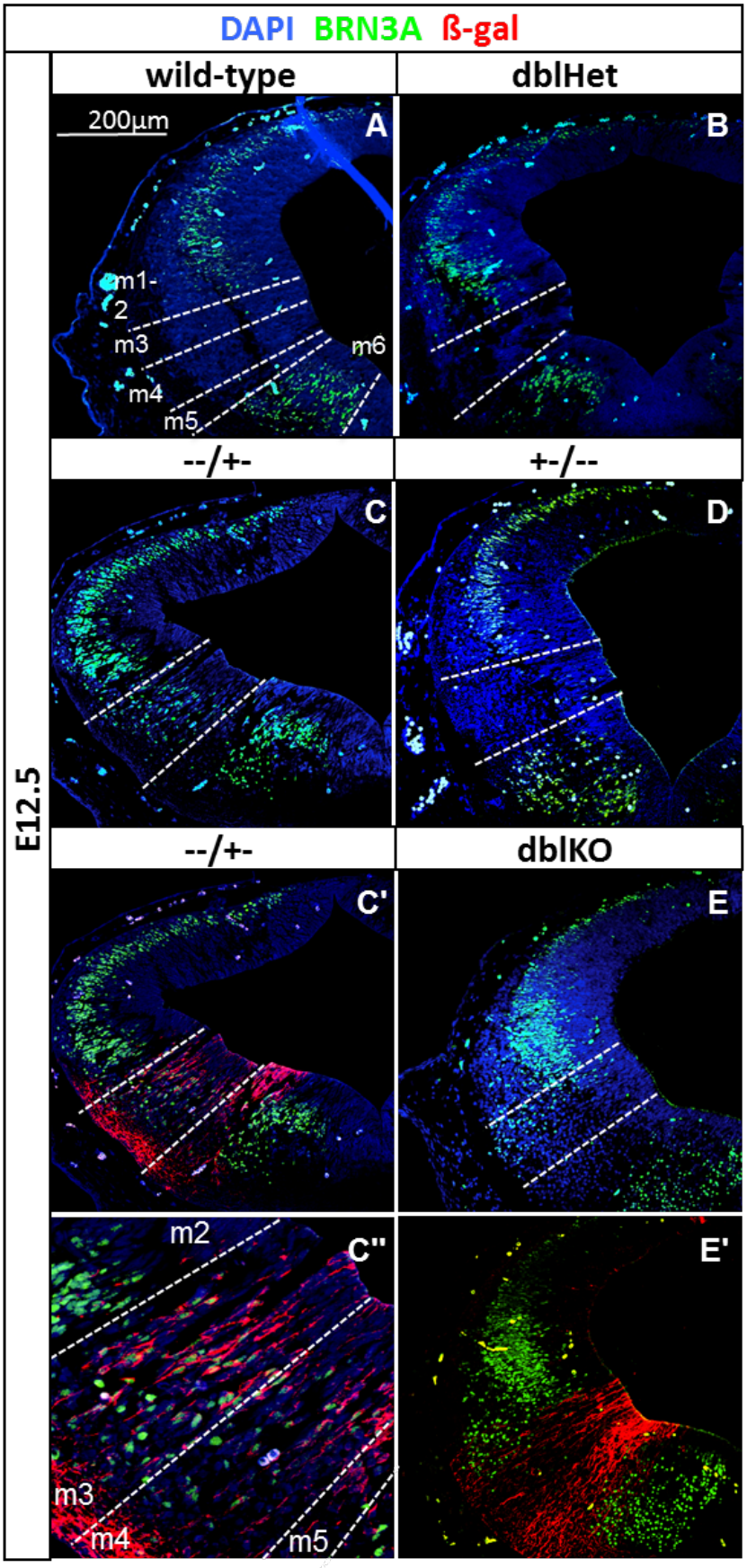

Figure 8.14: *Mgn* prevents *Brn3a* expression in m3-4 and regulates it in the dMB. Heterodimers of MGN and MASH1 ensure the right amount of *Brn3a* expression in the dorsal m1-2. Expression analysis of different *Mgn*/*Mash1* genotypes by DAPI staining and IHC with antibodies for BRN3A and ß-galactosidase on coronal sections of E12.5 MB. **(A)** in WT, *Brn3a* is detected in m1-2 and m6. **(B)** The expression of *Brn3a* in dblHet mutants is equivalent to WT. **(C, E)** the absence of two alleles of *Mgn* results in ectopic expression of BRN3A in m3-4 and a slight upregulation in the dMB**. (D)** *Mash1* expression has no impact on the number of BRN3A+ cells. **(C', C'', E')** BRN3A+ cells in m3-4 are likely to derive from the MGN+ domain.

8.8.3 MGN inhibits expression of *vGlut2* in m3-4.

As inactivation of *Mgn, Mash1* altered the expression of the glutamatergic marker *Brn3a* (Fig. 8.14), further fate specification analysis of a glutamatergic marker were mandatory. We therefore investigated possible trans-specification of the defective GABAn in single, compound and dblKO mutants by the expression pattern of *vGlut2*. We observed ventrolateral *Vglut2* expression only in m3-4 depended on *Mgn*. When both alleles of *Mgn* were missing, *vGlut2* was upregulated in m3-4 while remained unchanged in the other domains (Fig. 8.15; C, D, F). In contrast, the lack of expression of *Mash1* had no impact on *vGlut2* expression in the MB since *Mash1* sglMut and compound mutants with two mutated alleles of *Mash1* did not reveal an upregulation of *Vglut2* expression but was comparable to WT. The same observation accounted for dblHet mutants despite the presence of MGN/MASH1 heterodimers (Fig. 8.15).

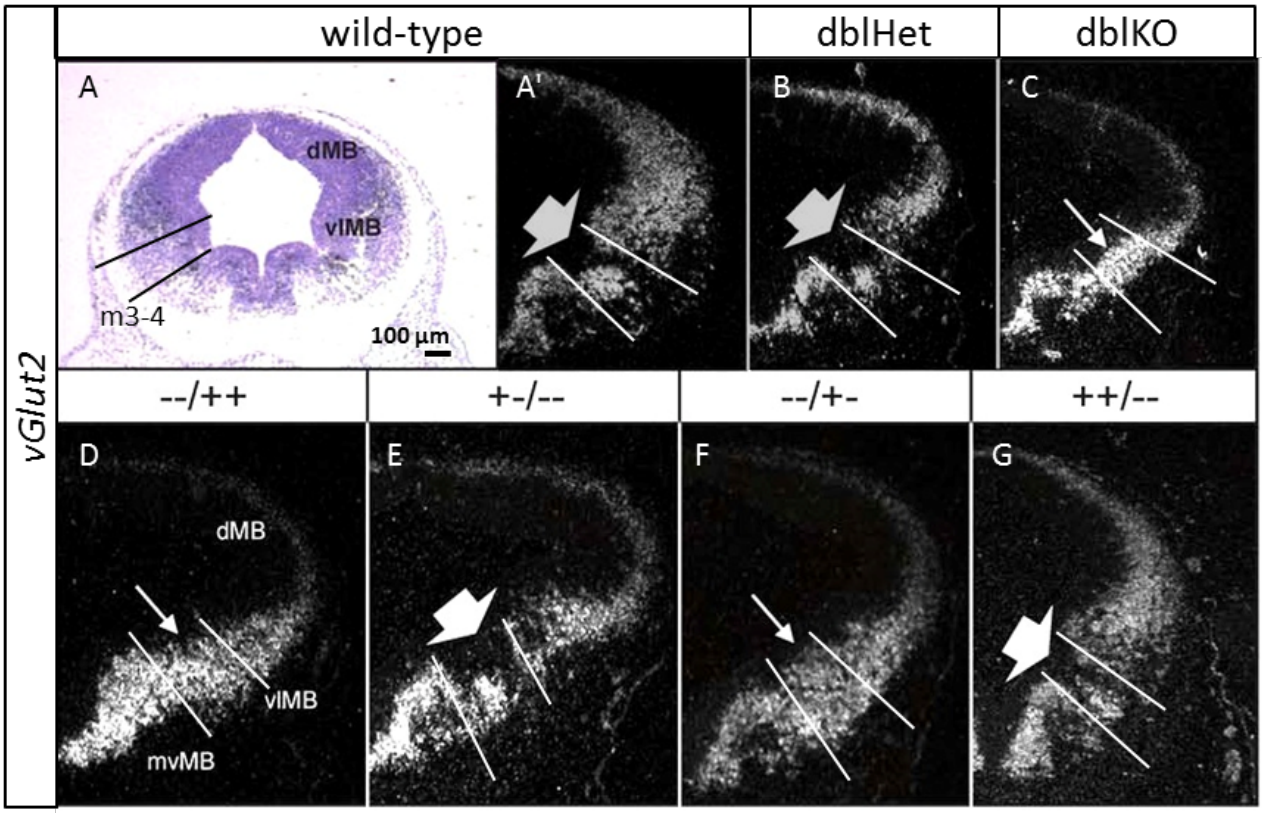

Figure 8.15: *Mgn* inhibits expression of *vGlut2* in m3-4.
Expression analysis by ISH on coronal sections of E12.5 MB on different *Mgn/Mash1* genotypes with a riboprobe of *vGlut2*. **(A)** brightfield image **(A' – G)** darkfield images. **(C, D, F)** upregulation of *Vglut2* expression in m3 and dm4 depends on missing Mgn but **(E, G)** neither on *Mash1* expression nor **(B)** the formation of MGN/MASH1 heterodimers. Thin arrows indicate upregulation of *vGlut2* in the m4 domain. Thick arrows indicate physiological expression of *vGlut2*.

8.8.4 MGN and MASH1 heterodimers regulate expression of a postmitotic NKX2.2+ population in the dMB

Interestingly, we discovered a NKX2.2+ subpopulation to be dependent on heterodimers of MGN and MASH1 (Fig. 8.16); *Nkx2.2* is expressed in the MB in two subpopulations – one in the dorsal MZ of m2 and one population in the vl VZ and MZ of m4-m6. The dorsal population appears to specifically mark postmitotic GABAn. This is in contrast to the population in the vlMB of m4-m6 where only some *Nkx2.2* expressing cells coexpress GABA in the MZ. Further, in the VZ, a few *Nkx2.2* expressing cells coexpress *Mgn* (Nakatani *et al.,* 2007). The dorsal postmitotic NKX2.2+ population is absent in both, *Mgn* and *Mash1* sglMut while the vl domain is unchanged (Nakatani *et al.,* 2007, Peltopuro *et al*., 2010). Likewise we observed this dorsal subpopulation to be missing in all single and compound mutants (Fig. 8.16; B, D, E; which did not allow heterodimerization of MGN and MASH1). As opposed to this, in compound mice allowing heterodimerization, the dorsal subpopulation was generated to the same extend as in WT (Fig. 8.16; A, C). We further confirmed the position of the remaining population of GABAergic cells in dblKO mutant brains to be located in the MZ of m5 by colocalization studies with GABA and NKX2.2. Notably, these cells did not colocalize with NKX2.2 (Fig. 8.16; B-B'') although in WT, most NKX2.2+ cells coexpress GABA (Fig. 8.16; A-A''). This correlates with the fact that the NKX2.2+ domain is known to overlap with that one of MGN and GABA (Nakatani *et al*., 2007). The change in specification of the MB domains supports the important role of dimerization of MGN and MASH1 protein for proper MB GABAergic development. Although the various subpopulations of MB GABAn follow different expression cascades, our results identified the two bHLH factors MGN and MASH1 to have common and unique targets and to govern MB GABAergic neurogenesis by particular bHLH codes with distinct roles ventrally versus dorsally.

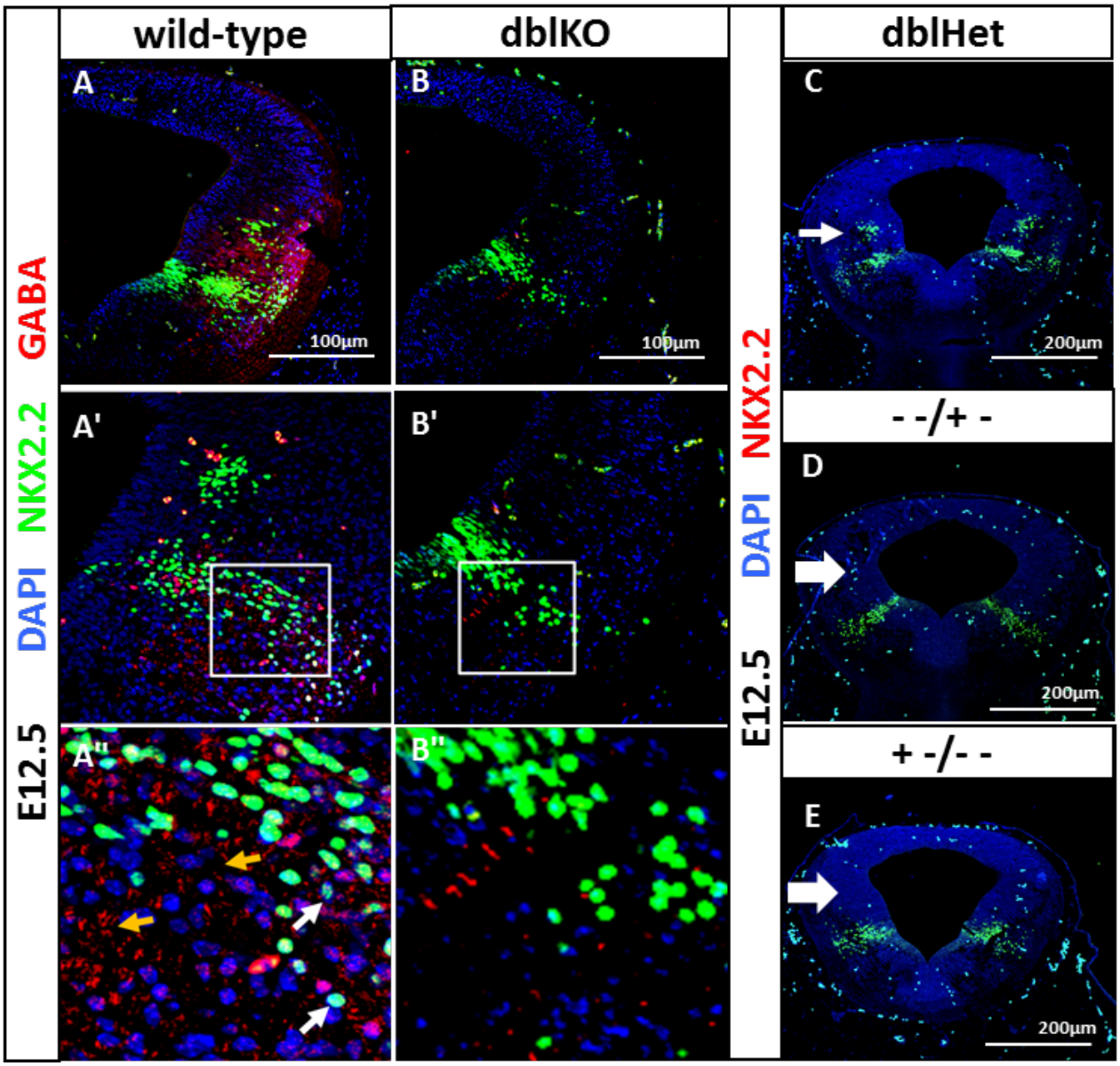

Figure 8.16: A subpopulation of NKX2.2+ cells depends on MGN/ MASH1 heterodimers.
DAPI staining and IHC on coronal sections of E12.5 MB with anti-NKX2.2 and anti-GABA antibodies. **(C)** the dorsal subpopulation of *Nkx2.2* (indicated by thin white arrow) expression domain in m2 is dependent on heterodimers of MGN and MASH1 while the NKX2.2+ vlMB population in m4-5 is independent of *Mgn* or *Mash1* **(B-E,** indicated by thick white arrows in D and E**). (B', B'')** the remaining GABAergic cells in m5 of dblKO mutants do not belong to NKX2.2 and GABA double positive neurons **(A'-A'').** White arrows in **(A'')** indicate coexpression of NKX2.2 and GABA, yellow arrows indicate neurons expressing GABA only.

8.8.5 The residual population of GAD67+ cells might comprise a different population

It was shown, that the vMB GABAergic population of the MRF and SNpr are populated by tangentially migrating neurons from the HB, (Achim *et al*., 2012) or from the MB itself (Madrigal *et al*., 2015). Further it was suggested that additionally, more GABAn could contribute to the populations in the MB by tangential migration from the FB (Achim *et al*., 2012). The GABAn, which migrate from the HB, arrive in the MB as postmitotic GABAergic precursors at E14.5 (Achim *et al*., 2012). Thus we had a closer look at neurons, expressing *tau-lacZ* under the endogenous *Mgn* regulatory elements of the *tau-lacZ* knocked in the *Mgn* locus (Guimera *et al.*, 2006b) at E14.5. Coronal sections of E14.5 *Mgn*-/- *Mash1*+/- were used due to availability, the stronger β-galactosidase staining upon ablation of both *Mgn* alleles and the migration cues described above. As described before, GABA+/β-galactosidase- (*Mgn* independent) neurons, migrating from the HB to the (presumptive) SNpr at this stage in the rostrally located sections of the MB, (indicated by thin white arrows in Fig. 8.17; A', A'') and more prominent in more caudally located sections (indicated by thin white arrows in Fig. 8.17; B, B''). Furthermore, we detected two different types of β-galactosidase+ neurons in the m5-6 domain. Most of the β-galactosidas+ neurons migrated radially from the MGN+ m3-5 domain, intermingled within GABA+ neurons. Yet, some of the β-galactosidase+ neurons differed in their shape from these neurons. These β-galactosidase+ neurons were clearly different from the radially migrating neurons since they were visible only as dotted spots (indicated by white thick arrows in Fig. 8.17; A', A'', B'). Thus they appeared not to display radial migration but rather to migrate tangentially. Addtionally, these GABAn appeared rather located in the m6 domain, suggesting an independency from *Mgn*.

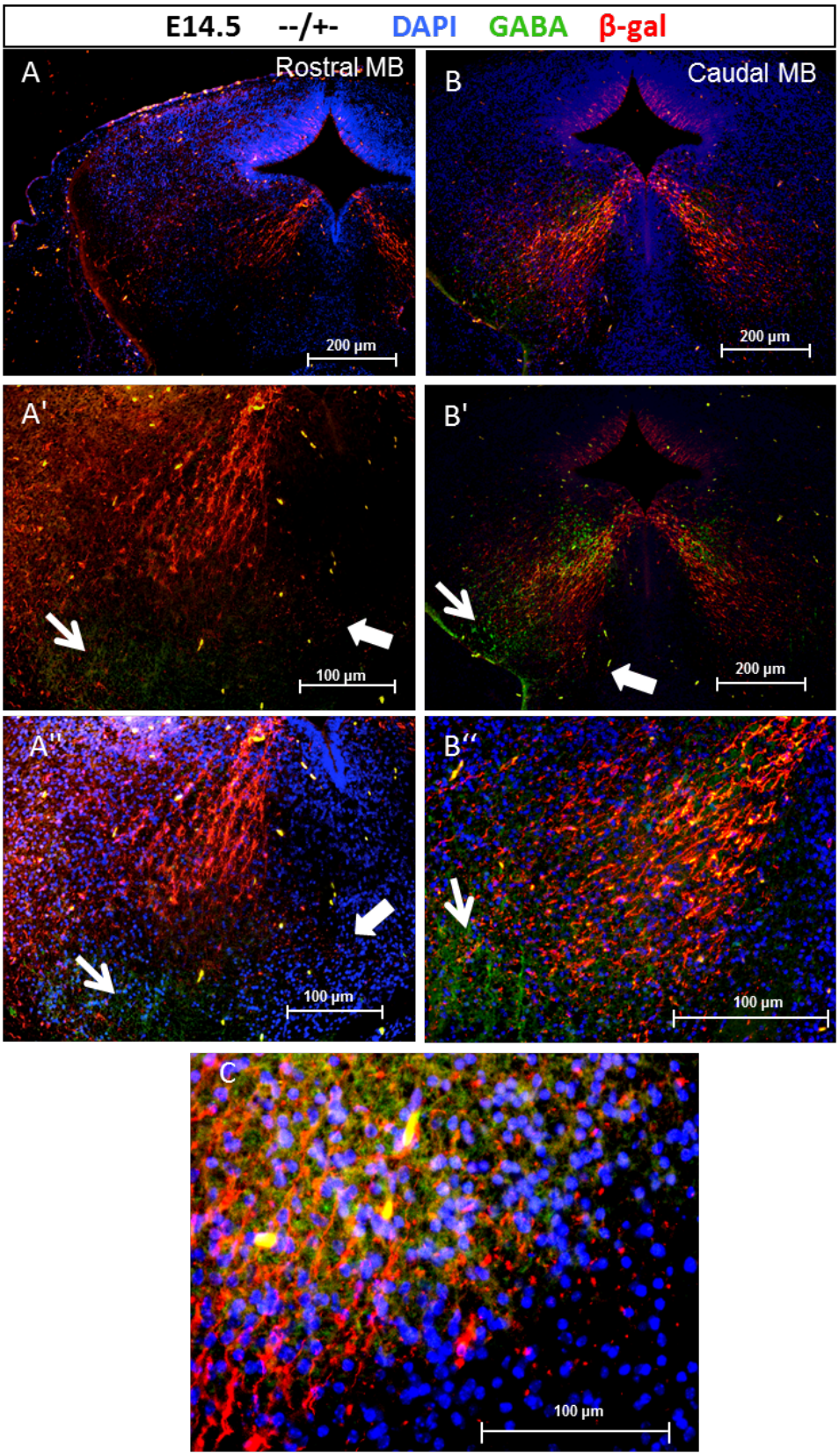

Figure 8.17: Some MGN+ deriveratives appear also to migrate tangentially travers the MB.
IHC on coronal sections of E12.5 MB with anti-ß-galactosidase, anti-GABA and DAPI staining.
The radially migrating neurons, deriving from the MGN+ domain, are ß-galactosidase+ and GABA+, while some ß-galactosidase+ neurons in more ventral areas (m5-6) of the MB appear to migrate tangentially and are not positive for GABA **(A, A'', B'')**; indicated by white thick arrows). The GABAn, populating the presumptive MRF do not coexpress *lac-Z* (**B, B''**; indicated by thin white arrows) and are independent from *Mgn* **(C)**. Close up of the eventually tangential migrating cells, located ventrally to the neurons, which derive from the MGN+ domain and are ß-galactosidase+ and GABA+.

9 DISCUSSION

9.1 DIFFERENT DORSO/VENTROLATERAL MECHANISMS FOR GABAERGIC NEUROGENESIS OPERATING IN THE MB

In the MB, *Mgn* and *Mash1* have been proven to function as the earliest key factors for the specification of GABAergic identity in the dMB (Guimera *et al*., 2006b, Peltopuro *et a*l., 2010). Both factors are coexpressed in progenitors of the VZ developing MB, where GABAergic precursor cells are born, prior and during the time of GABAergic induction (at E10.5-E12.5, in the vlMB and dMB, respectively). Strikingly, in the MB, loss-of-function experiments revealed that each single knock-out mouse revealed a very similar phenotype, regarding GABAn derived from the MB; In both mutants, GABAn induction fails in the dorsal aspect (m1-2) of the MB whereas GABAn in the vlMB (m3-5) develop normally (Guimera *et al.*, 2006b, Nakatani *et al*., 2007, Peltopuro *et al.*, 2010). Given that these GABAergic phenotype differences between the dorsal and vlMB and the fact that the underlying mechanisms operating in both sglMut, (*Mgn* sglMut: *Mgn-/- Mash1*+/+ and *Mash1* sglMut: *Mgn*+/+ *Mash1*-/-) were still poorly understood, the similar expression pattern of both genes (high expression in the vlMB and lower expression in the dMB (Peltopuro *et al*., 2010, Guimera *et al*., 2006b)) and the shared phenotypes indicate an apparent similar gene function during MB neurogenesis and the presence of a developmental program that functionally couples their activities for MB GABAergic neurogenesis Therefore, we focused on the role of these two factors and the mechanisms underlying their role in MB-GABAergic neurogenesis. In this study, we provide molecular, genetic and phenotypic evidence about two cooperating bHLH factors in the MB for the acquisition of GABAergic identity. We show distinct mechanisms by which MGN and MASH1 trigger the GABAergic cell fate, and suggest a model for d/vlMB-GABAergic neurogenesis during mouse development.

Given that MGN and MASH1 colocalize in most vlMB cells (Miyoshi *et al*., 2004) and the fact, that the GABAergic phenotype of sglMut mice is circumscribed in the dMB, we studied colocalization in that area. We could successfully determine MGN to colocalize with MASH1 in the entire MB neuroepithelium making an interaction likely. Albeit MGN appeared restricted to the MB VZ and to the GABAergic lineage, MASH1 is also expressed in postmitotic precursors suggesting possibly additional roles in neurogenesis since it has been also related to other neural lineages of different lineage including various neurotransmitter identities like noradrenergic, ACh+, 5-HT+, and TH+ lineages, but also oligodendrocytes and astrocytes (Kim *et al*., 2008, Guillemot *et al.*, 1993, Pattyn *et al*., 2006, Parras *et al.*, 2002). Protein-

protein interactions are intrinsic in eliciting the function of virtually all bHLH factors. We confirmed previous *in vivo* studies suggesting MGN protein was able to form homo- as well as heterodimers *in vitro*. Furthermore, we could demonstrate that MGN and MASH1 interacted at the protein level to form MGN/MASH1 heterodimers in physiological conditions at the time of the onset of MB GABAergic neurogenesis, dorsally and ventrally. Thus, we hypothesiszed that a different combination of homo- or/and heterodimers of MGN and MASH1 can result into a different transcriptional regulation of their downstream targets and therefore into different mechanisms of GABAergic specification.

Indeed, the present data provided compelling evidence that in the MB, the synergistic action of the two factors MGN and MASH1 are prerequisite to trigger GABAergic neurogenesis. By comparative phenotypic analysis of *Mgn* and *Mash1* sglMut (*Mgn+/+ Mash1-/-; Mgn-/- Mash1+/+*), dblHet (*Mgn+/- Mash1+/-)*, mutants carrying only one active allele of either *Mash1* or *Mgn* (*Mgn-/+ Mash1-/-; Mgn-/- Mash1+/-*) and dblKO (*Mgn-/- Mash1-/-*) mice, we identified *Mgn* and *Mash1* to function as selectors of GABAergic identity in a dorsal/ventrolateral mechanism – dependent on the formation of homo- and heterodimers. Thereby all four alleles have a crucial role in acquiring GABAergic phenotype and none of them has a dominant effect over the other; only when the genetic constellation allows MGN and MASH1 to form heterodimers, dMB GABAergic induction takes place while vlMB GABAergic neurogenesis functions in a dose dependent manner. Thus, we propose three main mechanisms for the acquisition of MB-GABAn during the three distinct phases of development separated in time and place;

I) the first wave in the vlMB: the earliest wave of GABAergic neurogenesis takes place at E9.5-E10.5 in the vlMB in domains m3-5 (ventral AP and dorsal BP) and corresponds with the highest expression level of *Mgn* and *Mash1* mRNA. At this time point, GABAergic neurogenesis is induced in the presence of MGN and/or MASH1 factors, indistinctly operating in a dose-dependent manner. Thus, MGN or MASH1 homodimers are sufficient for the induction of GABAn and heterodimers are not required.

II) the second wave in the dMB: the second phase takes place two days later at E12.5 in the dMB (domains m1-2; RP and dorsal AP) where the levels of *Mgn* and *Mash1* expression are only about a quarter of their vl expression profile; MGN/MASH1 heterodimers are *sine-qua-non condition* and each homodimer is not sufficient for the induction.

III) the third wave in the vMB: the third wave or population appears at E14.5 in the basal/floor plate (domains m6-7, the vmMB) comprising GABAn of the SNpr and VTA (MASH1+ but MGN negative territories). None of the *Mgn*/*Mash1* single, double or compound mutant embryos shows a GABAergic phenotype in the SN/VTA area. Thus MGN/MASH1 hetero-/ or homodimers seem not necessary for their specification or migration as most of them migrate from the HB into the MB where *Mgn* is not expressed.

Besides the time constrains and different d/vl expression profiles of *Mgn* and *Mash1*, the major mechanism underlying MB GABAergic neurogenesis is the different requirement of MGN/MASH1 homo and heterodimers in the dMB versus vlMB. Thus we propose that MB GABAergic neurogenesis complies with the following rules (Fig. 9.1).

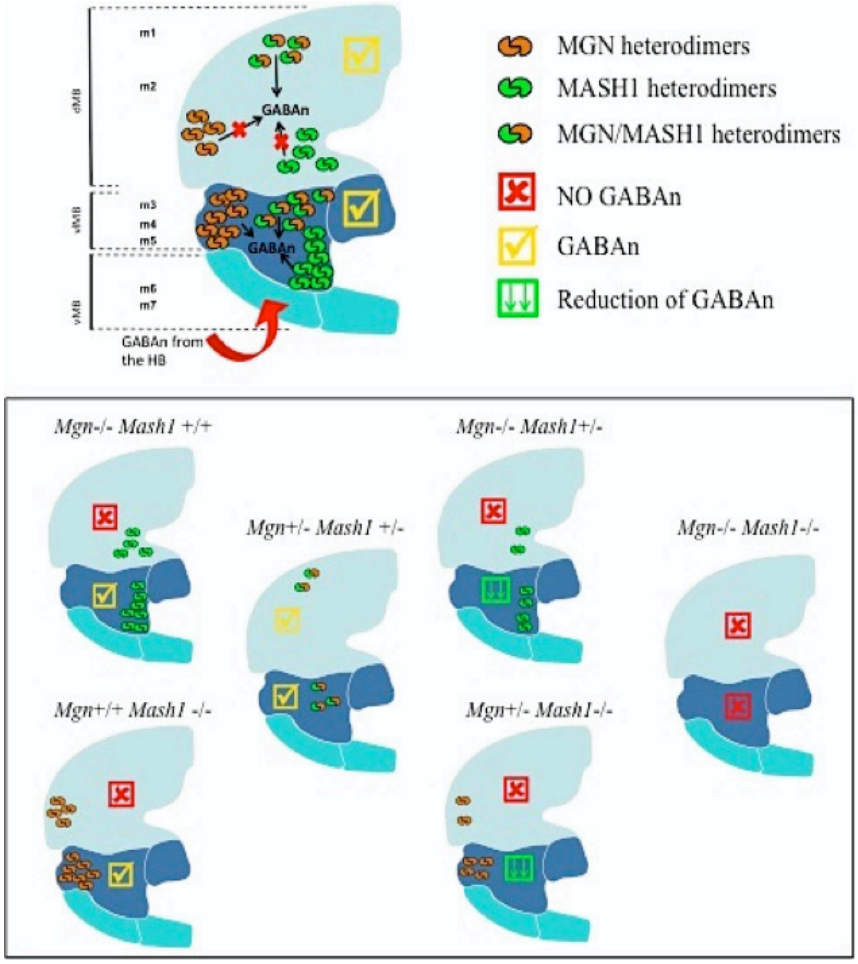

Figure 9.1: The dorsoventrolateral mechanism for the induction of MB GABAn by homo- and heterodimers of MGN and MASH1.

MGN/MASH1 heterodimers comprise the instructive role in specifying the identity of dMB-GABAn and neither MGN nor MASH1 homodimers can compensate for the loss of MGN/MASH1 heterodimer function in the dMB. The complete loss of dMB GABAn in the sglMut mice implies that MASH1 homodimers are insufficient to induce the GABAergic fate in the dMB. However, double heterozygous mice, carrying one allele from each locus are able to trigger dMB GABAergic induction (dorsally and ventrally) compared with WT animals, although still harboring the same number of total alleles. Thus, MGN/MASH1 cooperation is needed in the dMB and genotypes lacking either *Mash1* or *Mgn* (sglMut) and mutants carrying only one active allele of either *Mash1* or *Mgn* (*Mgn-/+ Mash1-/-; Mgn-/- Mash1+/-*) and therefore do not allow heterodimerization, no dMB but only vlMB GABAn are induced. Thus, MGN and MASH1 appear to have a synergistic role in specifying GABAergic fate in the dorsal aspect of the MB and heterodimers are prerequisite for it. A possible explanation why in sglMut mice appears to rely on different efficiency between MGN/MASH1 hetero-/ and homodimers is based on the different levels of expression of both genes which results in different capacities of homo/heterodimers to trigger GABAergic neurogenesis; the low expression levels of either *Mgn* or *Mash1* mRNAs in the dMB are not sufficient to induce GABAergic neurogenesis while the stronger expression of either *Mgn* or *Mash1* in the vlMB is sufficient. Thus, heterodimers appear to exert a higher efficiency over homodimers, thereby compensating for the low levels of *Mgn* and *Mash1* expression in the dMB (compared with the vlMB). This theory of the higher efficiency of heterodimers is not only supported by the fact that homo- or heterodimer combinations of bHLH TF can alter the strength of DNA binding thereby altering gene regulation (Fairman *et al*., 1993), but also by several previous studies showing a particular effect in target gene activation among the coincident expression of *Mgn* and *Mash1*: by testing yeast cultures, expressing different combinations of proneural factors in the presence 3-AT (which inhibits the synthesis of histidine (a vital amino acid in a strain of yeast that is auxotrophic for histidine), the cells expressing both factors were able to grow even in the presence of high concentration of 3-AT, whereas yeasts forming MGN/MGN or MASH1/MASH1 homodimers were not. Thus, MGN/MASH1 heterodimers – compared with homodimers – showed stronger affinity interaction. Moreover, β-galactosidase assays in liquid cultures showed that the strength of the MGN/MASH1 protein interaction is up to 4.0 times higher than that for the MGN/MGN and MASH1/MASH1 homodimers, respectively (Wende *et al*., 2015). Also in *vivo* experiments revealed similar observations: *Mgn* misexpression, in the presence of MASH1 at E10.5 results in premature GABAn in the dMB, despite GABAergic neurogenesis in this area starts only at E11.5-12.5. In the same experiment, ectopic GABAergic markers can be detected also in the mvMB area, which expresses *Mash1* only and does not give rise to MB derived GABAn at any stages (Miyoshi *et al.,* 2004). Further, mirroring our observations in the dMB GABAergic neurogenesis in compound mice, co-transfection of *Mgn* and *Mash1* potentiated GABAergic differentiation in cultured cells (Miyoshi *et al*., 2004). Although heterodimers have clearly the capacity to trigger GABAn, the massive expression of *Mgn*

and *Mash1* in the vlMB, may result in still more heterodimer formation compared to the dMB, also in dblHet mutants. This may explain the initial delay of GABAergic neurogenesis in the dMB in dblHet mutant embryos, which is overcome by the end of the second wave (E13.5). Nevertheless, we cannot rule out that in the presence of both proteins, also homodimers contribute to the generation of GABAn in the dMB. Thus, the combination of our phenotypic analysis of dblHet and compound mutant mice, supported by the molecular data from previous *in vitro* and *in vivo* experiments, provides a precedent for the hypothesis that the MGN/MASH1 heterodimers - despite low levels of *Mgn* and *Mash1* expression in the dMB – are sufficient to trigger GABAergic phenotype and are more efficient activating the GABAergic pathway compared with their homodimers.

In the vlMB, either MGN or MASH1 homodimers are sufficient to induce GABAn in a dose-dependent manner, resulting in a gradual phenotype from sglMut mutant mice to mutants carrying only one active allele of either *Mash1* or *Mgn* (*Mgn-/+ Mash1-/-; Mgn-/- Mash1+/-*). In contrast, MGN/MASH1 heterodimers are not needed for the induction of vlMB GABAn. Based on the fact that MGN and MASH1 can also form homodimers (MGN/MGN and MASH1/MASH1, respectively), we further propose that in the vlMB, homodimers of MASH1 in the absence of MGN – and vice versa – can take over the GABAergic cell fate function in the vlMB at these developmental stages of the first wave (E9.5-10.5) and trigger GABAn induction. The restriction of GABAn induction to the vlMB only in single and compound mutants can thus be explained by high level of expression of *Mgn* and *Mash1* in the vlMB compared to the dMB from which we further conclude that the massive amount of homodimers can circumvent and substitute the lack of MGN/MASH1 heterodimers and homodimers take over the function of GABAergic cell fate determination. Accordingly, analysis of compound mutants carrying only one active allele reveal, that the grade of GABAn induction is dependent on the number of active alleles of either *Mgn* or *Mash1* and therefore on the amount of homodimers. Even the presence of one single allele of either *Mgn* or *Mash1* (*Mgn-/+ Mash1-/-; Mgn-/- Mash1+/-*) was sufficient to induce vlMB GABAergic neurogenesis - although to a reduced level, when compared to sglMut mice (carrying two active alleles). Similar as with sglMut brains, no dMB GABAn were induced (due to the lack of heterodimers). These observations suggest that GABAergic induction in the vlMB is not only dependent on homodimerization of either MGN or MASH1 (as in sglMut) but also further dose dependent on the amount of dimers themselves: only one active allele contributes to less protein which therefore results in a less effective vlMB GABAn induction. At the same time, neither *Mgn* nor *Mash1* has a dominant effect over the other, as compound mutants with only one or two alleles – either from the *Mash1* or *Mgn* loci – displayed respective similar induction of GABAergic neurogenesis in the vlMB. This is in agreement with the observation that no compensatory mechanism existed between the levels of mRNA expression of *Mgn* and *Mash1* in dblHet mutant mice, as neither *Mgn* mRNA expression was upregulated in *Mash1* single mutant

mice and vice versa (Wende *et al*., 2015). Further, *Mash1* expression remains unaffected by ectopic expression or ablation of *Mgn* expression (Nakatani *et al*., 2007, Peltopuro *et al*., 2010, Miyoshi *et al.*, 2004).

In line with our hypothesis, in gain-of-function experiments, we ectopically expressed *Mgn* cDNA in organotypic cultures of WT mouse embryos at E10.5 induced *Gad65/67* expression throughout the CNS (Wende *et a*l., 2015). This suggested that *Mgn*, when expressed at high levels, does not need to cooperate with additional cell type-specific TFs to execute its function in a cell autonomous manner. Moreover, when *Mgn* is expressed at high levels by electroporation in the dMB of E12.5 *Mash1* single mutant embryos, GABAergic cell fate is also initiated (even in the absence of *Mash1* – and therefore in the absence of MGN/MASH1 heterodimers) (Wende *et al.*, 2015). Hence, high levels of MGN protein in the dorsal aspect have the capability to overcome the lower efficiency of heterodimers and mimic the *in vivo* conditions in the vlMB of the *Mash1* sglMut, where MGN homodimers are generated to high extend and are sufficient to induce GABAergic fate (neither MGN/MASH1 heterodimers nor MASH1 homodimers can be formed in the *Mash1* single mutant mice). Also overexpression of either *Mgn* or *Mash1* can induce GABAergic fate in other tissues: overexpression of *Mgn* in the FB is able to induce GABAergic fate (Nakatani *et al*., 2007, Sellers *et al*., 2014). A similar study revealed, that gain-of-function *Mgn* in the diencephalon is capable to induce specific rTH GABAergic fate in the adjacent caudal compartment (Sellers *et al*., 2014). This reflects the capacity that high levels of MGN homodimers to exert a GABA fate induction (Delogu *et al*., 2012, Guimera *et al*., 2006b). Albeit loss-of-function of *Mash1* did not alter *Gad67* expression in rTH progenitors, (Virolainen *et al.*, 2012, Peltopuro *et al.*, 2010) overexpression of *Mash1* in the FB and cortex (Fode *et al*., 2000, Parras *et al.*, 2002) but also in stem cells and even bone marrow mesenchymal stem cells was seen to result in profound GABAergic neurogenesis (Roybon *et al*., 2010, Wang *et al.*, 2013). Thus we suggest that the high levels of *Mgn* and *Mash1* expression in the vl-domain most likely reflect the limited efficiency of their homodimers to trigger GABAergic neurogenesis rather than an inherent functional difference between heterodimers and homodimers. Instead, MGN and MASH1 have the capacity to work either as homo- or heterodimers, and homodimers appear to act in a dose dependency while heterodimers can compensate for low levels of expression of either MGN or MASH1, dependent on their developmental origin in the neural tube.

The synergistic function of MGN and MASH1 can be proven as concomitant loss of function of both genes culminates in the loss of all dMB and vlMB GABAn (except for a small number of residual GABA+ cells in the ventrolateral m5 domain). As this phenotype persist until P0, it indicates that no other factor takes over the function of MGN/MASH1 homodimers in the vlMB, nor heterodimers in the dMB regarding the induction of *Gad67* expression. Nevertheless, we cannot rule out that a third factor is involved in the specification of GABAn in the MB, although our results indicate that both factors play a

pivotal role in regulating MB GABA fate. Yet, the plausibility and importance of the synergistic action of *Mgn/Mash1* is strengthened, as our hypothesis is the key explanation for observations about GABAergic neurogenesis in the FB by the group of Song *et al*. in 2014: They suggested a collaborative role of *Mgn* and *Mash1* (which are also coexpressed in the diencephalon) for the generation of GABAergic populations in the diencephalon. This suggestion is based on the observation that in sglMut, *Gad67* expression is largely unaffected in TH-R despite an almost complete lack or downregulation in pretectal neurons. By contrast, in dblKO mutants, there was a significant loss of *Gad67* expression in the TH-R domain (Song *et al.*, 2014). These spatial differences in the expression of *Gad65/67* in sglMut versus dblKO appear similar to what we observed in the MB. Thus, we propose that our mechanisms can be transferred to other brain parts. Hence, the absence of GABAn in dblKO FB as well as the spatial difference in *Gad67* expression between sglMut and dblKO in the FB depends presumptively also on the generation of homo/heterodimers of MGN/MASH1.

The GABAergic populations of the vmMB, which are associated with the DA system, are independent of *Mgn* or *Mash1*. Later on development, from E14.5-E15.5 onwards, a conspicuous subpopulation of GABAn is detected in the most ventral part of the MB (vmMB; domain m6-m7) in the dblKO mutants. Their presence in the absence of MGN and MASH1 can be explained as these subpopulations of GABAn, associated with the dopaminergic nuclei (SNpr and VTA), have their developmental origin outside the MB; these neurons migrate out of r1 of the HB, where GABAergic fate is independent of *Mgn* (*Mgn* is never expressed in the HB) and *Mash1* (Achim *et al.*, 2012).

The synergistic function of MGN and MASH1 unravels a new paradigm for the means of protein interaction between [*h/E(spl)*] and proneural factors. The proneural bHLH gene *Mash1* contributes to the specification of various neuronal fates of different lineage and has been particularly implicated with GABAergic fate in various brain compartments. This specification is highly dependent on the presence of other determinants of neuronal identity (Parras *et al*., 2002). Yet, the major role of *Mash1* conveys regulation of neurogenesis in the neural tube where TFs of the bHLH family play a phylogenetically conserved role in vertebrates and invertebrates. Neurogenesis in particular, depends on the balance between such proneural gene families and the members of the [*h/E(spl)*]. The latter ones are the direct effectors of NOTCH signaling, which maintain NOTCH active cells in a progenitor state by lateral inhibition, whereas the proneural genes typically promote neuronal identity (reviewed in Bertrand *et al*., 2002; Kageyama *et al*., 2008). These two major groups counterpart each other to control the number of neurons and their identity along the three primary brain vesicles of the neural tube. Albeit MGN belongs to the [*h/E(spl)*] family, MGN differs from [*h/E(spl)*]/HES TFs in several critical facts as conserved amino acid positions within the bHLH domain. Thus, these differences distinguishes it from other subfamilies related to the [*h/E(spl)*] family, including the mammalian HES, HEY, SHARP and DEC1 subfamilies and

define MGN to a new subclass of bHLH transcription factors (Guimera *et al.*, 2006a). Indeed, *Mgn* encodes a protein that shares structural homology within the bHLH-O region to the products of *Drosophila* [*h/E(spl)*] genes and promoter binding analysis performed *in vitro* suggest, that MGN homodimers act as a transcriptional repressors by binding to E-box class B and C1 sequences, which are typical recognition sequences for bHLH repressors. Notably, MGN shows also a different preference for the core sequence when compared with other bHLH-O repressors (Nakatani, 2004). Whether MGN activates neurogenesis *in vivo* by binding to the typical recognition sequence for activators, the E-box class A, or represses repressors of neurogenesis in either homodimer or heterodimer condition needs to be formally probed. In case that *Mgn* has solely a repressor function in physiological conditions, does not imply necessarily, that *Mgn* inhibits neurogenesis, since neurogenesis could also be activated by repression of repressors of neurogenesis. A typical example is *Hes6* (a repressor bHLH gene) promotes neurogenesis by repressing of neurogenesis (Bae *et al.,* 2000). Further, in our gain-of-function studies, *Mgn* also has the capacity to solely direct GABAergic fate thus it is exerting a promoting effect. Despite the fact that TFs belonging to the [*h/E(spl)*] have long been thought to mainly counteract proneural gene's function, this work uncovers the first example of de facto synergistic protein interaction of [*h/E(spl)*] and proneural factors. This interaction clearly underlies different context dependent mechanisms but provides a novel paradigm how these two families can cooperate for the proper acquisition of GABAergic neuronal identity.

9.2 IMPAIRED NEUROTRANSMITTER SPECIFICATION IN THE D/VLMB OF DBLKO MUTANTS

Data from *Mgn* and *Mash1* single knockout mice showed no proliferative deficits or cell death in the VZ/subventricular (SVZ) of the dMB. Nevertheless, the hypothesis, that *Mash1* and particularly *Mgn* - in regard to its [*h/E(spl)*] function – play a role in generating the proper number of GABAergic precursor cells in the MB cannot be excluded. Since *Mgn* or *Mash1* can take over each other function regarding the vlMB GABAergic specification, redundancy may also mask a proliferative function. To uncover a possible role in proliferation, extensive analysis of cell proliferation and cytoarchitecture at the time of GABAergic neurogenesis and later on in development have been performed. No reduction in cell proliferation was identified in the d/vlMB of double mutants at E10.5–E14.5 as revealed by IHC staining of mitotic cells surrounding the lumen of the neural tube with pHH3. Likewise, neurons, time-traced with BrdU, showed no proliferation deficits in the MB of dblKO, and the BrdU-labeled progenitors migrated radially to the MZ as in the littermate controls (Wende *et al*., 2015). There was also no evidence of increased apoptosis in the MB dblKO embryos, when compared with the littermate controls at the time of GABAergic neurogenesis, evidenced by apoptotic cCASP3 and TUNEL essays. Further, tracing of *Mgn* derivatives, which expressed *tau-lacZ* under the endogenous *Mgn* regulatory elements of the *tau-lacZ* knocked in the *Mgn* locus (Guimera *et al*., 2006b), the pattern of lacZ staining revealed, that the lacZ-stained neurons in dblHet and dblKO mutants were positioned in stream-like routes and initiated their radial migration toward the MZ through the intermediate zone, consistent with previous studies in single knockouts (Guimera *et al*., 2006a). Furthermore, the cytoarchitecture in dblHet and dblKO mutants revealed no significant difference as well as the cell density of differentiated neurons was comparable with WT mice, as determined by staining for NeuN. Interestingly, the neurons of dblKO mutants acquire the possibility to transduce GABAergic chemical signals since Ca^{2+}-binding proteins, which mark subpopulations of GABAn were expressed comparable to WT mice. Therefore, several lines of evidence indicate that in the absence of both, MGN and MASH1, d/vlMB-GABAergic precursor cells are generated properly and the progenitors that should have become GABAn, do not undergo apoptosis. Instead neurons are generated at proper numbers in VZ of d/vlMB during the first two waves of GABAergic neurogenesis (E10.5–E12.5) and the progenitors that should become GABAn do not enter into mutant-specific apoptotic programs but migrate radially towards the MZ (Fig. 7.8). The defective GABAn persist during development in dblKO mice and are maintained without expressing GABA until birth. Thus MGN and MASH1 control GABAergic neurotransmitter indentity whithout regulating the number of precursor cells.

Although *Mgn* function has already been shown not to be involved in progenitor domain formation or maintenance of *Mash1* (Kala *et al.*, 2009, Miyoshi *et al*., 2004) in m3–m5, *Mash1* in contrast, was shown

to regulate separation of neurogenic and neural stem cells, which results in a delay of GABAergic neurogenesis (Peltopuro *et al.*, 2010). In this study, the relative amount of MGN+ cells in *Mash1* sglMut is greatly increased in the vlMB: only few MASH+/MGN- cells were found in the *Mash1* sglMut VZ in domains m3-5, while in the dMB, *Mgn* (and neurogenesis) expression was completely unaffected. Concomitantly, the onset of GABAergic and Glutamatergic neurons is delayed in the vlMB at E11.5. Nevertheless, by E13.5 when GABAergic neurogenesis in the vlMB is already diminished, expression pattern of *Mgn/Mash1* is restored and the disturbation recovered. At that developmental stage, postmitotic precursors expressed GABAergic markers to their regular level. Therefore, we doubt that the claimed disturbance in progenitor formation is the reason for the compromised phenotype in dblKO and compound mutants observed in this study. Rather, the massive depletion of d/vlMB GABAergic markers in dblKO mutants occurs at the onset of neurogenesis by a failure of GABAergic fate commitment rather than deficits in the number of precursor cells or migration cues.

9.3 MGN AND MASH1 HOMO- AND HETERODIMERS ACTIVATE ESSENTIALLY THE SAME DOWNSTREAM TARGETS INVOLVED IN MB GABAERGIC NEUROGENESIS – A HYPOTHESIS OF HOMO- VERSUS HETERODIMER SENSITIVITY AND SYNERGY OF INTERPLAYERS

Although in the absence of *Mgn* and *Mash1*, the GABA-defective neurons are physically present, these generated neurons can no longer be called GABAn, as they lost their capacity to produce the neurotransmitter GABA and therefore their proper GABAergic identity. Nevertheless, all MGN+ cells coexpress MASH1 in the MB VZ and therefore share the same presumptive pool of GABAergic precursor cells. We considered that the genetic network behind MGH/MASH1 heterodimers and homodimers is essentially maintained along the d/vlMB axis and they can activate essentially the same downstream genetic cascades to induce neuronal differentiation. By phenotypic analysis of *Mgn/Mash1* sglMut, dblHet, mutants carrying only one active allele of either *Mash1* or *Mgn* (*Mgn-/+ Mash1-/-; Mgn-/- Mash1+/-*) and dblKO mutants for factors (*Gata2, Tal1, Tal2*, *Sox14*, and *Lim1*), which are known to be involved in MB GABAergic fate and are shown to follow similar expression cascades in the FB, we addressed possible change in the expression of these downstream targets, dependent on different combinations of homo-/heterodimer formation of MGN and MASH1. De facto, we could show that the defective postmitotic GABAn downregulate expression factors, predictive for their GABAergic fate.

All these factors showed a clear dependency on MGN/MASH dimers. Albeit these factors follow in the MB a similar expression cascade as in the FB, their expression in the MB consequential to different genotypes of *Mgn* and *Mash1* appeared individually distinct from each other: *Gata2* and *Tal1* expression followed the d/vl mechanism described for *Gad67*/GABA, while *Tal2*, *Sox14*, and *Lim1* appeared region specifically regulated by heterodimers only. Albeit *Tal2*, *Sox14*, and *Lim1* expression dependency on MGN/MASH1 in the MB differs from the d/vl mechanism (as for *Gad67*/GABA, GABA, *Gata2* and *Tal1*), it is in good agreement with our hypothesis, that MGN/MASH1 heterodimers appear to be more efficient. Heterodimers of MGN and MASH1 can trigger GABAergic markers (as *Gata2, Tal1, Sox14, Lim1* and *Gad67*) not only more efficiently than homodimers in the dMB but can also play an instructive role in the vlMB, where heterodimers are also required for the expression of *Tal2* (m5), *Lim1* (m3-4) and *Sox14* (m3-5). Therefore it appears as if different GABAergic markers are more sensitive to homodimers of MGN/MASH1 and can be activated already by homodimers (as *Gad67, Gata2* and *Tal1* in the vlMB), whereas some downstream targets (as *Sox14* and *Tal2*) require heterodimers for activation. Thus, despite similar expression cascades in different brain areas, the requirement of heterodimers triggering particular

downstream factors appears highly region specific, comparing the sole or mutual function of MGN and MASH1.

9.3.1 *Gata2* and *Tal1* follow the d/vlMB mechanism of MGN/MASH homo- and heterodimers

The zinkfinger TF GATA2 has been shown to promote GABAergic fate in the diencephalon and MB (Virolainen *et al*., 2012, Kala *et al.*, 2009). Partially coexpressed with *Mgn, Gata2* is a *Mgn* dependent marker of post-mitotic GABAergic precursors, which are about to exit the VZ and to differentiate. Markedly fewer GATA2+ cells could be observed also in the *Mash1* mutant MB (Peltopuro et al., 2010), making it likely that *Gata2* would also be regulated by the combinatorial genotype of *Mgn* and *Mash1*. Indeed by phenotypical analysis of dblKO, dblHet and compound mutants we identified *Gata2* expression to follow the d/vl dependency of heterodimers and homodimers of MGN/MASH1. Strikingly, *Gata2* knockout mice reveal a phenotype similar to that of the *Mgn/Mash1* dblKO – a complete lack of *Gata2* expression in the entire m1-5 except some residual cells in m5, respectively. Similar to the MB, *Gata2* is downstream of *Mgn/Mash1* in the diencephalon as it is reported to be absent, accompanied by the loss of *Gad67* expression (Virolainen *et al.*, 2012). Yet, the lack of *Gad67* expression in *Gata2* deficient mutants in the diencephalon is transient, in contrast to that of combined *Mgn*/*Mash1* mutants, which show persistent loss of GABAergic markers throughout later stages (Song *et al.*, 2014). This is different from the MB, where the loss of *Gata2* results in enduring loss of GABAergic markers. Thus, *Gata2* may have a more abiding role in the MB for GABAergic neurogenesis. Since *Gata2* in the MB follows our proposed d/vl mechanism of MGN and MASH1 while not affecting cell cycle exit in the MB it emphasizes the crucial role of *Mgn* and *Mash1* for earliest MB GABA fate acquisition.

In the MB, the bHLH TF TAL1 is coexpressed with GATA2 in presumptive MB GABAn and both participate in their neuronal subtype selection (Achim *et al*., 2013, Kala *et al*., 2009). TAL1 alone is not required for GABAergic neuron differentiation from the MB neuroepithelium but is thought to act in concert with GATA2 in a complex to probably maintain GABAergic identity (Achim *et al*., 2013). We confirm *Tal1* to be downstream of *Gata2* and that both factors are expressed on the same pathway for MB GABAergic neurogenesis. Consequently, like *Gata2*, *Tal1* expression in m1-5 appears directed by the combinatorial expression of *Mgn* and *Mash1*. Similar dependency to the dMB was shown to act in the rTH and pretectum, where GATA2+ and TAL1+ neurons, contributing to the same lineage, were downregulated upon combinatorial ablation of *Mgn* and *Mash1* (Song *et al.*, 2014). At E14.5, we noticed a population of neurons defined to the VTA and SNpr of dblKO brains, which expressed *Tal1* and *Gata2*. As mentioned above, *Mgn* is never expressed in the HB, neither affects *Mash1* GABAergic neurogenesis in the HB (Peltopuro *et al.,* 2010). Therefore, ablation of *Mgn/Mash1* did not alter the expression of the

specific markers TAL1 and GATA2 in the HB. Thus the TAL1+/GATA2+ population in the dblKO comprises the postmitotic GABAergic precursors which migrate from the HB, expressing their specific markers TAL1 and GATA2 and arrive in the MB at E14.5-E15-5 (Achim *et al*., 2013).

9.3.2 *Tal2* expression is dependent upon MGN/MASH1 heterodimers in m5

Notably, the phenotype regarding residual GABAergic cells in the MB m5 domain of *Mgn/Mash1* dblKO mutant resembles greatly the phenotype of the *Tal2* knockout as in both mutants, the MB is completely devoid of GABAn (Achim *et al.*, 2013). Albeit the *Gata2* knockout mutant shows a similar downregulation of GABAergic markers in the MB (Kala *et al*., 2009*),* in contrast to *Gata2*, we observed *Tal2* expression not to follow the d/vl mechanism of MGN/MASH1 – except for the m5 domain – where heterodimers of MGN/MASH1 were prerequisite. Strikingly, only upon ablation of both, *Mgn* and *Mash1,* in the FB, *Tal2 was* downregulated only in the rTH whereas ablation of one gene alone had no effect on *Tal2* expression (Song *et al*., 2014). Therefore, *Tal2* expression appears to be activated by MGN/MASH1 heterodimers, but only in certain regions of the neuroepithelium. Its exact regulation appears different from the mechanism for *Gata2* and *Tal1* and more complex as defined to particular GABAergic lineages (m5 in the MB). *Tal2* is plays also a role for proper tectum morphology since *Tal2* knockout mutants show a distinct dysgenesis of the midbrain tectum. Due to the loss of superficial gray and optical layers, the SC is reduced in size and the IC colliculus is abnormally rounded and protruding in mutants after E15.5 (Bucher *et al.*, 2000). Since we did not observe any changes in size nor morphology in dblKO mutants, additional, so far unknown roles of *Tal2* might explain the independency its expression from the MGN/MASH1 – GATA2 pathway.

Markedly, *Gata2* – although mainly coexpressed with *Tal2* – is activated independently from *Tal2,* as its expression is unaffected in the *Tal2* mutant (and *Tal1/2* dblKO). Another intriguing aspect is, that MB GABAn appear only to be generated to proper extend when both, *Tal2* and *Gata2* – albeit acting individually - are coincidently expressed (at least in m1-4): In single mutants, only *Tal2* is expressed in the dMB, but not *Gata2*, while both are expressed in the vlMB m3-4. Concomitantly, GABAn could be observed in single mutants only in the vlMB. In dblHet mutants of *Mgn/Mash1*, both factors are expressed in the entire m1-5 domain, which in turn correlates with normal GABAergic marker expression in these areas (Fig. 9.2). Moreover, *Tal1* is absent in both, the *Gata2* and *Tal2* mutant (Achim *et al*., 2013). Yet, some *Gata3* expressing cells in the m5 domain were still detected of the *Tal1/2 dblKO* MB (Achim *et al*., 2013). Just like *Tal1*, *Gata3* is expressed in GABAergic postmitotic progenitors and was shown to be downstream of *Gata2* (Kala *et al*., 2009) and further to follow the d/vl mechanism of MGN/MASH1 (Wende *et al*., 2015).

This suggests that even in *Tal1/2* dblKO, the loss of GABAergic identity is still incomplete - at least in this m5 domain. Further it proposes, in the MB, two individual but mutual pathways for GABAergic neurogenesis might be linked together at the time of beginning *Tal1/Gata3* expression: one pathway guided by MGN and MASH1 - regulating *Gata2* by heterodimers and homodimers in a d/vlMB fashion - and one pathway which is linked to *Tal2,* only dependent on heterodimers in m5. Alternatively – although unlikely – considering *Tal2* not being expressed in the VZ of the MB, another factor might be involved in early GABAergic specification, additional to *Mgn* and *Mash1*. Yet*, Gata2* and *Tal2* expression are activated very early during GABAergic neuron differentiation but are mainly confined to the IZ. Further, *Mgn* and *Mash1* are detected in the VZ to normal extent in both, *Gata2* and *Tal2* knockout mutants (Achim *et al*., 2013, Kala *et al*., 2009). This indicates, that the absence of these factors results in alterations in GABAergic fate only at the postmitotic differentiation stage, after the expression of *Mgn* or *Mash1*. Therefore, the most notable difference between these two factors and MGN/MASH1 may be the timing of misregulation; *Mgn* and *Mash1* appear to function as primary selectors of GABAergic identity in mitotically active GABAergic precursors, whereas *Gata2* and *Tal2* are selectors expressed in postmitotic neurons of the intermediate and MZ driving GABAergic fate.

9.3.3 *Sox14* expression requires heterodimers of MGN and MASH1 in the MB

Sox14 was recently described as one of the latest GABAergic markers in the diencephalon. A*s* a marker for all nuclei of the subvisual shell VS it is required to drive development of a functional network supporting light-entrained circadian behaviors (Delogu *et al.,* 2012). In the diencephalon, it acts downstream of *Mgn* and is activated sequentially with *Mgn, Tal1* and *Gad67*. Further, it was reported downregulated in the entire diencephalon in the *Mgn/Mash1* dblKO (Song *et al*., 2014). Since *Sox14* is also expressed along GABAergic lineages deriving from the MB (m1-5) and its expression is absent in *Tal1/2* double mutant concomitant with *Gad67* (Virolainen *et al*., 2012), we addressed *Sox14* expression in different *Mgn/Mash1* genotypes. Although we observed *Tal2* dependent on MGN/MASH1 heterodimers in the MB domain m5, we detected a strong dependency of *Sox14* on MGN/MASH1 heterodimers in the entire MZ of m1-5. Except some scattered *Sox14*+ cells in m3-4, which appeared independent from *Mgn* and/or *Mash1, Sox14* expression was lost in the entire MB MZ in all genotypes that did not allow heterodimerization. Since these phenotypes regarding *Sox14* expression did not alter over time and the amount of the independent cells remained starting from E11.5, and no persistent proliferative function is attributed to *Mgn/Mash1* (Wende *et al*., 2015), we rather suggest that the scattered cells in m3-4 are independent of *Mgn/Mash1* (similar to m5 for *Gad67, Gata2* and *Tal1* expression in m5). This is reinforced by the contrasting, prominent capacity of heterodimers, to direct *Sox14* fate in the

entire MB (also in m3-4; the vlMB) comparable to WT, while completely missing in the dblKO (except the mentioned residual cells).

9.4 THE INVOLVEMENT OF MGN/MASH1 IN THE REGULATION OF GABAERGIC VERSUS GLUTAMATERGIC FATE

As MB GABA defective cells in *Mgn* and *Mash1* single and dblKO mutants are not arrested into a progenitor-like state, the keep migrating radially out of the VZ towards the MZ and integrate themselves into the unchanged neuronal cytoarchitecture as, we considered neurotransmitter switch possibly to glutamatergic fate. Such fate switch is conceivable, as GABA is converted from glutamate and MB GABAn have been shown to switch into a partial and transient glutamatergic fate upon ablation of GABAergic factors (Achim *et al.*, 2012, Achim *et al.*, 2013, Kala *et al.*, 2009, Anderson *et al.*, 1997, Hoshino *et al.,* 2005).

Likewise, *Mgn* was shown to promote induction of the GABAergic related LIM1 TF by repression of the proneural genes *Ngn1/2* which in turn promote glutamatergic fate via induction of *Brn3a* (Nakatani *et al.,* 2007). In the MB, *Lim1* is coexpressed with *Gad67* in the m1-5 domains at the single cell level, but also in m6, which is a glutamatergic domain (Nakatani *et al.,* 2007). Consistent with the results from Nakatani's group, *Lim1* was absent in m1-2 and downregulated in m3-4 upon *Mgn* ablation, while m5 (and m6) was independent from MGN/MASH. In their study, *Lim1* was also absent in m3-4 in the *Mgn* knockout. However, we detected some LIM+ cells in m3-4, which were independent from both *Mgn* and *Mash1* as they appeared also in the dblKO. Also for *Lim1* expression, heterodimers had the capacity to allow the proper expression to the same level as in WT mice. Thus, similar to *Sox14* expression: also *Lim1* is also subordinated to heterodimers to ensure proper expression except for some residual cells in m3-4.

Particularly, the dorsal MB generates both GABAergic and glutamatergic neurons in a mosaic fashion. In the dMB of *Mash1* and *Mgn* knockout mutants, *Brn3a* is upregulated driving the cells towards a glutamatergic fate at the expense of GABAn (Peltopuro *et al*., 2010, Nakatani *et al.*, 2007). Since *Mgn* sglMut brains also showed *Brn3a* expressed ectopically to the extent of *Lim1* and *Gad67* (Nakatani *et al*., 2007), we checked whether *Brn3a* would be conversely regulated to *Lim1* by MGN/MASH1 as mentioned by the group of Nakatani. Indeed, mutants lacking two alleles of *Mgn* revealed ectopic *Brn3a*+ cells in the m3-4 area, which is normally devoid of *Brn3a* expression. Besides this ectopic expression, *Mgn* also affects *Brn3a* expression in the dMB, since we confirmed a slight upregulation of *Brn3a* in m1-2 upon *Mgn* ablation (Nakatani *et al*., 2007, Peltopuro *et al.,* 2010). As *Brn3a* is linked to glutamatergic neurons expressing the vesicular glutamate transporter vGLUT2 in the MB (Nakatani *et al.*, 2007), this indicates a

potential neurotransmitter switch. Therefore, it was not surprising that the same dependency accounted for *vGlut2*, which was ectopically expressed in m3 and m4 in the absence of *Mgn.* Strikingly, in dblHet mutants, just like *Lim1*, also *Brn3a* (and *vGlut2*) expression was not altered and GABAergic cells were also generated to physiological level. This again reinforces the capacity of heterodimers to trigger the generation of the GABAergic lineages.

Besides a shared neurotransmitter fate, the GABAn and Glutamatergic neurons emerging from the m1-5 domains have distinct identities, marked by the coincident expression of different sets of postmitotic TF, which are linked to a specific neurotransmitter fate. Also in mutants of the *Mgn* downstream player *Gata2*, GABAergic neurons switch from GABAergic to a glutamatergic fate in m1-4, along with a partial loss of *Lim1* (Kala *et al*., 2009). Besides, in *Tal2* mutants a neurotransmitter switch from GABAergic to Glutamatergic fate occurs (Achim *et al*., 2013). Nevertheless, despite the similarity in transmitter switch, the ectopic glutamatergic neurons in *Gata2* and *Tal2* mutants differ in their expression of the domain/neurotransmitter specific TF; in both mutants, the neurotransmitter switch does not occur in all cells but the cells rather adopt the postmitotic TF fate of adjacent, glutamatergic domains. NKX2.2 is such a postmitotic TF, which selectively marks GABAn the dorsal m2 MZ (Nakatani *et al*., 2007) and GABAergic mixed with some glutamatergic neurons in the entire m4 domain (VZ and MZ). Since *Mgn* (and *Mash1*) regulates the expression of *Gata2* and *Tal2* (at least in m5), we investigated the expression of *Nkx2.2* to test a possible change in such a postmitotic marker expression in the combinatorial absence of *Mgn* and/or *Mash.*

We confirmed that when either *Mgn* or *Mash1* is missing, expression of *Nkx2.2* in the dorsal subpopulation in m2 is absent, while it is independent from *Mgn* or *Mash1* in m4 (Nakatani *et al*., 2007, Miyoshi *et al.*, 2004). Despite the partial neurotransmitter switch from GABAergic to glutamatergic in m4 in *Mgn* sglMut, this d/vl discrepancy is similar to the expression pattern of *Gad65/67* in sglMut, where only vlMB GABAn are generated. Notably, in dblHet mutants, the expression pattern of *Nkx2.*2 was not altered compared with WT brains, correlating with our expression analysis for GABAergic markers in these mutants. This suggests, that MGN/MASH1 heterodimers can shape up the full profile of a certain MB GABAergic lineage, while *Mgn* exerts its function mainly as cell fate determinant for GABAergic neurotransmitter identity.

9.5 HETERODIMERS OF MGN/MASH1 ENSURE THE PROPER EXPRESSION PROFILE OF THE MB COMPARABLE TO WT MICE

Since *Mgn* and *Mash1* specify the presumptive GABAn very early, and clearly control the expression of genes ensuring GABAergic fate decision, alterations in the postmitotic marker pattern is not surprising, when these genes are misregulated. Although this control differs in place for each factor, we noticed that only heterodimers of MGN/MASH1 are able to ensure the correct expression of all markers and therefore also correct GABAn distribution and postmitotic refinement in all domains (Fig. 9.2). Noticeably, all markers that are so far known to be involved in specifically MB GABAn (*Gad67, Gata2, Tal1, Sox14, Lim1,* and *Nkx2.2*, although not *Tal2*) were dependent on heterodimers of MGN/MASH1 in m1-4. Only when heterodimerization was possible, all markers along GABAn maturation were expressed to their proper extent at the right time and the postmitotic identity of the GABAn was maintained. This is reflected in the expression of *Gata2* and *Tal2*; they appear to ensure GABAergic fate in a mutual way, which in turn is only possible upon possible heterodimers. Further, *Lim1* appears to have a major role in specifying GABA versus glutamatergic fate, also highly dependent on heterodimers. Only when *Lim1* is properly expressed in m1-5 (as in dblHet mutants) comparable to WT, no switch to glutamatergic fate is coincident. In sglMut and dlbMut mice the lack of *Lim1* expression in m1-4 coincidences with ectopic or upregulated glutamatergic cells - exactly in these areas. This might also explain why *Lim1* in m6 defines glutamatergic neurons: *Mash1* but not *Mgn* is expressed here, indicating that *Lim1*, when expressed in areas where it is under control of *Mgn* drives preferentially GABAergic fate. Thus, we propose that in the m1-4 domain, GABAergic versus glutamatergic fate is partially specified by MGN and MASH1. This might occur via the correct expression of *Lim1*, since only heterodimers ensure the right neurotransmitter fate (GABA versus glutamate). This suggests that in the absence of *Mgn*, the cells become preferentially glutamatergic, while in the presence of heterodimers of MGN/MASH1 the proper expression of all interrogated markers retain the accurate GABAergic identity (Fig. 9.2).

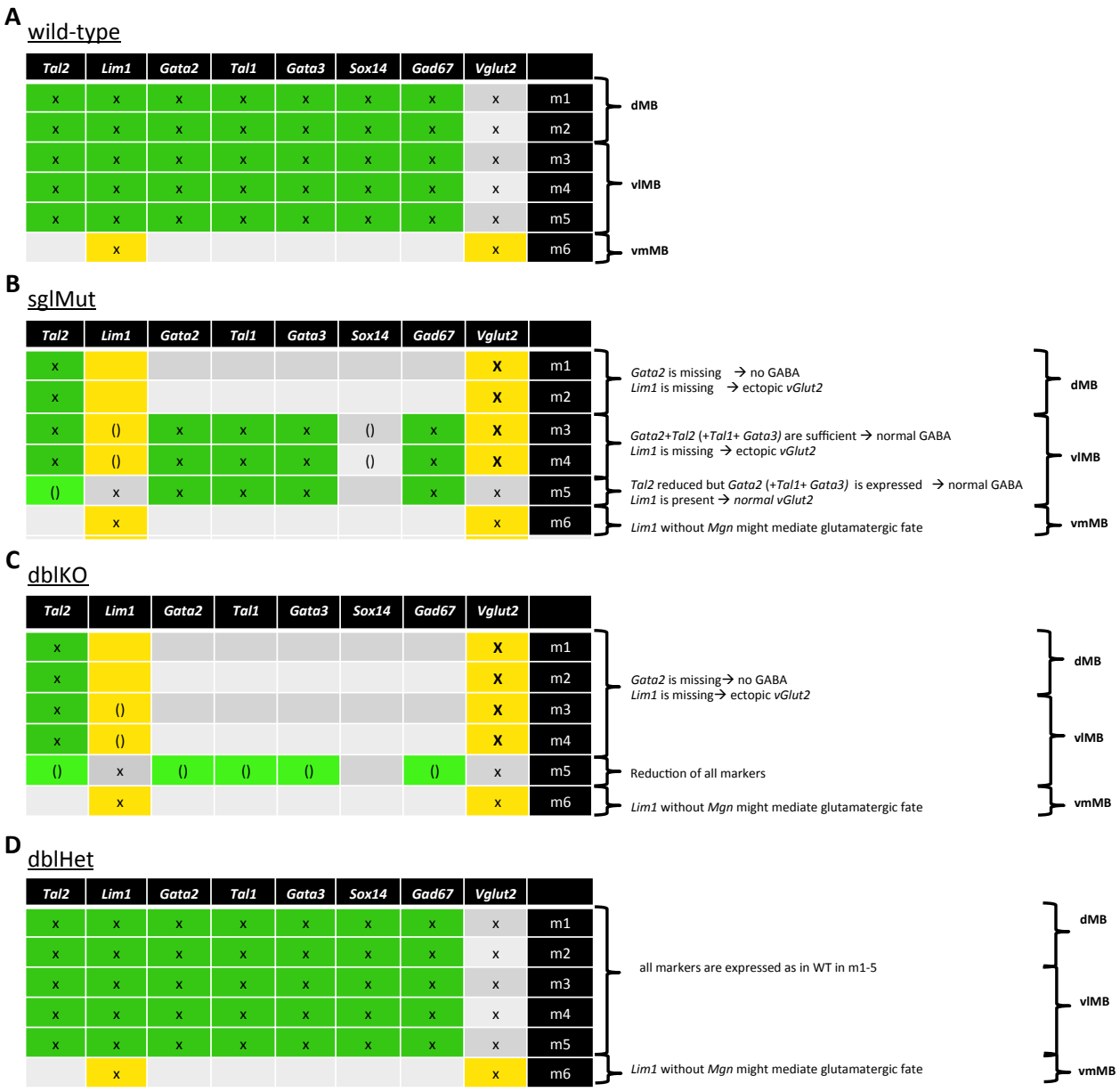

Figure 9.2: Heterodimers of MGN/MASH1 ensure the proper expression profile of the MB comparable to WT mice.
Tal2 and *Gata2* appear to collaborate for *Gad67* expression while *Lim1* appears to be involved in GABAergic over glutamatergic fate. **(A, D)** in double heterozygous mutants (dblHet) all markers are expressed as in WT. When *Lim1* is missing, *vGlut2* is upregulated. **(B)** in single mutants (sglMut), *Gata2*, *Tal1*, *Gata3* and *Gad67* are following the d/vl mechanism of MGN/MASH1. *Gata2* and *Tal2* are only expressed together in the vlMB (m3-5) - coinciding with *Gad67* expression in these areas**. (C)** on double knockout mutants (dblKO), all markers involved in GABAergic neurogenesis - except *Tal2* - are absent in m1-4 and downregulated in m5 (either spread (*Tal2*), or in a correlating subpopulation (*Gata2, Tal1, Gata1, Gad67*)). Abbreviations: **x:** marker expressed; **()**: some remaining (*Mgn/Mash1* independent) cells are expressed; **X**: gene is upregulated.

9.6 DIFFERENT POPULATION OF MB GABAN APPEAR TO POPULATE THE MB FROM DIFFERENT NEUROEPITHELIA BY RADIAL AND TANGENTIAL MIGRATION

Our proposed mechanisms regarding the m1-5 domain, the areas where *Mgn* and *Mash1* are coexpressed. Nevertheless, some GABAn in the domain m5 however, appear to be regulated slightly different. Albeit most markers in m5 were downregulated in the single and dblKO mutants, some residual cells in the vlMB m5 domain still express *Tal1* and *Gata2* (*Gata3*) in the dblKO mutant – correlating with the remaining GAD67+ population in the dblKO mutant. When tracing *lac-Z* expressing cells under the promoter of *Mgn,* theses GABAergic cells appeared not to colocalize with β-galactosidase. Thus it is likely, that these cells do not derive from the MGN+ domain. It has been proven that the SNpr GABAn are partially derived from r1, expressing *Gata2* and *Tal1,* and migrate tangentially towards their final location in the MB and concentrate in the caudal SNpr (Achim *et al*., 2013). Nevertheless, these postmitotic precursors arrive at the MB at E14.5. Although most GABAn in m1-5 are thought to migrate only radially, it was recently reported that some of them in the vlMB also show little tangential migration already at E12.5 to populate the rostral SNpr (Madrigal *et al*., 2015). The SNpr is not a homogeneous population and the origins of these GABAn are distributed in two opposite rostrocaudal gradients: one from r1 (dependent on *Tal1*) – being more abundant in the caudal SNpr and almost absent in the rostral part (Achim *et al.*, 2013) and one from the ventricular zone of the vlMB itself (dependent on *Nkx6.2* and marked by *Six3*) – comprising the more caudally located GABAn. However, GABAn associated with the dopaminergic nuclei in the VTA and SN were reported not to require *Mgn* or *Mash1* (Peltopuro et al., 2010). As they develop independently of the known MB transcriptional regulators, the VTA and SNpr GABAn appear molecularly distinct (Guimera *et al*., 2006b, Kala *et al*., 2009) and are therefore likely to have a different origin. Strikingly, in the *Gata2* knockout mutant, all the MB GABAn populations switch to a glutamatergic phenotype, except for the SNpr and MRF (Lahti *et al.,* 2013) indicating that the remaining MB GABAn could be born in a region of the MB that does not require *Gata2* (Kala *et al*., 2009). In the *Gata2* knockout embryo, the expression of *Six3* is altered but does not disappear (Kala *et al.*, 2009). In contrast, in the *Tal2* mutant, besides *Gad67*, *Six3* expression is completely lost and GABAn differentiation is absent specifically in the domain of the NKX6.2+ ventricular domain. As expected, the generation of the SNpr is also strongly affected, corroborating the role of *Tal2* in SNpr GABAn differentiation (Achim *et al*., 2013). Since *Tal2* is only absent in the dblKO in the m5 but not m4, where most of the SNpr originate, it would be possible that the residual GABAn observed in the dblKO are part of the *Nkx6.2* derivatives which migrate in a rostro-ventral direction to colonize the rostral portion of the SNpr. Further, the *Nkx6.2* derivatives also populate the MRF, which lies more dorsally. Thus this emphasizes the possibility that the remaining GABAn population in m5 derives from the NKX6.2+

domain. Further, by β-galactosidase staining, we noticed *Mgn* derivatives in the m5-6 domain, which appeared rather to migrate tangentially, differing from the radial migrating neurons in m1-5. Since *Mgn* and *Mash1* are also expressed in the diencephalon, where they also direct GABAergic fate, it might also be possible that a population of GABAn migrates from the diencephalon into the MB, contributing to MB GABAn and these neurons might be the ones, visualized by the remaining cells in the dblKO. This is further plausible as – despite brain compartment specific differences – the genetic cascades for GABAn are similar between FB and MB and such a migratory stream was also suggested by other groups (Achim *et al.*, 2012, Madrigal *et al.*, 2015). Yet, our analysis revealed that the m5 domain appears differently regulated compared to MB and the genetic pathway providing GABAergic neuronal identity to this small subpopulation of GABAn in the m5 domain needs to be elucidated.

In summary, we have provided molecular, genetic and phenotypic evidence that the two bHLH factors MGN and MASH1 are the major players in the MB for the acquisition of GABAergic identity. Nevertheless, considering the structure of bHLH proteins, in particular their multiple HLH domains, it could well be that MGN and MASH1 are likely to interact with additional factors which also/in turn might facilitate the establishment of functional interactions. This is so far reasonably, since in the entire CNS many of the genes implicated in neuronal differentiation, are structurally related to bHLH proteins. Despite some TFs are found in different GABAergic domains, none of them is present in all of the GABAergic progenitor domains specific for the GABAergic phenotype. Instead, each domain has adopted an individual set of genes either exclusively or in spatially coherent groups and cascades leading to GABAn specific for the respective region. This may result from the capacity of bHLH genes, reasoned in their structure, to elicit different biological responses when expressed in different cellular contexts. In each context, they have a pivotal role in integrating positional information as well as in the acquisition of neural lineages (migration and fate) in neural progenitor cells (Parras *et al*., 2002). Thus, the cooperation with regionally expressed determinants and the transcriptional control of these specification genes results in the variety of neuronal specificity (Wong *et a*l., 2003, Lee, 1997, Jan and Jan, 1993). Since many of such regionally expressed determinants and how they are directly regulated are not known so far, more research on this field is needed until the exact regulation of each MB GABAn subtype will be elucidated.

Yet, MGN and MASH1 play an undoubtedly important role in early specifying MB GABAergic neurogenesis, particular in the populations deriving from the MB itself and it is therefore likely that the two genes have the capacity to control many so far specification factors. Further, the change in GABA expression in single, compound and dblKO mutants might have a more widespread effect on maturation of the NS, as *in vitro* GABA promotes neuronal survival and differentiation (LoTurco *et al*., 1995, Ikeda *et al*., 1997) as well as forming, stabilizing, and strengthening synaptic connections in general (LoTurco *et al*., 1995, Nguyen *et al*., 2003, Kneussel and Betz, 2000). Albeit we did not observe any change in

maturation of proliferation and the mutants maturated, it cannot be excluded that the lack of MB GABA changes the formation of circuits since GABA also regulates glutamatergic synapse and dendritic spine formation, thus also final circuit formation (Ben-Ari *et al.,* 1989, Ben-Ari *et al*., 2007, Wang and Kriegstein, 2009, Huang, 2009). Since GABAergic alteration in *Mgn/Mash1* defective brains obviously changes the molecular unique signature of genetic markers (thus also the correct functional composition), it raises the question whether the neurons would exert their proper function. Albeit the expression of GABA-transporters (as for example GAT1) puts themselves forward to answer this question, the combination with electrophysiological studies appears as the accurate technique to gain insight into the physiological behavior of the "defective" GABAn and the physiological actions with afferent and efferent neurons. Since in the MB, most nuclei comprise important integration centers, which project to various nuclei in the FB and HB, it would be very interesting to test the physiological and also behavioral outcome of combinatorial alteration in *Mgn* or *Mash1* expression. This would not only define their individual function for specific nuclei and thus their function in the brain, but also give more insights in the functionality of the nuclei themselves. This can also help to further uncover the function of GABA and its receptors in general - in the immature as well as in the mature brain - and how perturbations in GABAergic transmission have the potential to result in severe psychiatric and neurological disturbances, like bipolar disorders, ADHD, autism but also addiction and anxiety.

10 REFERENCES

ACHIM, K., PELTOPURO, P., LAHTI, L., LI, J., SALMINEN, M. & PARTANEN, J. 2012. Distinct developmental origins and regulatory mechanisms for GABAergic neurons associated with dopaminergic nuclei in the ventral mesodiencephalic region. *Development,* 139**,** 2360-70.

ACHIM, K., PELTOPURO, P., LAHTI, L., TSAI, H.-H., ZACHARIAH, A., ÅSTRAND, M., SALMINEN, M., ROWITCH, D. & PARTANEN, J. 2013. The role of Tal2 and Tal1 in the differentiation of midbrain GABAergic neuron precursors. *Biology Open,* 2**,** 990-997.

DELOGU, A., SELLERS, K., ZAGORAIOU, L., BOCIANOWSKA-ZBROG, A., MANDAL, S., GUIMERA, J., RUBENSTEIN, J. L., SUGDEN, D., JESSELL, T. & LUMSDEN, A. 2012. Subcortical visual shell nuclei targeted by ipRGCs develop from a Sox14+-GABAergic progenitor and require Sox14 to regulate daily activity rhythms. *Neuron,* 75**,** 648-62.

GUIMERA, J., WEISENHORN, D. V. & WURST, W. 2006. Megane/Heslike is required for normal GABAergic differentiation in the mouse superior colliculus. *Development,* 133**,** 3847-57.

KALA, K., HAUGAS, M., LILLEVALI, K., GUIMERA, J., WURST, W., SALMINEN, M. & PARTANEN, J. 2009. Gata2 is a tissue-specific post-mitotic selector gene for midbrain GABAergic neurons. *Development,* 136**,** 253-62.

MADRIGAL, M. P., MORENO-BRAVO, J. A., MARTINEZ-LOPEZ, J. E., MARTINEZ, S. & PUELLES, E. 2015. Mesencephalic origin of the rostral Substantia nigra pars reticulata. *Brain Struct Funct*.

MIYOSHI, G., BESSHO, Y., YAMADA, S. & KAGEYAMA, R. 2004. Identification of a novel basic helix-loop-helix gene, Heslike, and its role in GABAergic neurogenesis. *J Neurosci,* 24**,** 3672-82.

NAKATANI, T., MINAKI, Y., KUMAI, M. & ONO, Y. 2007. Helt determines GABAergic over glutamatergic neuronal fate by repressing Ngn genes in the developing mesencephalon. *Development,* 134**,** 2783-93.

PELTOPURO, P., KALA, K. & PARTANEN, J. 2010. Distinct requirements for Ascl1 in subpopulations of midbrain GABAergic neurons. *Dev Biol,* 343**,** 63-70.

ACAMPORA, D., GULISANO, M., BROCCOLI, V. & SIMEONE, A. 2001. Otx genes in brain morphogenesis. *Prog Neurobiol,* 64**,** 69-95.

ACHIM, K., PELTOPURO, P., LAHTI, L., LI, J., SALMINEN, M. & PARTANEN, J. 2012. Distinct developmental origins and regulatory mechanisms for GABAergic neurons associated with dopaminergic nuclei in the ventral mesodiencephalic region. *Development,* 139**,** 2360-70.

ACHIM, K., PELTOPURO, P., LAHTI, L., TSAI, H.-H., ZACHARIAH, A., ÅSTRAND, M., SALMINEN, M., ROWITCH, D. & PARTANEN, J. 2013. The role of Tal2 and Tal1 in the differentiation of midbrain GABAergic neuron precursors. *Biology Open,* 2**,** 990-997.

ACHIM, K., SALMINEN, M. & PARTANEN, J. 2014. Mechanisms regulating GABAergic neuron development. *Cell Mol Life Sci,* 71**,** 1395-415.

AGARWALA, S. & RAGSDALE, C. W. 2002. A role for midbrain arcs in nucleogenesis. *Development,* 129**,** 5779-88.

AKAZAWA, C., SASAI, Y., NAKANISHI, S. & KAGEYAMA, R. 1992. Molecular characterization of a rat negative regulator with a basic helix-loop-helix structure predominantly expressed in the developing nervous system. *J Biol Chem,* 267**,** 21879-85.

ANDERSON, S. A., EISENSTAT, D. D., SHI, L. & RUBENSTEIN, J. L. 1997. Interneuron migration from basal forebrain to neocortex: dependence on Dlx genes. *Science,* 278**,** 474-6.

ARTAVANIS-TSAKONAS, S., RAND, M. D. & LAKE, R. J. 1999. Notch signaling: cell fate control and signal integration in development. *Science,* 284**,** 770-6.

ASADA, H., KAWAMURA, Y., MARUYAMA, K., KUME, H., DING, R., JI, F. Y., KANBARA, N., KUZUME, H., SANBO, M., YAGI, T. & OBATA, K. 1996. Mice lacking the 65 kDa isoform of glutamic acid decarboxylase (GAD65) maintain normal levels of GAD67 and GABA in their brains but are susceptible to seizures. *Biochem Biophys Res Commun,* 229**,** 891-5.

ASADA, H., KAWAMURA, Y., MARUYAMA, K., KUME, H., DING, R. G., KANBARA, N., KUZUME, H., SANBO, M., YAGI, T. & OBATA, K. 1997. Cleft palate and decreased brain gamma-aminobutyric acid in mice lacking the 67-kDa isoform of glutamic acid decarboxylase. *Proc Natl Acad Sci U S A,* 94**,** 6496-9.

ATCHLEY, W. R. & FITCH, W. M. 1997. A natural classification of the basic helix-loop-helix class of transcription factors. *Proc Natl Acad Sci U S A,* 94**,** 5172-6.

ATTWELL, D., BARBOUR, B. & SZATKOWSKI, M. 1993. Nonvesicular release of neurotransmitter. *Neuron,* 11**,** 401-7.

AWAPARA, J., LANDUA, A. J., FUERST, R. & SEALE, B. 1950. Free gamma-aminobutyric acid in brain. *J Biol Chem,* 187**,** 35-9.

BAE, S., BESSHO, Y., HOJO, M. & KAGEYAMA, R. 2000. The bHLH gene Hes6, an inhibitor of Hes1, promotes neuronal differentiation. *Development,* 127**,** 2933-43.

BALASKAS, N., RIBEIRO, A., PANOVSKA, J., DESSAUD, E., SASAI, N., PAGE, K. M., BRISCOE, J. & RIBES, V. 2012. Gene regulatory logic for reading the Sonic Hedgehog signaling gradient in the vertebrate neural tube. *Cell,* 148**,** 273-84.

BATTAGLIOLI, G., LIU, H. & MARTIN, D. L. 2003. Kinetic differences between the isoforms of glutamate decarboxylase: implications for the regulation of GABA synthesis. *J Neurochem,* 86**,** 879-87.

BEHAR, T., LI, Y., TRAN, H., MA, W., DUNLAP, V., SCOTT, C. & BARKER, J. 1996. GABA stimulates chemotaxis and chemokinesis of embryonic cortical neurons via calcium-dependent mechanisms. *The Journal of Neuroscience,* 16**,** 1808-1818.

BEHBEHANI, M. M. 1995. Functional characteristics of the midbrain periaqueductal gray. *Prog Neurobiol,* 46**,** 575-605.

BELL, E., LUMSDEN, A. & GRAHAM, A. 1999. Expression of GATA-2 in the developing avian rhombencephalon. *Mech Dev,* 84**,** 173-6.

BEN-ARI, Y. 2014. The GABA excitatory/inhibitory developmental sequence: A personal journey. *Neuroscience,* 279**,** 187-219.

BEN-ARI, Y., CHERUBINI, E., CORRADETTI, R. & GAIARSA, J. L. 1989. Giant synaptic potentials in immature rat CA3 hippocampal neurones. *J Physiol,* 416**,** 303-25.

BEN-ARI, Y., GAIARSA, J. L., TYZIO, R. & KHAZIPOV, R. 2007. GABA: a pioneer transmitter that excites immature neurons and generates primitive oscillations. *Physiol Rev,* 87**,** 1215-84.

BERTRAND, N., CASTRO, D. S. & GUILLEMOT, F. 2002. Proneural genes and the specification of neural cell types. *Nat Rev Neurosci,* 3**,** 517-30.

BOND, R. W., WYBORSKI, R. J. & GOTTLIEB, D. I. 1990. Developmentally regulated expression of an exon containing a stop codon in the gene for glutamic acid decarboxylase. *Proc Natl Acad Sci U S A,* 87**,** 8771-5.

BORDEN, L. A. 1996. GABA transporter heterogeneity: pharmacology and cellular localization. *Neurochem Int,* 29**,** 335-56.

BORMANN, J. 1988. Electrophysiology of GABAA and GABAB receptor subtypes. *Trends Neurosci,* 11**,** 112-6.

BOWERY, N. 1989. GABAB receptors and their significance in mammalian pharmacology. *Trends Pharmacol Sci,* 10**,** 401-7.

BOWERY, N. G., HILL, D. R., HUDSON, A. L., DOBLE, A., MIDDLEMISS, D. N., SHAW, J. & TURNBULL, M. 1980. (-)Baclofen decreases neurotransmitter release in the mammalian CNS by an action at a novel GABA receptor. *Nature,* 283**,** 92-4.

BRISCHOUX, F., MAINVILLE, L. & JONES, B. E. 2008. Muscarinic-2 and orexin-2 receptors on GABAergic and other neurons in the rat mesopontine tegmentum and their potential role in sleep-wake state control. *J Comp Neurol,* 510**,** 607-30.

BRISCOE, J., PIERANI, A., JESSELL, T. M. & ERICSON, J. 2000. A homeodomain protein code specifies progenitor cell identity and neuronal fate in the ventral neural tube. *Cell,* 101**,** 435-45.

BROCCOLI, V., BONCINELLI, E. & WURST, W. 1999. The caudal limit of Otx2 expression positions the isthmic organizer. *Nature,* 401**,** 164-8.

BRUNET, J. F. & GHYSEN, A. 1999. Deconstructing cell determination: proneural genes and neuronal identity. *Bioessays,* 21**,** 313-8.

BUCHER, K., SOFRONIEW, M. V., PANNELL, R., IMPEY, H., SMITH, A. J., TORRES, E. M., DUNNETT, S. B., JIN, Y., BAER, R. & RABBITTS, T. H. 2000. The T cell oncogene Tal2 is necessary for normal development of the mouse brain. *Dev Biol,* 227**,** 533-44.

BURDSAL, C. A., DAMSKY, C. H. & PEDERSEN, R. A. 1993. The role of E-cadherin and integrins in mesoderm differentiation and migration at the mammalian primitive streak. *Development,* 118**,** 829-44.

CANTOR, A. B. & ORKIN, S. H. 2002. Transcriptional regulation of erythropoiesis: an affair involving multiple partners. *Oncogene,* 21**,** 3368-76.

CASAROSA, S., FODE, C. & GUILLEMOT, F. 1999. Mash1 regulates neurogenesis in the ventral telencephalon. *Development,* 126**,** 525-34.

CASTRO, D. S., SKOWRONSKA-KRAWCZYK, D., ARMANT, O., DONALDSON, I. J., PARRAS, C., HUNT, C., CRITCHLEY, J. A., NGUYEN, L., GOSSLER, A., GOTTGENS, B., MATTER, J. M. & GUILLEMOT, F. 2006. Proneural bHLH and Brn proteins coregulate a neurogenic program through cooperative binding to a conserved DNA motif. *Dev Cell,* 11**,** 831-44.

CAVINESS, V. S., JR., TAKAHASHI, T. & NOWAKOWSKI, R. S. 2000. Neuronogenesis and the Early Events of Neocortical Histogenesis. *In:* GOFFINET, A. & RAKIC, P. (eds.) *Mouse Brain Development.* Springer Berlin Heidelberg.

CHEN, H., THIAGALINGAM, A., CHOPRA, H., BORGES, M. W., FEDER, J. N., NELKIN, B. D., BAYLIN, S. B. & BALL, D. W. 1997. Conservation of the Drosophila lateral inhibition pathway in human lung cancer: a hairy-related protein (HES-1) directly represses achaete-scute homolog-1 expression. *Proc Natl Acad Sci U S A,* 94**,** 5355-60.

CHENG, L., ARATA, A., MIZUGUCHI, R., QIAN, Y., KARUNARATNE, A., GRAY, P. A., ARATA, S., SHIRASAWA, S., BOUCHARD, M., LUO, P., CHEN, C. L., BUSSLINGER, M., GOULDING, M., ONIMARU, H. & MA, Q. 2004. Tlx3 and Tlx1 are post-mitotic selector genes determining glutamatergic over GABAergic cell fates. *Nat Neurosci,* 7**,** 510-7.

CHENG, L., SAMAD, O. A., XU, Y., MIZUGUCHI, R., LUO, P., SHIRASAWA, S., GOULDING, M. & MA, Q. 2005. Lbx1 and Tlx3 are opposing switches in determining GABAergic versus glutamatergic transmitter phenotypes. *Nat Neurosci,* 8**,** 1510-5.

CLEAVER, O. & KRIEG, P. A. 2001. Notochord patterning of the endoderm. *Dev Biol,* 234**,** 1-12.

COHEN, J. Y., HAESLER, S., VONG, L., LOWELL, B. B. & UCHIDA, N. 2012. Neuron-type-specific signals for reward and punishment in the ventral tegmental area. *Nature,* 482**,** 85-8.

CONNOR, J. A., TSENG, H. Y. & HOCKBERGER, P. E. 1987. Depolarization- and transmitter-induced changes in intracellular Ca2+ of rat cerebellar granule cells in explant cultures. *J Neurosci,* 7**,** 1384-400.

CRANDALL, J. E., MCCARTHY, D. M., ARAKI, K. Y., SIMS, J. R., REN, J. Q. & BHIDE, P. G. 2007. Dopamine receptor activation modulates GABA neuron migration from the basal forebrain to the cerebral cortex. *J Neurosci,* 27**,** 3813-22.

CRAVEN, S. E., LIM, K. C., YE, W., ENGEL, J. D., DE SAUVAGE, F. & ROSENTHAL, A. 2004. Gata2 specifies serotonergic neurons downstream of sonic hedgehog. *Development,* 131**,** 1165-73.

CROSSLEY, P. H., MARTINEZ, S. & MARTIN, G. R. 1996. Midbrain development induced by FGF8 in the chick embryo. *Nature,* 380**,** 66-8.

DAVIS, R. L. & TURNER, D. L. 2001. Vertebrate hairy and Enhancer of split related proteins: transcriptional repressors regulating cellular differentiation and embryonic patterning. *Oncogene,* 20**,** 8342-57.

DELOGU, A., SELLERS, K., ZAGORAIOU, L., BOCIANOWSKA-ZBROG, A., MANDAL, S., GUIMERA, J., RUBENSTEIN, J. L., SUGDEN, D., JESSELL, T. & LUMSDEN, A. 2012.

Subcortical visual shell nuclei targeted by ipRGCs develop from a Sox14+-GABAergic progenitor and require Sox14 to regulate daily activity rhythms. *Neuron,* 75**,** 648-62.

DIRKX, R., JR., THOMAS, A., LI, L., LERNMARK, A., SHERWIN, R. S., DE CAMILLI, P. & SOLIMENA, M. 1995. Targeting of the 67-kDa isoform of glutamic acid decarboxylase to intracellular organelles is mediated by its interaction with the NH2-terminal region of the 65-kDa isoform of glutamic acid decarboxylase. *J Biol Chem,* 270**,** 2241-6.

DYCE, J., GEORGE, M., GOODALL, H. & FLEMING, T. P. 1987. Do trophectoderm and inner cell mass cells in the mouse blastocyst maintain discrete lineages? *Development,* 100**,** 685-98.

ECHEVARRIA, D., VIEIRA, C., GIMENO, L. & MARTINEZ, S. 2003. Neuroepithelial secondary organizers and cell fate specification in the developing brain. *Brain Res Brain Res Rev,* 43**,** 179-91.

EISENSTAT, D. D., LIU, J. K., MIONE, M., ZHONG, W., YU, G., ANDERSON, S. A., GHATTAS, I., PUELLES, L. & RUBENSTEIN, J. L. 1999. DLX-1, DLX-2, and DLX-5 expression define distinct stages of basal forebrain differentiation. *J Comp Neurol,* 414**,** 217-37.

EL WAKIL, A., FRANCIUS, C., WOLFF, A., PLEAU-VARET, J. & NARDELLI, J. 2006. The GATA2 transcription factor negatively regulates the proliferation of neuronal progenitors. *Development,* 133**,** 2155-65.

ELLIOTT, K. A. & FLOREY, E. 1956. Factor I--inhibitory factor from brain; assay; conditions in brain; simulating and antagonizing substances. *J Neurochem,* 1**,** 181-92.

ELLIOTT, K. A. & JASPER, H. H. 1959. Gammaaminobutyric acid. *Physiol Rev,* 39**,** 383-406.

EPHRUSSI, A., CHURCH, G. M., TONEGAWA, S. & GILBERT, W. 1985. B lineage--specific interactions of an immunoglobulin enhancer with cellular factors in vivo. *Science,* 227**,** 134-40.

ERLANDER, M. G., TILLAKARATNE, N. J., FELDBLUM, S., PATEL, N. & TOBIN, A. J. 1991. Two genes encode distinct glutamate decarboxylases. *Neuron,* 7**,** 91-100.

ESCLAPEZ, M., TILLAKARATNE, N. J., KAUFMAN, D. L., TOBIN, A. J. & HOUSER, C. R. 1994. Comparative localization of two forms of glutamic acid decarboxylase and their mRNAs in rat brain supports the concept of functional differences between the forms. *J Neurosci,* 14**,** 1834-55.

FAIRMAN, R., BERAN-STEED, R. K., ANTHONY-CAHILL, S. J., LEAR, J. D., STAFFORD, W. F., 3RD, DEGRADO, W. F., BENFIELD, P. A. & BRENNER, S. L. 1993. Multiple oligomeric states regulate the DNA binding of helix-loop-helix peptides. *Proc Natl Acad Sci U S A,* 90**,** 10429-33.

FELSEN, G. & MAINEN, Z. F. 2008. Neural substrates of sensory-guided locomotor decisions in the rat superior colliculus. *Neuron,* 60**,** 137-48.

FLEMING, T. P. 1987. A quantitative analysis of cell allocation to trophectoderm and inner cell mass in the mouse blastocyst. *Dev Biol,* 119**,** 520-31.

FODE, C., MA, Q., CASAROSA, S., ANG, S. L., ANDERSON, D. J. & GUILLEMOT, F. 2000. A role for neural determination genes in specifying the dorsoventral identity of telencephalic neurons. *Genes Dev,* 14**,** 67-80.

FON, E. A. & EDWARDS, R. H. 2001. Molecular mechanisms of neurotransmitter release. *Muscle Nerve,* 24**,** 581-601.

GARCIA-LOPEZ, R., VIEIRA, C., ECHEVARRIA, D. & MARTINEZ, S. 2004. Fate map of the diencephalon and the zona limitans at the 10-somites stage in chick embryos. *Dev Biol,* 268**,** 514-30.

GARDA, A. L., ECHEVARRIA, D. & MARTINEZ, S. 2001. Neuroepithelial co-expression of Gbx2 and Otx2 precedes Fgf8 expression in the isthmic organizer. *Mech Dev,* 101**,** 111-8.

GERHART, J. 2001. Evolution of the organizer and the chordate body plan. *Int J Dev Biol,* 45**,** 133-53.

GLASGOW, S. M., HENKE, R. M., MACDONALD, R. J., WRIGHT, C. V. & JOHNSON, J. E. 2005. Ptf1a determines GABAergic over glutamatergic neuronal cell fate in the spinal cord dorsal horn. *Development,* 132**,** 5461-9.

GRILLNER, S., HELLGREN, J., MENARD, A., SAITOH, K. & WIKSTROM, M. A. 2005. Mechanisms for selection of basic motor programs--roles for the striatum and pallidum. *Trends Neurosci,* 28**,** 364-70.

GUILLEMOT, F., LO, L. C., JOHNSON, J. E., AUERBACH, A., ANDERSON, D. J. & JOYNER, A. L. 1993. Mammalian achaete-scute homolog 1 is required for the early development of olfactory and autonomic neurons. *Cell,* 75**,** 463-76.

GUIMERA, J., VOGT WEISENHORN, D., ECHEVARRIA, D., MARTINEZ, S. & WURST, W. 2006a. Molecular characterization, structure and developmental expression of Megane bHLH factor. *Gene,* 377**,** 65-76.

GUIMERA, J., WEISENHORN, D. V. & WURST, W. 2006b. Megane/Heslike is required for normal GABAergic differentiation in the mouse superior colliculus. *Development,* 133**,** 3847-57.

HATAKEYAMA, J., BESSHO, Y., KATOH, K., OOKAWARA, S., FUJIOKA, M., GUILLEMOT, F. & KAGEYAMA, R. 2004. Hes genes regulate size, shape and histogenesis of the nervous system by control of the timing of neural stem cell differentiation. *Development,* 131**,** 5539-50.

HEMMATI-BRIVANLOU, A. & MELTON, D. 1997. Vertebrate embryonic cells will become nerve cells unless told otherwise. *Cell,* 88**,** 13-7.

HENRIQUE, D., HIRSINGER, E., ADAM, J., LE ROUX, I., POURQUIE, O., ISH-HOROWICZ, D. & LEWIS, J. 1997. Maintenance of neuroepithelial progenitor cells by Delta-Notch signalling in the embryonic chick retina. *Curr Biol,* 7**,** 661-70.

HIDALGO-SANCHEZ, M., MILLET, S., SIMEONE, A. & ALVARADO-MALLART, R. M. 1999. Comparative analysis of Otx2, Gbx2, Pax2, Fgf8 and Wnt1 gene expressions during the formation of the chick midbrain/hindbrain domain. *Mech Dev,* 81**,** 175-8.

HOBERT, O., CARRERA, I. & STEFANAKIS, N. 2010. The molecular and gene regulatory signature of a neuron. *Trends Neurosci,* 33**,** 435-45.

HOBERT, O. & WESTPHAL, H. 2000. Functions of LIM-homeobox genes. *Trends Genet,* 16**,** 75-83.

HONJO, T. 1996. The shortest path from the surface to the nucleus: RBP-J kappa/Su(H) transcription factor. *Genes Cells,* 1**,** 1-9.

HORTON, S., MEREDITH, A., RICHARDSON, J. A. & JOHNSON, J. E. 1999. Correct coordination of neuronal differentiation events in ventral forebrain requires the bHLH factor MASH1. *Mol Cell Neurosci,* 14**,** 355-69.

HOSHINO, M., NAKAMURA, S., MORI, K., KAWAUCHI, T., TERAO, M., NISHIMURA, Y. V., FUKUDA, A., FUSE, T., MATSUO, N., SONE, M., WATANABE, M., BITO, H., TERASHIMA, T., WRIGHT, C. V., KAWAGUCHI, Y., NAKAO, K. & NABESHIMA, Y. 2005. Ptf1a, a bHLH transcriptional gene, defines GABAergic neuronal fates in cerebellum. *Neuron,* 47**,** 201-13.

HOUART, C., CANEPARO, L., HEISENBERG, C., BARTH, K., TAKE-UCHI, M. & WILSON, S. 2002. Establishment of the telencephalon during gastrulation by local antagonism of Wnt signaling. *Neuron,* 35**,** 255-65.

HUANG, X. & SAINT-JEANNET, J. P. 2004. Induction of the neural crest and the opportunities of life on the edge. *Dev Biol,* 275**,** 1-11.

HUANG, Z. J. 2009. Activity-dependent development of inhibitory synapses and innervation pattern: role of GABA signalling and beyond. *J Physiol,* 587**,** 1881-8.

IKEDA, Y., NISHIYAMA, N., SAITO, H. & KATSUKI, H. 1997. GABAA receptor stimulation promotes survival of embryonic rat striatal neurons in culture. *Brain Res Dev Brain Res,* 98**,** 253-8.

IMAYOSHI, I. & KAGEYAMA, R. 2014. bHLH factors in self-renewal, multipotency, and fate choice of neural progenitor cells. *Neuron,* 82**,** 9-23.

ISHIBASHI, M., ANG, S. L., SHIOTA, K., NAKANISHI, S., KAGEYAMA, R. & GUILLEMOT, F. 1995. Targeted disruption of mammalian hairy and Enhancer of split homolog-1 (HES-1) leads to up-regulation of neural helix-loop-helix factors, premature neurogenesis, and severe neural tube defects. *Genes Dev,* 9**,** 3136-48.

JAN, Y. N. & JAN, L. Y. 1993. HLH proteins, fly neurogenesis, and vertebrate myogenesis. *Cell,* 75**,** 827-30.

KAGEYAMA, R. & NAKANISHI, S. 1997. Helix-loop-helix factors in growth and differentiation of the vertebrate nervous system. *Curr Opin Genet Dev,* 7**,** 659-65.

KAGEYAMA, R., OHTSUKA, T., HATAKEYAMA, J. & OHSAWA, R. 2005. Roles of bHLH genes in neural stem cell differentiation. *Exp Cell Res,* 306**,** 343-8.

KAGEYAMA, R., OHTSUKA, T. & KOBAYASHI, T. 2007. The Hes gene family: repressors and oscillators that orchestrate embryogenesis. *Development,* 134**,** 1243-51.

KAGEYAMA, R., OHTSUKA, T. & KOBAYASHI, T. 2008. Roles of Hes genes in neural development. *Dev Growth Differ,* 50 Suppl 1**,** S97-103.

KAGEYAMA, R., OHTSUKA, T., SHIMOJO, H. & IMAYOSHI, I. 2009. Dynamic regulation of Notch signaling in neural progenitor cells. *Curr Opin Cell Biol,* 21**,** 733-40.

KAILA, K. 1994. Ionic basis of GABAA receptor channel function in the nervous system. *Prog Neurobiol,* 42**,** 489-537.

KALA, K., HAUGAS, M., LILLEVALI, K., GUIMERA, J., WURST, W., SALMINEN, M. & PARTANEN, J. 2009. Gata2 is a tissue-specific post-mitotic selector gene for midbrain GABAergic neurons. *Development,* 136**,** 253-62.

KARUNARATNE, A., HARGRAVE, M., POH, A. & YAMADA, T. 2002. GATA proteins identify a novel ventral interneuron subclass in the developing chick spinal cord. *Dev Biol,* 249**,** 30-43.

KAWAGUCHI, Y. & KUBOTA, Y. 1997. GABAergic cell subtypes and their synaptic connections in rat frontal cortex. *Cereb Cortex,* 7**,** 476-86.

KELLER, R., SHIH, J., SATER, A. K. & MORENO, C. 1992. Planar induction of convergence and extension of the neural plate by the organizer of Xenopus. *Dev Dyn,* 193**,** 218-34.

KHIRUG, S., YAMADA, J., AFZALOV, R., VOIPIO, J., KHIROUG, L. & KAILA, K. 2008. GABAergic depolarization of the axon initial segment in cortical principal neurons is caused by the Na-K-2Cl cotransporter NKCC1. *J Neurosci,* 28**,** 4635-9.

KIM, E. J., BATTISTE, J., NAKAGAWA, Y. & JOHNSON, J. E. 2008. Ascl1 (Mash1) lineage cells contribute to discrete cell populations in CNS architecture. *Mol Cell Neurosci,* 38**,** 595-606.

KNEUSSEL, M. & BETZ, H. 2000. Clustering of inhibitory neurotransmitter receptors at developing postsynaptic sites: the membrane activation model. *Trends Neurosci,* 23**,** 429-35.

KUNISCH, M., HAENLIN, M. & CAMPOS-ORTEGA, J. A. 1994. Lateral inhibition mediated by the Drosophila neurogenic gene delta is enhanced by proneural proteins. *Proc Natl Acad Sci U S A,* 91**,** 10139-43.

LAHTI, L., ACHIM, K. & PARTANEN, J. 2013. Molecular regulation of GABAergic neuron differentiation and diversity in the developing midbrain. *Acta Physiol (Oxf),* 207**,** 616-27.

LAKSHMANAN, G., LIEUW, K. H., LIM, K. C., GU, Y., GROSVELD, F., ENGEL, J. D. & KARIS, A. 1999. Localization of distant urogenital system-, central nervous system-, and endocardium-specific transcriptional regulatory elements in the GATA-3 locus. *Mol Cell Biol,* 19**,** 1558-68.

LEE, J. D. & ANDERSON, K. V. 2008. Morphogenesis of the node and notochord: the cellular basis for the establishment and maintenance of left-right asymmetry in the mouse. *Dev Dyn,* 237**,** 3464-76.

LEE, J. E. 1997. Basic helix-loop-helix genes in neural development. *Curr Opin Neurobiol,* 7**,** 13-20.

LEE, J. E., HOLLENBERG, S. M., SNIDER, L., TURNER, D. L., LIPNICK, N. & WEINTRAUB, H. 1995. Conversion of Xenopus ectoderm into neurons by NeuroD, a basic helix-loop-helix protein. *Science,* 268**,** 836-44.

LEVINE, H., 3RD 1999. Structural features of heterotrimeric G-protein-coupled receptors and their modulatory proteins. *Mol Neurobiol,* 19**,** 111-49.

LOTURCO, J. J., OWENS, D. F., HEATH, M. J., DAVIS, M. B. & KRIEGSTEIN, A. R. 1995. GABA and glutamate depolarize cortical progenitor cells and inhibit DNA synthesis. *Neuron,* 15**,** 1287-98.

LOUVI, A. & ARTAVANIS-TSAKONAS, S. 2006. Notch signalling in vertebrate neural development. *Nat Rev Neurosci,* 7**,** 93-102.

LU, J., KARADSHEH, M. & DELPIRE, E. 1999. Developmental regulation of the neuronal-specific isoform of K-Cl cotransporter KCC2 in postnatal rat brains. *J Neurobiol,* 39**,** 558-68.

LUPPI, P. H., CLEMENT, O., SAPIN, E., GERVASONI, D., PEYRON, C., LEGER, L., SALVERT, D. & FORT, P. 2011. The neuronal network responsible for paradoxical sleep and its dysfunctions

causing narcolepsy and rapid eye movement (REM) behavior disorder. *Sleep Med Rev,* 15**,** 153-63.

MA, Q., CHEN, Z., DEL BARCO BARRANTES, I., DE LA POMPA, J. L. & ANDERSON, D. J. 1998. neurogenin1 is essential for the determination of neuronal precursors for proximal cranial sensory ganglia. *Neuron,* 20**,** 469-82.

MA, Q., FODE, C., GUILLEMOT, F. & ANDERSON, D. J. 1999. Neurogenin1 and neurogenin2 control two distinct waves of neurogenesis in developing dorsal root ganglia. *Genes Dev,* 13**,** 1717-28.

MA, Q., SOMMER, L., CSERJESI, P. & ANDERSON, D. J. 1997. Mash1 and neurogenin1 expression patterns define complementary domains of neuroepithelium in the developing CNS and are correlated with regions expressing notch ligands. *J Neurosci,* 17**,** 3644-52.

MADRIGAL, M. P., MORENO-BRAVO, J. A., MARTINEZ-LOPEZ, J. E., MARTINEZ, S. & PUELLES, E. 2015. Mesencephalic origin of the rostral Substantia nigra pars reticulata. *Brain Struct Funct*.

MARTIN, D. L. & RIMVALL, K. 1993. Regulation of gamma-aminobutyric acid synthesis in the brain. *J Neurochem,* 60**,** 395-407.

MARTINEZ, S. & PUELLES, L. 2000. Neurogenetic compartments of the mouse diencephalon and some characteristic gene expression patterns. *Results Probl Cell Differ,* 30**,** 91-106.

MASSARI, M. E. & MURRE, C. 2000. Helix-loop-helix proteins: regulators of transcription in eucaryotic organisms. *Mol Cell Biol,* 20**,** 429-40.

MEINHARDT, H. 2001. Organizer and axes formation as a self-organizing process. *Int J Dev Biol,* 45**,** 177-88.

MELONE, M., BARBARESI, P., FATTORINI, G. & CONTI, F. 2005. Neuronal localization of the GABA transporter GAT-3 in human cerebral cortex: A procedural artifact? *Journal of Chemical Neuroanatomy,* 30**,** 45-54.

MILLET, S., CAMPBELL, K., EPSTEIN, D. J., LOSOS, K., HARRIS, E. & JOYNER, A. L. 1999. A role for Gbx2 in repression of Otx2 and positioning the mid/hindbrain organizer. *Nature,* 401**,** 161-4.

MIYOSHI, G., BESSHO, Y., YAMADA, S. & KAGEYAMA, R. 2004. Identification of a novel basic helix-loop-helix gene, Heslike, and its role in GABAergic neurogenesis. *J Neurosci,* 24**,** 3672-82.

MORENO, N., BACHY, I., RETAUX, S. & GONZALEZ, A. 2004. LIM-homeodomain genes as developmental and adult genetic markers of Xenopus forebrain functional subdivisions. *J Comp Neurol,* 472**,** 52-72.

MORI, S., SUGAWARA, S., KIKUCHI, T., TANJI, M., NARUMI, O., STOYKOVA, A., NISHIKAWA, S. I. & YOKOTA, Y. 1999. The leukemic oncogene tal-2 is expressed in the developing mouse brain. *Brain Res Mol Brain Res,* 64**,** 199-210.

MUROYAMA, Y., FUJIWARA, Y., ORKIN, S. H. & ROWITCH, D. H. 2005. Specification of astrocytes by bHLH protein SCL in a restricted region of the neural tube. *Nature,* 438**,** 360-3.

MURRE, C., BAIN, G., VAN DIJK, M. A., ENGEL, I., FURNARI, B. A., MASSARI, M. E., MATTHEWS, J. R., QUONG, M. W., RIVERA, R. R. & STUIVER, M. H. 1994. Structure and function of helix-loop-helix proteins. *Biochimica et Biophysica Acta (BBA) - Gene Structure and Expression,* 1218**,** 129-135.

MURRE, C., MCCAW, P. S. & BALTIMORE, D. 1989. A new DNA binding and dimerization motif in immunoglobulin enhancer binding, daughterless, MyoD, and myc proteins. *Cell,* 56**,** 777-83.

NAIR-ROBERTS, R. G., CHATELAIN-BADIE, S. D., BENSON, E., WHITE-COOPER, H., BOLAM, J. P. & UNGLESS, M. A. 2008. Stereological estimates of dopaminergic, GABAergic and glutamatergic neurons in the ventral tegmental area, substantia nigra and retrorubral field in the rat. *Neuroscience,* 152**,** 1024-31.

NAKATANI, T. 2004. Helt, a novel basic-helix-loop-helix transcriptional repressor expressed in the developing central nervous system. *J Biol Chem,* 279**,** 16356-67.

NAKATANI, T., MINAKI, Y., KUMAI, M. & ONO, Y. 2007. Helt determines GABAergic over glutamatergic neuronal fate by repressing Ngn genes in the developing mesencephalon. *Development,* 134**,** 2783-93.

NARDELLI, J., THIESSON, D., FUJIWARA, Y., TSAI, F. Y. & ORKIN, S. H. 1999. Expression and genetic interaction of transcription factors GATA-2 and GATA-3 during development of the mouse central nervous system. *Dev Biol,* 210**,** 305-21.

NGUYEN, L., MALGRANGE, B., BREUSKIN, I., BETTENDORFF, L., MOONEN, G., BELACHEW, S. & RIGO, J. M. 2003. Autocrine/paracrine activation of the GABA(A) receptor inhibits the proliferation of neurogenic polysialylated neural cell adhesion molecule-positive (PSA-NCAM+) precursor cells from postnatal striatum. *J Neurosci,* 23**,** 3278-94.

NICHOLS, D. H. 1981. Neural crest formation in the head of the mouse embryo as observed using a new histological technique. *J Embryol Exp Morphol,* 64**,** 105-20.

NICOLL, R. A. 1988. The coupling of neurotransmitter receptors to ion channels in the brain. *Science,* 241**,** 545-51.

NORDSTROM, U., JESSELL, T. M. & EDLUND, T. 2002. Progressive induction of caudal neural character by graded Wnt signaling. *Nat Neurosci,* 5**,** 525-32.

OHTSUKA, T., ISHIBASHI, M., GRADWOHL, G., NAKANISHI, S., GUILLEMOT, F. & KAGEYAMA, R. 1999. Hes1 and Hes5 as notch effectors in mammalian neuronal differentiation. *EMBO J,* 18**,** 2196-207.

OLIVER, D. L., WINER, J. A., BECKIUS, G. E. & SAINT MARIE, R. L. 1994. Morphology of GABAergic neurons in the inferior colliculus of the cat. *J Comp Neurol,* 340**,** 27-42.

OLSON, V. G. & NESTLER, E. J. 2007. Topographical organization of GABAergic neurons within the ventral tegmental area of the rat. *Synapse,* 61**,** 87-95.

PAROUSH, Z., FINLEY, R. L., JR., KIDD, T., WAINWRIGHT, S. M., INGHAM, P. W., BRENT, R. & ISH-HOROWICZ, D. 1994. Groucho is required for Drosophila neurogenesis, segmentation, and sex determination and interacts directly with hairy-related bHLH proteins. *Cell,* 79**,** 805-15.

PARRAS, C. M., SCHUURMANS, C., SCARDIGLI, R., KIM, J., ANDERSON, D. J. & GUILLEMOT, F. 2002. Divergent functions of the proneural genes Mash1 and Ngn2 in the specification of neuronal subtype identity. *Genes Dev,* 16**,** 324-38.

PARVIZ, M., VOGEL, K., GIBSON, K. M. & PEARL, P. L. 2014. Disorders of GABA metabolism: SSADH and GABA-transaminase deficiencies. *J Pediatr Epilepsy,* 3**,** 217-227.

PATTYN, A., GUILLEMOT, F. & BRUNET, J. F. 2006. Delays in neuronal differentiation in Mash1/Ascl1 mutants. *Dev Biol,* 295**,** 67-75.

PATTYN, A., SIMPLICIO, N., VAN DOORNINCK, J. H., GORIDIS, C., GUILLEMOT, F. & BRUNET, J. F. 2004. Ascl1/Mash1 is required for the development of central serotonergic neurons. *Nat Neurosci,* 7**,** 589-95.

PELTOPURO, P., KALA, K. & PARTANEN, J. 2010. Distinct requirements for Ascl1 in subpopulations of midbrain GABAergic neurons. *Dev Biol,* 343**,** 63-70.

PORTER, T. G., SPINK, D. C., MARTIN, S. B. & MARTIN, D. L. 1985. Transaminations catalysed by brain glutamate decarboxylase. *Biochem J,* 231**,** 705-12.

PUELLES, L., HARRISON, M., PAXINOS, G. & WATSON, C. 2013. A developmental ontology for the mammalian brain based on the prosomeric model. *Trends Neurosci,* 36**,** 570-8.

RIVERA, C., VOIPIO, J., PAYNE, J. A., RUUSUVUORI, E., LAHTINEN, H., LAMSA, K., PIRVOLA, U., SAARMA, M. & KAILA, K. 1999. The K+/Cl- co-transporter KCC2 renders GABA hyperpolarizing during neuronal maturation. *Nature,* 397**,** 251-5.

ROBERTS, E. & FRANKEL, S. 1950. gamma-Aminobutyric acid in brain: its formation from glutamic acid. *J Biol Chem,* 187**,** 55-63.

ROYBON, L., MASTRACCI, T. L., RIBEIRO, D., SUSSEL, L., BRUNDIN, P. & LI, J. Y. 2010. GABAergic differentiation induced by Mash1 is compromised by the bHLH proteins Neurogenin2, NeuroD1, and NeuroD2. *Cereb Cortex,* 20**,** 1234-44.

RUBENSTEIN, J. L., SHIMAMURA, K., MARTINEZ, S. & PUELLES, L. 1998. Regionalization of the prosencephalic neural plate. *Annu Rev Neurosci,* 21**,** 445-77.

SANCHEZ-CATALAN, M. J., KAUFLING, J., GEORGES, F., VEINANTE, P. & BARROT, M. 2014. The antero-posterior heterogeneity of the ventral tegmental area. *Neuroscience,* 282**c,** 198-216.

SAXEN, L. 1989. Neural induction. *Int J Dev Biol,* 33**,** 21-48.

SCARDIGLI, R., SCHUURMANS, C., GRADWOHL, G. & GUILLEMOT, F. 2001. Crossregulation between Neurogenin2 and pathways specifying neuronal identity in the spinal cord. *Neuron,* 31**,** 203-17.

SCHOLPP, S. & LUMSDEN, A. 2010. Building a bridal chamber: development of the thalamus. *Trends Neurosci,* 33**,** 373-80.

SELLERS, K., ZYKA, V., LUMSDEN, A. G. & DELOGU, A. 2014. Transcriptional control of GABAergic neuronal subtype identity in the thalamus. *Neural Dev,* 9**,** 14.

SERAFINI, R., VALEYEV, A. Y., BARKER, J. L. & POULTER, M. O. 1995. Depolarizing GABA-activated Cl- channels in embryonic rat spinal and olfactory bulb cells. *J Physiol,* 488 (Pt 2)**,** 371-86.

SHIMAMURA, K., HARTIGAN, D. J., MARTINEZ, S., PUELLES, L. & RUBENSTEIN, J. L. 1995. Longitudinal organization of the anterior neural plate and neural tube. *Development,* 121**,** 3923-33.

SHIMOJO, H., OHTSUKA, T. & KAGEYAMA, R. 2008. Oscillations in notch signaling regulate maintenance of neural progenitors. *Neuron,* 58**,** 52-64.

SHIVDASANI, R. A., MAYER, E. L. & ORKIN, S. H. 1995. Absence of blood formation in mice lacking the T-cell leukaemia oncoprotein tal-1/SCL. *Nature,* 373**,** 432-434.

SKINNER, M. K., RAWLS, A., WILSON-RAWLS, J. & ROALSON, E. H. 2010. Basic helix-loop-helix transcription factor gene family phylogenetics and nomenclature. *Differentiation,* 80**,** 1-8.

SMITH, J. L. & SCHOENWOLF, G. C. 1989. Notochordal induction of cell wedging in the chick neural plate and its role in neural tube formation. *J Exp Zool,* 250**,** 49-62.

SOGHOMONIAN, J. J. & MARTIN, D. L. 1998. Two isoforms of glutamate decarboxylase: why? *Trends Pharmacol Sci,* 19**,** 500-5.

SONG, H., LEE, B., PYUN, D., GUIMERA, J., SON, Y., YOON, J., BAEK, K., WURST, W. & JEONG, Y. 2014. Ascl1 and Helt act combinatorially to specify thalamic neuronal identity by repressing Dlxs activation. *Dev Biol*.

STERN, C. D. 2005. Neural induction: old problem, new findings, yet more questions. *Development,* 132**,** 2007-21.

SZABO, G., KATAROVA, Z. & GREENSPAN, R. 1994. Distinct protein forms are produced from alternatively spliced bicistronic glutamic acid decarboxylase mRNAs during development. *Mol Cell Biol,* 14**,** 7535-45.

TAN, S. S., VALCANIS, H., KALLONIATIS, M. & HARVEY, A. 2002. Cellular dispersion patterns and phenotypes in the developing mouse superior colliculus. *Dev Biol,* 241**,** 117-31.

TOMITA, K., MORIYOSHI, K., NAKANISHI, S., GUILLEMOT, F. & KAGEYAMA, R. 2000. Mammalian achaete-scute and atonal homologs regulate neuronal versus glial fate determination in the central nervous system. *Embo j,* 19**,** 5460-72.

VAN EEKELEN, J. A., BRADLEY, C. K., GOTHERT, J. R., ROBB, L., ELEFANTY, A. G., BEGLEY, C. G. & HARVEY, A. R. 2003. Expression pattern of the stem cell leukaemia gene in the CNS of the embryonic and adult mouse. *Neuroscience,* 122**,** 421-36.

VASUDEVAN, A., WON, C., LI, S., ERDELYI, F., SZABO, G. & KIM, K. S. 2012. Dopaminergic neurons modulate GABA neuron migration in the embryonic midbrain. *Development,* 139**,** 3136-41.

VIEIRA, C., POMBERO, A., GARCIA-LOPEZ, R., GIMENO, L., ECHEVARRIA, D. & MARTINEZ, S. 2010. Molecular mechanisms controlling brain development: an overview of neuroepithelial secondary organizers. *Int J Dev Biol,* 54**,** 7-20.

VIROLAINEN, S. M., ACHIM, K., PELTOPURO, P., SALMINEN, M. & PARTANEN, J. 2012. Transcriptional regulatory mechanisms underlying the GABAergic neuron fate in different diencephalic prosomeres. *Development,* 139**,** 3795-805.

WADMAN, I. A., OSADA, H., GRUTZ, G. G., AGULNICK, A. D., WESTPHAL, H., FORSTER, A. & RABBITTS, T. H. 1997. The LIM-only protein Lmo2 is a bridging molecule assembling an erythroid, DNA-binding complex which includes the TAL1, E47, GATA-1 and Ldb1/NLI proteins. *Embo j,* 16**,** 3145-57.

WANG, D. D. & KRIEGSTEIN, A. R. 2009. Defining the role of GABA in cortical development. *J Physiol,* 587**,** 1873-9.

WANG, K., LONG, Q., JIA, C., LIU, Y., YI, X., YANG, H., FEI, Z. & LIU, W. 2013. Over-expression of Mash1 improves the GABAergic differentiation of bone marrow mesenchymal stem cells in vitro. *Brain Res Bull,* 99**,** 84-94.

WEINMASTER, G. 2000. Notch signal transduction: a real rip and more. *Curr Opin Genet Dev,* 10**,** 363–9.

WENDE, C. Z., ZOUBAA, S., BLAK, A., ECHEVARRIA, D., MARTINEZ, S., GUILLEMOT, F., WURST, W. & GUIMERA, J. 2015. Hairy/Enhancer-of-Split MEGANE and Proneural MASH1 Factors Cooperate Synergistically in Midbrain GABAergic Neurogenesis. *PLoS One,* 10**,** e0127681.

WONG, C. G., BOTTIGLIERI, T. & SNEAD, O. C., 3RD 2003. GABA, gamma-hydroxybutyric acid, and neurological disease. *Ann Neurol,* 54 Suppl 6**,** S3-12.

WURST, W. & BALLY-CUIF, L. 2001. Neural plate patterning: upstream and downstream of the isthmic organizer. *Nat Rev Neurosci,* 2**,** 99-108.

YUSTE, R. & KATZ, L. C. 1991. Control of postsynaptic Ca2+ influx in developing neocortex by excitatory and inhibitory neurotransmitters. *Neuron,* 6**,** 333-44.

ZHOU, Y., YAMAMOTO, M. & ENGEL, J. D. 2000. GATA2 is required for the generation of V2 interneurons. *Development,* 127**,** 3829-38.

11 APPENDIX

11.1 ABBREVIATIONS

A

A	purine base/amino acid adenine
A/P	antero-posterior
ACh	acetylcholine
ADHD	attention deficit hyperactivity disorder
AP	alar plate

B

BCA	bicinchoninic acid
BG	basal ganglia
bHLH	basic helix-loop-helix
BMPs	BONE MORPHOGENIC PROTEINS
BP	basal plate
bp	basepair
Brn3a	*POU domain, class 4, transcription factor 1 (Pou4f1); brain-specific homeobox/POU domain protein 3A*

C

C	amino acid cysteine / pyrimidine base cytosine
c	centi (10-2)
ca.	circa
Ca^{2+}	calcium
cCASP3	cleaved caspase3
CGE	caudal ganglionic eminences
CH_3COOH	acetic acid
Cl^-	chloride anions
CNS	central nervous system
CO_2	carbon dioxide
Co-IP	Co-Immunoprecipitation
CoP	commissural pretectum

cpm	counts per minute
CSP	caudal secondary prosencephalon
cTH	caudal thalamus
CTP	cytosine triphosphate

D

d/v	dorsal-ventral
DAB	3-3'Diaminobenzidine
DAn	dopaminergic neurons
DAPI	4',6-Diamidino-2-phenylindole
dblHet	double-heterozygous mutants (*Mgn+/- / Mash1+/-*)
dblKO	double knockout (*Mgn-/- / Mash -/-*)
DEPC-H_2O	UltraPure diethylpyrocarbonate (DEPC) - treated water
DH5α	*E.coli* strain
DLL1	delta like 1
dm H_2O	demineralized water
dMB	dorsal midbrain
DNA	desoxyribonucleic acid
DNase	desoxyribonuclease
dNTP	desoxyribonucleotide triphosphate
DTT	dithiotreitol

E

E	embryonic day
E. coli	*Escherichia coli*
e.g.	for example
EDTA	ethylenediaminetetraacetic acid
ES cells	embryonic stem cells

F

FB	forebrain (prosencephalon)
FBv	the vesicles of the rostral forebrain
FGF	FIBROBLAST GROW FACTORS
Fig.	figure
FP	floor plate

G

GABA	ɣ-amino-butyric acid
GABAn	GABAergic neurons
GABA-R	GABA receptors
Gad	*glutamic acid decarboxylase*
Gad65	*Glutamate Decarboxylase 2 (65kDa) Glutamate Decarboxylase 65 KDa Isoform*
Gad67	*Glutamate Decarboxylase 1 (67kDa); Glutamate Decarboxylase 67 KDa Isoform*
Gata2	*GATA Binding Protein 2*

H

h	hour(s)
H_2O_2	water
HB	hindbrain (rhombencephalon)
HCl	hydrochloric acid
HD	homeodomain
HEK293	Human Embryonic Kidney 293 cells
het	heterozygous

I

IC	inferior colliculus
IHC	immunohistochemistry
ISH	hot in situ hybridisation
IsO	isthmic organizer
IVC	individually ventilated cages
IZ	intermediate zone

J

JcP	juxtacommissural pretectum

K

K^+	potassium anions
kb	kilobase pairs
KCC2	potassium-Cloride-cotransporter 2
KCl	potassium chloride
kDa	kilo Dalton
kg	kilogram

KH_2PO_4	monopotassium phosphate
KOH	potassium hydroxide

L

l	liter
lac-Z	*lac-Z gene*
LB	Luria Broth
LGE	lateral ganglionic eminence
Lim1	*Lim homeobox 1* (*Lhx1*)

M

m	meter
m	milli (10^{-3})
M	molar (mol/l)
Mash1	*Achaete-Scute1 (Ascl1)* Family BHLH Transcription Factor
MB	midbrain (mesencephalon)
$MgCl_2$	magnesium chloride
MGE	medial ganglionic eminence
Mgn	*Megane (Helt, Heslike)*
MH	medullary hindbrain
MHB	midhindbrain
min	minute(s)
MRF	midbrain reticular formation
mRNA	messenger ribonucleic acid
MZ	mantle zone

N

n	nano ($10^{-9)}$
Na^+	sodium kations
Na_2HPO_4	disodium phosphate
Na-Citrat buffer	trisodium citrate buffer (10x)
NaCl	sodium cloride
$NaHPO_4$	sodium phosphate
NaOAc	sodium acetate
NeuN	*Neuronal Nuclei*
Ngn1	*Neurogenin1*

NH_4OAc	ammonium acetate
NICD	NOTCH intracellular domain
NKCC1	sodium-potassium-2-cloride cotransporter 1
NP-40	Nonidet P-40
NS	nervous system
NTE	NaCl-Tris-EDTA

O

o/n	overnight
OD	optical density

P

p1	pretectum
p2	thalamus
p3	prethalamus
PAG	periaqueductal gray
PBS	phosphate buffered saline
PcP	precomissural pretectum,
PCR	polymerase chain reaction
PFA	paraformaldehyde
PH	pontine hindbrain
pH	potential hydrogen
pHH3	phosphohistone 3
PMH	pontomedullary hindbrain
POA	preoptic area
PCR	Polymerase chain reaction
PPH	prepontine hindbrain
pTHr	rostral population of thalamic progenitors

Q

R

RIPA	protein lysis buffer
RNA	ribonucleic acid
RNase	ribonuclease
RNasin	ribonuclease I inhibitor

rNTP	ribonucleoside tri-phosphate Solution Mix containing adenine (A), cytosine (C) and guanine (G), as diifferent bases (rATP; rCTP; rGTP)
rpm	rounds per minutes
RSP	rostral secondary prosencephalon
RT	room temperature
rTH	rostral thalamus

S

s	second(s)
SC	superior colliculus
SDS	sodium dodecylsulfate
SDS-PAGE	sodium dodecyl sulfate polyacrylamide gel electrophoresis
sglMut	single mutant (*Mgn-/- / Mash -/-*)
SHH	SONIC HEDGEHOG
SN	substantia nigra
SNpc	substantia nigra pars compacta
SNpr	substantia nigra pars reticulata
Sox14	*SRY (Sex Determining Region Y)-Box*
SSC	saline sodium citrate

T

TAE (electrophoresis)	tris acetate with EDTA
Tal1	*T-Cell Acute Lymphocytic Leukemia 1; (Scl1)*
Tal2	*T-Cell Acute Lymphocytic Leukemia 2 ; (Scl2)*
TEA (ISH)	triethanolamine-HCl
temp.	temperature
TF(s)	transcription factor(s)
TH	dopamine
Tris	trishydroxymethyl-aminoethane

U

U	unit(s)
UV	ultra-violet
V	volt(s)

V

VGAT	vesicular GABA transporter 2; *vGlut2 Glutamate Transporter 2 (Solute Carrier Family 17 Vesicular Glutamate Transporter, Member 6; Vesicular)*
vl	ventrolateral
vlMB	ventrolateral midbrain
VTA	ventral tegmental area
VZ	ventricular zone

W

WB	Western Blot
WT	wild-type

X

x	symbol for crosses between mouse strains

Y

Y2H	yeast two hybrid system

Z

ZLI	zona limitans intrathalamica

β-gal	β-galactosidase
µ	micro (10^{-6})
%	percentage
°C	celsius degree
35S	isotope of sulfur
5-HT	serotonin
∞	until eternity

11.2 INDEX OF FIGURES

11.3 DANKSAGUNG

Ich danke Prof. Dr. Wolfgang Wurst für die Möglichkeit, diese Arbeit am Institut für Entwicklungsgenetik anzufertigen sowie für die Unterstützung in wissenschaftlichen Fragenstellungen.

Ferner danke ich Prof. Dr. Nilima Prakash und Dr. Jovica Ninkovic für die Teilnahme an meinem Thesis Committee und die hilfreichen Anregungen, die das Projekt maßgeblich vorrangetrieben haben.

Mein Dank gilt Prof. Dr. Siegfried Scherer für die Übernahme des Vorsitzes der Prüfungskommission und Prof. Dr. Heiko Lickert für die Übernahme der Aufgabe des Zweitprüfers.

Insbesondere möchte ich meinen Dank Dr. Jordi Guimera für die intensive, professionelle und warmherzige Betreuung aussprechen. Die Kombination aus seiner Wertschätzung gegenüber meiner Arbeit und Person, jede erdenkliche, hilfreiche Unterstützung zu jeder Zeit und die Möglichkeit, eigenständig zu arbeiten waren die Grundsteine, die zum Gelingen dieser Arbeit beigetragen haben. Auch weil er mich in meinem Glauben bestärkt hat, dass Probleme nur Herausforderungen sind und der Frieden mit sich selbst ungeahnte Kräfte weckt.

Ein ganz besonderer Dank geht an meine Mitdoktoranden sowie alle Mitarbeiter und Mitarbeiterinnen des Instituts - insbesondere an das Büro 8031 mit Anke, Benedict, Constantin, Luise und Michi, die entstandenen Freundschaften und ihre Bereitschaft, mir bei kleineren oder größeren Problemen jederzeit zuzuhören.

Ich danke meiner Schwester, dass sie mir immer wieder das bestärkende Gefühl gibt, dass alles im Leben seinen Sinn hat und der ich ein Vorbild sein darf. Ich danke meinen Großmüttern, die mich Stärke gelehrt haben und meinem Großvater, der mir beigebracht hat, die Dinge zu hinterfragen und dass Neues zu lernen glücklich macht. Natürlich danke ich vor allem meinen Eltern für ihre Unterstützung und ihre Art, die mich gelehrt hat, das Leben zu umarmen und gleichzeitig sich zu fordern – und: „denn sonst gäbe es mich ja nicht“.
Josef bin ich dankbar für die fachliche Unterstützung in Layout-Fragen, seine endlose Geduld und sein Talent, mich lachend ans Meer und noch viel weiter zu bringen. Meiner Cousine Suse danke ich für ihre allumfassende fachliche, interdisziplinäre, moralische, lebenstechnische und kulinarische Unterstützung. Armin danke ich, weil er Armin ist und immer da ist, wenn ich ihn brauche. Besonderer Dank gilt der Häberl-WG (mit Maria und Philip), der Balde-WG (mit Thomas und Philipp) und Stephie, die meine Zeit der Doktorarbeit zu einer Zeit meines Lebens gemacht haben, die erfüllt von großartigen Erinnerungen an gute Freundschaft ist. Stefanie danke ich für den sportlich-fachlichen Austausch in zweifelnden Zeiten. Letztlich danke ich allen meinen lieben Freunden für die Ausdauer, Ruhe und Geduld, mit denen sie mir stets zur Seite standen und mich immer wieder aufgemuntert haben, auch wenn sie es eigentlich nicht mehr hören konnten.